Ferdowsi University of Mashhad

Print ISSN 2008-9147
Online ISSN 2717-3364
Numbers: 27

JCMR

Journal of Cell and Molecular Research

Volume 14, Number 1, Summer, 2022

بسم الله الرحمن الرحیم

Issuance License No. 124/902-27.05.2008 from Ministry of Culture and Islamic Guidance
Scientific Research Issuance License No. 161675 from the Ministry of Science, Research and Technology, Iran

Journal of Cell and Molecular Research (JCMR)

Volume 14, Number 1, Summer, 2022

JCMR Office: Department of Biology, Faculty of Sciences, Ferdowsi University of Mashhad, Mashhad, Iran.
Postal Code: 9177948953
P.O. Box: 917751436
Tel: +98-513-8804063/+98-9156996326
Fax: +98-513-8795162
E-mail: jcmr@um.ac.ir
Online Submission: http://jcmr.um.ac.ir

Table of Contents

Expressed Cellobiohydrolase Enzyme of Thermobifidia fusca in Pichia pastoris as Host Can Act on Cotton Substrate 1
Karim Imangholiloo; Nasrin Moshtaghi; Seyed Hasan Marashi; Abdolreza Bagheri; Ahmad Sharifi

Phytochemical Analysis of Volatile and Non-volatile Fractions, Antioxidant, and Anti-Cancer Activities of *Dracocephalum polychaetum* and *Dracocephalum kotschyi* 11
Marzieh Taghizadeh; Sara Soltanian; Nahid Nasibi

Effect of Intramuscular and Intraperitoneal Injections of conjugated MSTN-siRNA-cholesterol on Inhibition of Myostatin Gene expression 20
Mitra Riasi; Sina Mozaffari Jovin; Ali Javadmanesh

Conversion of Membrane Lipids to Jasmonates as a Key Pathway to Develop Somatic Embryos in Arabidopsis thaliana 28
Azadeh Khadem; Nasrin Moshtaghi; Abdolreza Bagheri

Evaluation of CD86 rs17281995Gene Polymorphism in Gastric and Intestinal Cancer Subjects in Tehran and Khorramabad Cities 37
Masoumeh Aalipour; Asghar Aalipour; Mohammad Mousaei Ghasroldasht

Comparative Transcriptome Analyses of a Transgenic Sugar Beet Resistant to Beet Necrotic Yellow Vein Virus 44
Mahdieh Yousefiara; Mohammad Ali Malboobi; Abdolreza Bagheri; Nasrin Moshtaghi

Investigating the Effect of Stable Glutamine on the Neuronal Differentiation of PC-12 Cells in 2D- and 3D-Culture Media 54
Seyed Majid Jalalian Hosseini; Javad Baharara; Shahrbanoo Oryan; Mohammad Amin Kerachian

Study of lncRNA NEAT1 Gene Expression in Ovarian Cancer 63
Amin Moqadami; Mohammad Khalaj-Kondori

 DOI: 10.22067/jcmr.2022.74925.1029

Research Article

Expressed Cellobiohydrolase Enzyme of *Thermobifidia fusca* in *Pichia pastoris* as Host Can Act on Cotton Substrate

Karim Imangholiloo[1], Nasrin Moshtaghi[2*], Seyed Hasan Marashi[2], Abdolreza Bagheri [2], Ahmad Sharifi[3]

[1] *Agricultural Biotechnology, Ferdowsi University of Mashhad, Mashhad, Iran*
[2] *Biotechnology and Plant Breeding Department, Ferdowsi University of Mashhad, Mashhad, Iran*
[3] *Ornamental Biotechnology Department, ACECR, Mashhad Branch, Mashhad, Iran*

Received 24 January 2022 Accepted 7 June 2022

Abstract

Cellulose which is extremely produced by plants, can be used for biofuel production but this function needs chemical or enzymatic digestion. Cellulose hydrolysis of plant wastes for ethanol production requires a mixture of three enzyme groups, including endoglucanases, exoglucanases, and beta-glucosidases. The cellobiohydrolase enzyme (Cel6B) from *Thermobifidia fusca* has been used for cellulase activity extensively. This research aimed to express recombinant Cel6B enzyme in *Pichia pastoris*. For this purpose, *cel*6B gene in control of AOX1 promoter (methanol inducible) was introduced into *Pichia pastoris.* Amplification of *cel6B* gene was performed by PCR technique and then introduced into the Phil-S1 yeast vector. The recombinant construct contained the *cel6B* gene sequence and PHO1 signal sequence as secretion signal was transferred into *Pichia pastoris* GS115 strain. The transformed yeast cells expressed the recombinant Cel6B to yield 2.104 U (µmol/min)/ml of culture medium. Purified recombinant enzyme showed the best activity at 60 °C and pH 4.5 and this was agreed with optimum conditions for recombinant Cel6B enzymes which were produced in other systems. The purity of the enzyme was examined by SDS–PAGE technique, and a single band with a molecular weight about 59.6 kDa was observed. As *cel6B* gene sequence was not optimized for expression in the *Pichia pastoris* yeast, this could be one of the reasons for low level activity of recombinant Cel6B enzyme. This thermostable enzyme can be used for cellulolytic digestion of biomaterials in biofuel production research and other uses.

***Keywords*:** Cellulose, Cel6B, yeast, AOX1 promoter, Expression

Introduction

Cellulose produces by plant photosynthesis and can be used as a renewable biological material. Cellulose biodegradation by cellulase enzymes or cellulolytic microorganisms produces CO_2 and CH_4 in nature. Main cellulase enzymes include endoglucanases (EC 3.2.1.4) that make free ends on cellulose chains; cellobiohydrolases or CBHs (EC 3.2.1.91) that degrade cellulose chains from free ends and produce cellobiose units and β-glucosidase (EC 3.2.1.21) that hydrolyze cellobiose to glucose (Zhang et al. 2009). All of these enzymes are necessary for the hydrolysis of crystalline cellulose (Sun and Cheng, 2002; Kazzaz and Fatehi, 2020; Xiao et al. 2019).

Thermobifida fusca is an anaerobic bacterium and it hydrolyzes the cellulose using synergistic cellulase activities to supply its sole carbon source. Cel6B enzyme (a cellulase enzyme) is necessary for the function of this synergistic hydrolysis, therefore its mobility usually is weak on the substrates. Cel6B is an exocellulase and cuts β-glycosidic bonds from the end of cellulose chains (Vuong and Wilson, 2009; Wu et al. 2013; Gomez del Pulgar and Saadeddin, 2014). More amounts of this valuable enzyme could be obtained by expressing *cel6B* gene in non-original hosts such as yeast cells. *Pichia pastoris* was a desirable host for producing of CBH enzyme from *Trichoderma reesei*. This host can secrete the recombinant enzyme into the culture medium due to secretion signal peptide that attached to the protein, can do protein folding and post translational modification for normal function of recombinant proteins (Fang and Xia, 2015; Fang et al. 2019).

Zhang *et al*. (2018) expressed GHF9 (an endoglucanase enzyme) from *Reticulitermes speratus* microorganism in *P. pastoris* and

*Corresponding author's e-mail address: moshtaghi@um.ac.ir

recombinant enzyme showed suitable stability at pHs between 4.0 and 11.0 and temperatures lower than 40℃ in RsEGm mutant (Zhang et al. 2018; Zhang et al. 2020). Cellobiohydrolase II from *Trichoderma reesei* was expressed in *P. pastoris* and exhibited the highest activity at pH 5.0 and 50℃ temperature (Fang and Xia, 2015). Various enzymes for cellulose and hemicellulose degrading such as xyloglucanases, exoglucanases, and xylanases have been produced in *P. pastoris* (Tenkanen et al. 2012; Sun et al. 2016). *P. pastoris* can produce high levels of heterologous proteins. It is possible to obtain up to 12 g/L of recombinant proteins in high biomass *P. pasroris* fermentations (Lindenmuth and McDonald, 2011; Srivastava et al. 2018).

In this study, an exocellulase gene, *cel6B*, from filamentous soil bacterium *Thermobifida fusca*, was expressed in *P. pastoris*. In the following, optimum conditions (pH and temperature) were determined for recombinant enzyme.

Materials and Methods

Vector construction and transformation

We used the CDS of *cel6*B gene presented in plasmid pSZ143 gifted by Dr. Wilson from California University. Gene amplification performed by PCR technique, and primers designed by PrimerBlast software. The following primer pairs were used, Cel6B F (5′-TCCATACGAATTCGCCGGCTGCTCG-3′; the underlined sequence was *Eco*RI site) and Cel6B R (5′-TCACTCCGGGATCCAGAGGCGGGTA-3′; the underlined sequence was *BamH*I site). PCR was performed for 35 cycles by Pfu DNA polymerase (Fermentase Company): Cycles programmed as 95°C for 1 min (denaturation step), 60°C for 40 s (annealing step), and 72°C for 2 min (extension step), and 72 °C for 5 min to final extension. PCR products were digested using *Eco*RI and *BamH*I, and DNA fragment purified by NaOAc (1 M) and ethanol method. Yeast plasmid pHIL-S1 was also digested using of *Eco*RI and *BamH*I, and then purified (Table 1). Cloning of *cel6*B gene in pHIL-S1 plasmid was done by T4 ligase enzyme (Table 2), and the recombinant plasmid was transferred into *Escherichia coli* DH5α. Successful transformation was confirmed by DNA sequencing (Macro Gene Company). Figure 1 showed the recombinant plasmid pHIL-S1 containing *cel6B* gene.

The *cel6B* gene was ligated to the pHIL-S1 vector along with its PHO1 sequence, a signal sequence. The recombinant vector was amplified in the *E. coli* DH5α strain. The expression construct, PhilS1-Cel6B was extracted from *E. coli* and linearized by *Stu*I restriction enzyme according to manufacture protocol (Fermentase). The linearized plasmid was transformed into *P. pastoris* GS115 strain by electroporation technique (Agilent Technologies). The linearized recombinant DNA (2 µg) was used for electroporation using an electroporator Gene PulserXcell™ (BIORAD). The mixture (DNA and yeast cells) was transferred into a pre-chilled electroporation cuvette (2 ml) and incubated on the ice for 5 min. The voltage and time constant were, 2kV and 5 milli-seconds, respectively. After electroporation, 1 mL of ice-cold sorbitol (1M) was added to the cuvette.

Screening of transformed *P. pastoris* colonies

P. pastoris culture media included BMGY, BMMY, MD, MM and, YPD (Invitrogen protocol, Invitrogen | Thermo Fisher Scientific – US). According to the Invitrogen instructions, if the recombinant construct is linearized with StuI enzyme and transferred to *P. pastoris* yeast cells GS115 strain. Although most transformants must be Mut $^{+}$ phenotype in the presence of AOX1, recombination is likely to occur at the AOX1 site and disrupt the wild AOX1 gene and resulting in His^{+} Mut^{S} transformants. Therefore, the test was performed on minimum dextrose (MD) and minimum methanol (MM) media. Mut^{+} phenotype colonies could grow on both culture media, and the Mut^{S} phenotype colonies, would only grow on MD medium and not on MM medium.
After the transformation process, cells were transferred onto MD and MM media. A sterile toothpick was used for picking one colony from MD medium, and streaking or patching on MM and MD media on the same pattern of primary plate. Mut^{+} transformants grew well on both MD and MM plates, but Mut^{S} transformants grew well only on MD plates, and show little or no growth on the MM plates (http://tools.thermofisher.com).

Confirmation of *P. pastoris* transformants

The genomic DNA of *P. pastoris* was extracted using Volossiouk et al. (1995) method. The insertion of gene cassette into the yeast genome was confirmed by PCR technique using AOX1 primers, forward primer (5′-GACTGGTTCCAATTGACAAGC-3′) and, reverse primer (5′- GGCAAATGGCATTCTGACATCCT-3′). PCR was programmed as 94℃ for 5 min, 30 cycles of 94℃ for 1 min, 60℃ for 1 min, 72℃ for 2 min, and final extension at 72℃ for 5 min.

Recombinant soluble protein detection

One recombinant colony was transferred into a 100 mL BMGY medium (http://tools.thermofisher.com) and incubated at 30℃ overnight. Then, the whole culture medium was centrifuged at 3000×g for 5 min, then supernatant removed and pellet transferred into 100 mL BMMY medium (http://tools.thermofisher.com) until OD_{600} = 1. Methanol (0.5% (v/v) was added to the medium every 24 h, the culturing was carried out at 250 rpm and 30℃ for 96 h. The content of soluble protein was determined using Bradford reagent (Sigma Aldrich). Protein standard curve was determined using serial concentrations of bovine serum albumin. Then the standard curve was used for quantifying soluble protein content produced by different transformed yeast colonies. Absorbancies of all samples were read at 595 nm.

Cellobiohydrolase assay

Phosphoric acid-treated cotton (2.5 mg/ml) as PC was utilized as the substrate of enzyme reactions. PC was prepared according to Vuong and Wilson method (Vuong and Wilson, 2009). The reaction mixtures were prepared at one ml volumes (three replications) in 50 mM sodium acetate buffer (pH 5.5) and maintained at 50°C for 16 h. Reducing sugar concentrations were measured using phenol-sulfuric acid reagent (PAS) and a standard curve of glucose. Enzyme activities of different recombinant colonies were determined and expressed as a percentage of activity. One unit of enzyme activity is defined as the content of an enzyme that releases one µmol of reducing sugars per milliliter for one minute.

SDS-PAGE

Recombinant enzyme was detected by SDS-PAGE technique (Laemmli, 1970). SDS–PAGE was performed on the precast 12% polyacrylamide gel (Bio-Rad). Polyacrylamide gel was rinsed twice by water after electrophoresis, and stained by Coomassie blue.

Recombinant enzyme properties

The pH range of 3.5-7.5 was tested for determining the optimum pH of CBH activity. pH adjustment was done by 50 mM sodium acetate buffer (NaOAc buffer pH 5.5) solution (pH 3.5-6) and 50 mM potassium phosphate buffer (pH 6-7.5). The optimum temperature of CBH activity was determined by enzyme assays at the temperature range of 40℃ to 60℃ with 10 ° C intervals using 50 mM NaOAc buffer solution, pH 5.5.

Table 1. Reaction compounds of pHIL-S1 plasmid digestion.

Component	Volume (µl)	Concentration in final reaction
pHIL-S1 vector	6	9 µg
Tango 10X buffer	6 of 10X	2X
*Eco*RI enzyme	1	1 (U/µl)
*Bam*HI enzyme	1	1 (U/µl)
Distilled water	16	Up to 30 µl

Table2. Ligation reaction of *cel6*B gene subcloning into the pHIL-S1 vector

Component	Volume (µl)
digested and purified gene fragment (1673 bp. 15.2 ng / µl)	8
Digested and purified pHIL-S1 vector (20 ng / µl)	2
T4 ligase enzyme buffer (10X)	2
T4 DNA Ligase enzyme (5U / µl)	1
Distilled water	7

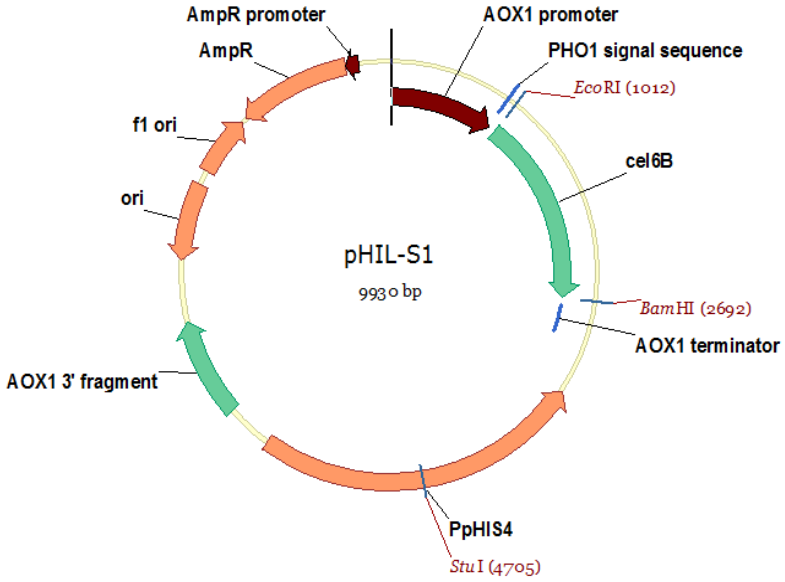

Figure 1. Recombinant pHIL-S1 plasmid containing *cel6B* gene, (pHIL-S1: *P. pastoris* vector for expression of a secreted recombinant protein).

Results and Discussion

Construction of the Cel6B expression vector

The *cel6B* gene was cloned into the vector pHIL-S1 to obtain a good expression. At first, we cut plasmid pHIL-S1 using *EcoR*I and *BamH*I enzymes for transferring CDS of Cle6B gene to this vector. Enzymatic digestion of the vector was confirmed by gel electrophoresis method, and the size of digested and uncut pHIL-S1 vectors was compared on agarose gel (Figure 2). The *cel6B* gene (a 1.6 Kb fragment) was observed on the agarose gel, that indicated the expression vector was correctly constructed. For testing the successful ligation, the expression cassette was digested with *Stu*I restriction enzyme, and linearized and uncut recombinant vectors were compared on the agarose gel (Figure 3).

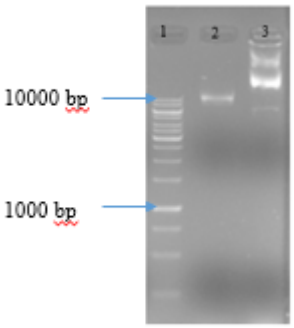

Figure 2. Confirmation of recombinant pHIL-S1 construction. Lane 1: 1 kb DNA size marker (Fermentas), Lane 2: pHIL-S1 vector was cut using *Eco*RI and *BamH*I restriction enzymes, Lane 3: uncut pHIL-S1.

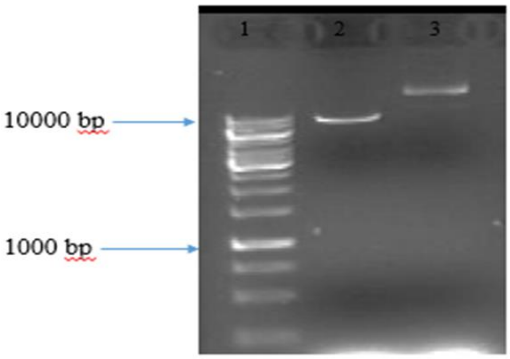

Figure 3. Linearization of recombinant pHIL-S1 vector. Lane 1: 1 kb DNA size marker. Lane 2: linearized recombinant pHIL-S1 containing *cel6*B gene. Vector was linearized by *Stu*I restriction enzyme, Lane 3: Uncut recombinant pHIL-S1 plasmid.

Electroporation and the primary screening

The linearized recombinant DNA, pHIL-S1-Cel6B, was transferred into *P. pastoris* GS115 host using electroporation technique. Then yeast cells were transferred onto the MD plate, and transformed colonies were grown. These colonies were able to produce and secret the Cel6B recombinant protein. These transformants had different capacities for enzyme production because of varied gene

integration modes and gene copy numbers (http://tools.thermofisher.com). It has been shown that increasing the copy numbers up to more than 10 copies, could increase protein expression (Sun et al. 2016). Figure 4 shows *Pichia pastoris* colonies after transformation step on two different MD and MM media. These cultures were prepared to identify rapid-growth yeast colonies and strains.

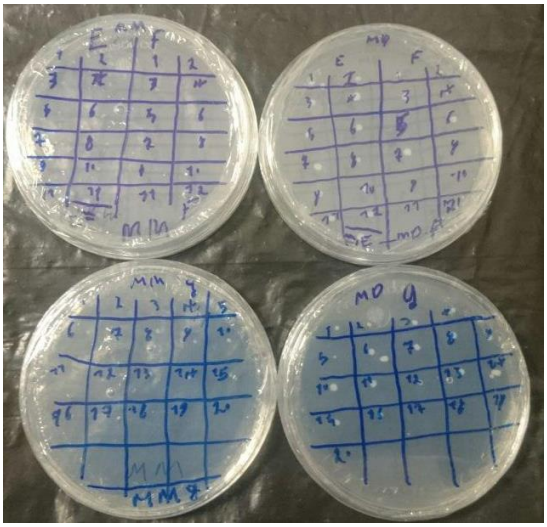

Figure 4. Colonies of *P. pastoris* after transformation step on two different media, MD (right) and MM (left).

Confirmation of transformants

The transformants that had grown on the MM and MD plates were Mut$^+$ GS115 strains. These colonies were used for PCR confirmation (Figure 5). Figure 5, lanes 1 and 2, showed the PCR products amplified from the genomic DNAs of yeast transformants using specific primers of *cel6B* gene and lanes 4 and 5 showed the PCR products amplified from the genomic DNAs of yeast transformants using *AOX1* primers. Figure 5 confirmed the integration and stability of *cel6B* gene into the yeast genomic DNA, sometimes genetic traits might be lost from one generation to the next (Sun et al. 2016).

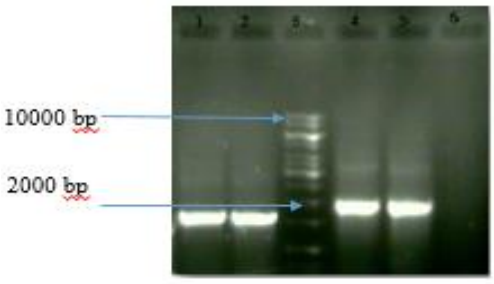

Figure 5. PCR products of *P. pastoris* transformants carried the expression construct containing *cel6*B gene. Lane 1 and 2: PCR products using specific primers of *cel6*B gene, Lane 3: 1kb DNA size marker. Lane 4 and 5 PCR products using AOX1 primers, Lane 6: negative control.

Soluble protein content of transgenic yeast cells

After transferring the construct into the yeast cells and confirming it by PCR technique, selected recombinant colonies containing AOX1 must produce recombinant enzyme by inducing the colonies in the induction medium. Since this yeast plasmid has a secretory signal, the protein must be secreted into the yeast culture medium. For this purpose, transgenic colonies were induced in BMMY induction medium for 4 days. Sampling was performed every 24 hours and the best day and strain were determined in terms of protein production, using Bradford method. A BSA standard curve with R^2 = 0.98 and line equation y = 0.1513x + 0.5484 was obtained by Excel software (Figure 6). Then the amount of produced protein was calculated and the results showed that colony 4E, showed the highest protein production among the transgenic colonies, 24 hours after induction. Figure 7 shows the Bradford assay results of two colonies.

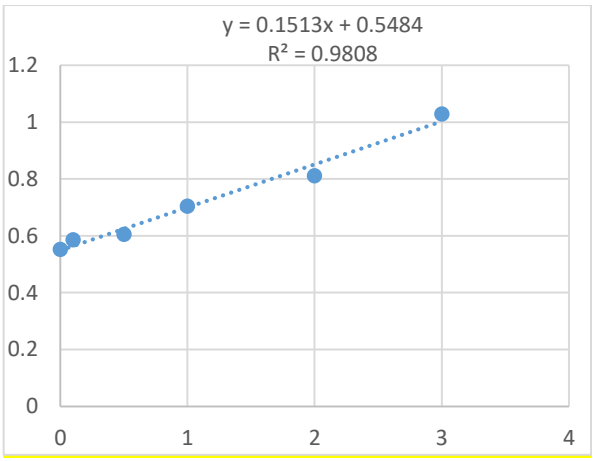

Figure 6. Bovine serum albomin standard curve

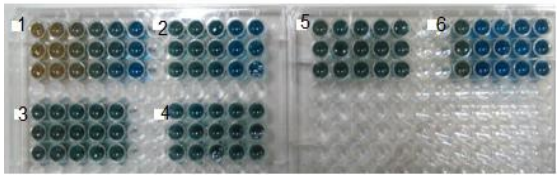

Figure 7. Bradford assay of yeast colonies. (1) BSA, (2) non-recombinant *P. pastoris* GS115 colony, (3) non-induced recombinant colony 7A, (4) non-induced recombinant colony 4E, (5) induced recombinant colony 7A, and (6) induced recombinant colony 4E.

Statistical analysis was performed using JMP 8 software for 4E and 7A strains and their controls which were non-transgenic colonies: 4eni, 7ani, and gs115 non-transgenic colonies. The mean comparison was performed at 1% significance level. As shown in Figure 8, 4E colony had the highest protein production after 24 hours of induction and was significantly different from other colonies.

Screening recombinant yeast colonies with high activity

Multi-copy yeast colonies were screened to determine the expression level of Cel6B enzyme (Figure 8). Three colonies were cultured on a BMMY medium and induced by 0.5% methanol (v/v) for 96 h to detect the Cel6B activity. Colony-4E (Figure 8) showed a slightly higher CBH activity (0.11 U/mL). Therefore, Colony-4E was selected for the next phase of the experiment. SDS-PAGE analysis of the Colony-4E culture medium (a 72 h-culture) confirms the expression of Cel6B protein (Figure 9). A protein band with 59.6 kDa molecular weight can verify the Cel6B expression.

Enzymatic properties of recombinant Cel6B

The effects of different pHs and temperatures were studied on the activity of recombinant Cel6B on microcrystalline cellulose (Sigma Aldrich) (Figures 10 and 11). pH 4.5 and 60℃ temperature were determined as the optimum pH and temperature for Cel6B enzymatic activity, respectively. There were no significant differences in enzyme activity levels at 40 and 50℃, and higher activity was observed at 60℃.

Optimal temperature of fermentation process can play a role in mRNA synthesis regulation of cells. Temperature can affect extracellular enzyme secretion by changing the physical properties of the cell membrane (Abd Rahman et al., 2004).

The level of enzyme secretion can directly affect the amount and activity of the enzyme (Murao et al. 1988). Lu et al. (2003) reported that the optimum temperature for enzyme production varies from one microorganism to another. Rai et al. (2012) reported that the optimal activity of cellulase enzyme in *Candida* yeast is about 50 °C. Taha et al. (2015) has stated that the cellulase enzyme activity of *Trichoderm viride* is at the highest levels at 50 °C.

It has been reported that 45°C and pH 4.5 led to the highest activity of cellulase enzyme (Alami et al., 2017). The effects of pH on the enzyme activity levels is due to changing of ionic charge of the enzyme active site and thus changing the conformation of the active site.

Taha et al. (2015) observed the high activity of cellulase enzyme from *Trichoderma viride* at pH 6. Harshvardha et al. (2013) stated that the highest activity of cellulases could be observed at pH between 3 and 9.

Various hosts can be used for expression of recombinant proteins. *P. pastoris* is a better host than bacteria, fungi or plants. This species has advantages such as a strong AOX1 promoter and the ability of protein secretion. In this study the codon optimization was not done for *cel6B* gene, so the expression was low. Therefore, in following this change should be done. Moreover, Cel6B of *T. fusca* was expressed in *E. coli* but its product was limited to the outer membrane and unable to be excreted (Zhang et al. 2018). As a result, *P. pastoris*, could be a good alternative for producing enzymes such as CBH due to simple separation and purification.

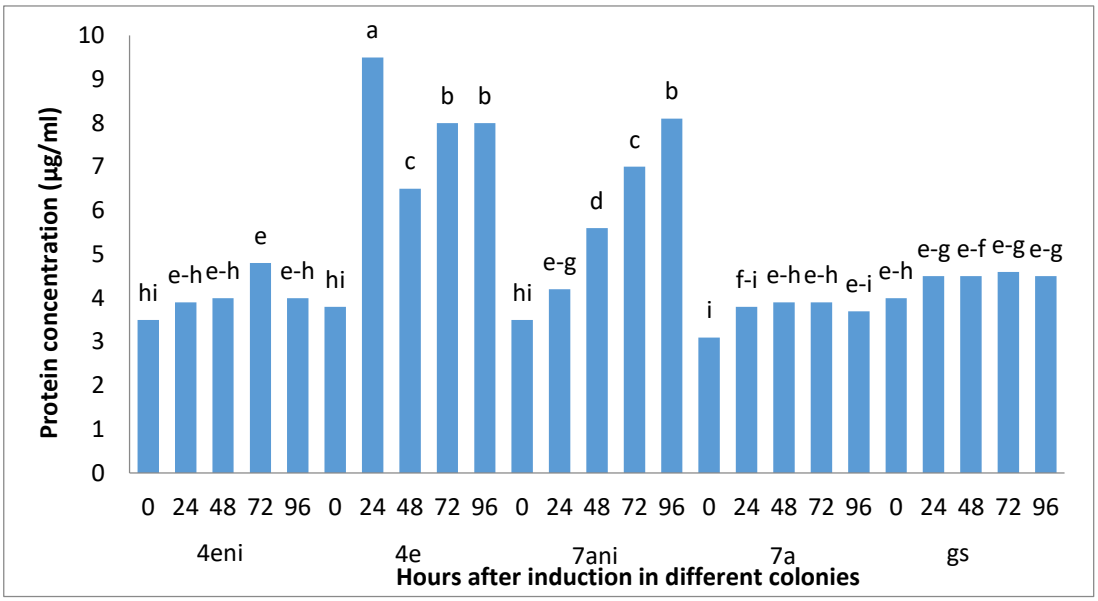

Figure 8. Protein production (µg/mL) by *P. pastoris* strains 4E, 4eni, 7A, 7ani, and GS115 (gs) during 96 hours of induction, columns with the same letters showed no significant differences (α = 5%).

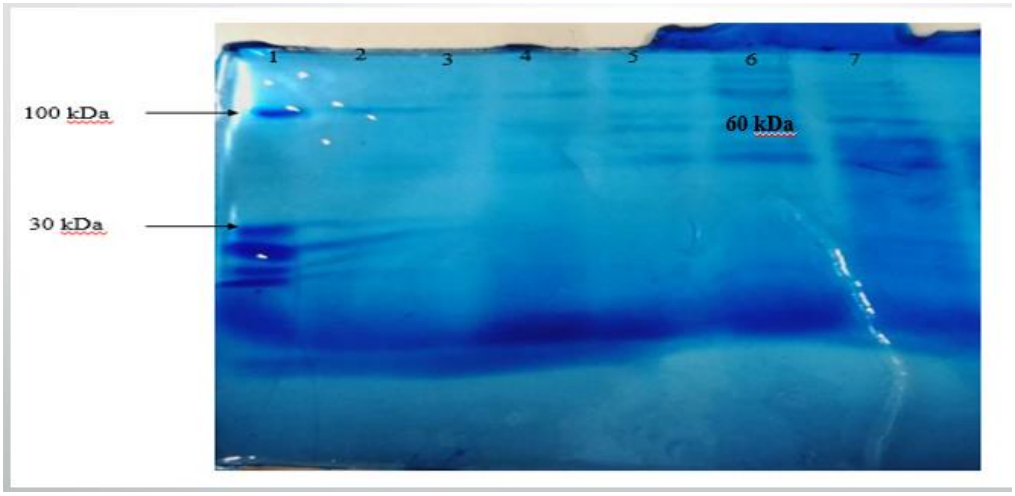

Figure 9. SDS-PAGE analysis of the culture medium of recombinant *P. pastoris*. Lane 1: protein size marker, Lane 2 and 3: culture medium of control *P. pastoris* colonies, Lane 4 to 7: Cel6B protein band. All samples were collected at 72 hours during fermentation.

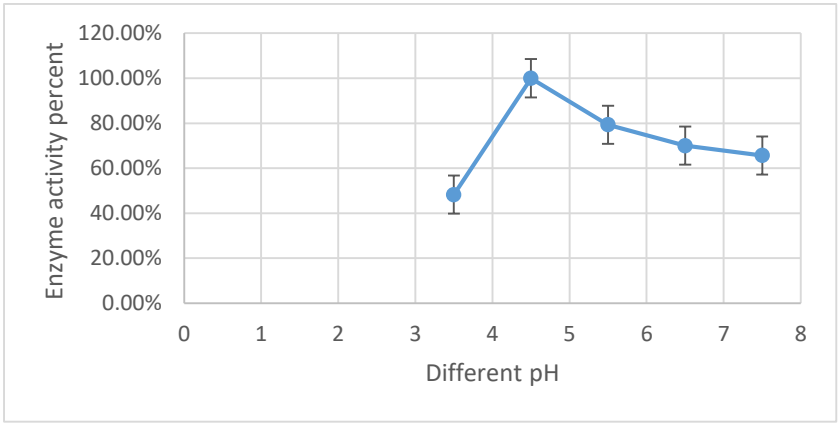

Figure 10. Determination of optimum pH for Cel6B enzyme activity expressed in P. pastoris yeast cells. The activity of recombinant Cel6B enzyme was assayed at 50℃ and various pHs (3.5-7.5). Cel6B enzyme showed the highest activity at pH 4.5.

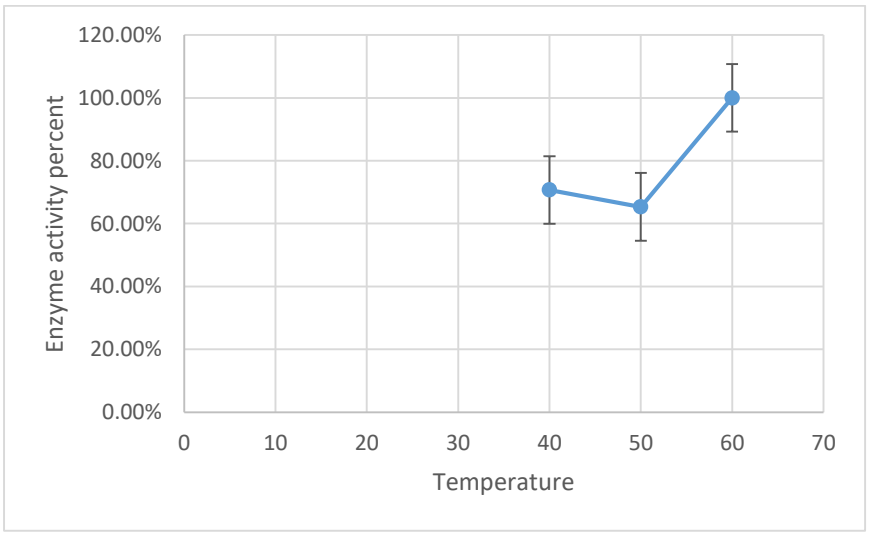

Figure 11. Determination of optimum temperature for Cel6B enzyme activity expressed in *P. pastoris* yeast cells. The activity of recombinant Cel6B enzyme was assayed at pH 4.5 and various temperatures (40-60℃). Cel6B enzyme showed the highest activity at 60℃.

Conclusion

Here we report the production of *T. fusca* cellobiohydrolase in *P. pastoris* yeast cells. The strain GS115 (high methanol-utilizing) showed the highest yield of Cel6B as 2.104 U(µmol/min)/ml culture medium. The optimum temperature and pH were 60℃ and 4.5, respectively, which coincide with similar research. The enzyme purity was studied using SDS–PAGE technique, and a single band was observed with a molecular weight of 59.6 kDa. AOX1 promoter is inducible by methanol, therefore we could have a rapid and easy cloning selection and controlled expression. This thermostable enzyme can be used in future research after codon optimization and other optimal conditions.

Acknowledgements

This research was conducted using the research grant from Ferdowsi University of Mashhad, Iran. We have to thank ACECR (Khorasan Razavi branch) for their guidance and facilities and Dr. Javanmard, Ph.D. of Biology from Ferdowsi University of Mashhad for her guidance.

Conflict of Interest: The authors declare that they have no conflict of interest.

References

Abd Rahman R. N. Z., Geok L. P., Basri M. and Saleh, A. B. (2004) Physical factors affecting the production of organic solvent-tolerant protease by

Pseudomonas aeruginosa strain K. Bioresource Technology 96:429-43

Alami N. H., Kuswytasari N. D., Zulaika E. and Shovitri M. (2017) Optimization of cellulase production by Candida G3.2 from the rhizosphere of gunung anyar mangrove surabaya. Proceeding of International Conference on Green Technology 8 (1):399-406.

Fang H. and Xia L. (2015) Heterologous expression and production of *Trichoderma reesei* cellobiohydrolase II in *Pichia pastoris* and the application in the enzymatic hydrolysis of corn stover and rice straw. Biomass and Bioenergy 78:99-109.

Fang H., Zhao R., Li C. and Zhao C. (2019) Simultaneous enhancement of the beta–exo synergism and exo–exo synergism in *Trichoderma reesei* cellulase to increase the cellulose degrading capability. Microbial Cell Factories 18(1):1-14.

Gomez del Pulgar E.M. and Saadeddin A. (2014) The cellulolytic system of *Thermobifida fusca*. Critical Reviews in Microbiology 40(3):236-247.

Harshvardhan K., Mishr A. and Jha B. (2013). Purification and characterization of cellulase from a marine Bacillus sp. H1666: a potential agent for single step saccharification of seaweed biomass. Journal of Molecular Catalysis B: Enzymatic 93:51-56.

Kazzaz A. E. and Fatehi P. (2020) Technical lignin and its potential modification routes: a mini-review. Industrial Crops and Products 154:112732.

Laemmli U. K. (1970). Cleavage of structural proteins during the assembly of the head of bacteriophage T4. Nature 227(5259):680-685.

Lindenmuth B. E. and McDonald K. A. (2011) Production and characterization of *Acidothermus cellulolyticus* endoglucanase in *Pichia pastoris*. Protein Expression and Purification 77(2):153-158.

Murao S., Sakamoto R. and Arai M. (1988) Cellulase of *Aspergillus aculeatus*. In methods in Enzymology. Academic Press. London, 274-299 pp.

Lu W., Li D. and Wu Y. (2003) Influence of water activity and temperature on xylanase biosynthesis in pilot-scale solid-state fermentation by *Aspergillus sulphurous*. Enzyme and Microbial Technology 32:305-311.

Rai P., Tiwari S. and dan Gaur R. (2012). Optimization of process parameters for cellulase production by novel thermotolerant yeast**.** BioResources 7:5401-5414.

Srivastava N., Srivastava M., Mishra P. K., Gupta V. K., Molina G., Rodriguez-Couto S., et al. (2018) Applications of fungal cellulases in biofuel production: advances and limitations. Renewable and Sustainable Energy Reviews 82:2379-2386.

Sun F. F., Bai R., Yang H., Wang F., He J., Wang C., et al. (2016). Heterologous expression of codon optimized *Trichoderma reesei* Cel6A in *Pichia pastoris*. Enzyme and Microbial Technology 92:107-116.

Sun Y. and Cheng J. (2002) Hydrolysis of lignocellulosic materials for ethanol production: A review. Bioresource Technology 83(1):1-11.

Taha, A. S. J., Taha, A. J., & Faisal, Z. G. (2015). Purification and kinetic study on cellulase produced by local Trichoderma viride. Nature and Science, 13(1), 87-90.

Taha, A. S. J., Taha, A. J. and Faisal, Z. G. (2015) Purification and kinetic study on cellulase produced by local *Trichoderma viride.* Nature and Science 13:87-90.

Tenkanen M., Vršanská M., Siika-aho M., Wong D. W., Puchart V., Penttilä M., et al. (2012) Xylanase XYN IV from *Trichoderma reesei* showing exo- and endo-xylanase activity. FEBS Journal 280(1):285-301.

Volossiouk T., Robb E. J. and Nazar R. N. (1995) Direct DNA extraction for PCR-mediated assays of soil organisms. Applied and Environmental Microbiology 61(11):3972-3976.

Vuong T. V. and Wilson D. B. (2009). Processivity, synergism, and substrate specificity of *Thermobifida fusca* Cel6B. Applied and Environmental Microbiology 75(21):6655-6661.

Vuong T. V. and Wilson D. B. (2009). The absence of an identifiable single catalytic base residue in *Thermobifida fusca* exocellulase Cel6B. The FEBS Journal 276(14):.3837-3845.

Wu M., Bu L., Vuong T.V., Wilson D.B., Crowley M.F., Sandgren M., et al. (2013). Loop motions important to product expulsion in the *Thermobifida fusca* glycoside hydrolase family 6 cellobiohydrolase from structural and computational studies. Journal of Biological Chemistry 288(46):33107-33117.

Xiao W., Li H., Xia W., Yang Y., Hu P., Zhou S., et al.(2019) Co-expression of cellulase and xylanase

genes in *Sacchromyces cerevisiae* toward enhanced bioethanol production from corn stover. Bioengineered 10(1):513-521.

Zhang N., Wright T., Wang X., Savary B. J. and Xu J. (2020) Production of thermostable endo-1, 5-α-L-arabinanase in *Pichia pastoris* for enzymatically releasing functional oligosaccharides from sugar beet pulp. Applied Microbiology and Biotechnology 104(4):1595-1607.

Zhang P., Yuan X., Du Y. and Li J. J. (2018). Heterologous expression and biochemical characterization of a GHF9 endoglucanase from the termite *Reticulitermes speratus* in *Pichia pastoris*. BMC Biotechnology, 18(1):1-9.

Zhang Y.P., Hong J. and Ye X. (2009). Cellulase assays. In Biofuels. Humana Press, Totowa, NJ, 213-231 pp.

Research Article

Phytochemical Analysis of Volatile and Non-volatile Fractions, Antioxidant, and Anti-Cancer Activities of *Dracocephalum polychaetum* and *Dracocephalum kotschyi*

Marzieh Taghizadeh [1*], Sara Soltanian [2], Nahid Nasibi [2]

[1] *Department of Plant and Animal Biology, Faculty of Biological Science and Technology, University of Isfahan, Isfahan, Iran.*
[2] *Department of Biology, Faculty of Science, Shahid Bahonar University of Kerman, Kerman, Iran*

Received 06 February 2022 Accepted 20 August 2022

Abstract

The present study was conducted to determine the volatile and non-volatile fractions and the antioxidant and anti-cancer activities of ethanolic extracts of *Dracocephalum polychaetum* and *D. kotschyi*. The volatile and non-volatile fractions were investigated by gas chromatography-mass spectrometry (GC-MS) and high-performance liquid chromatography (HPLC). The cytotoxicity effect of two ethanol extracts and the major phenolic components has been evaluated on breast and colon cancer cells by the MMT assay. GC-MS of the essential oils identified about 50 compounds, and perillylaldehyde and D-limonene were the main constituents in the essential oils of the two species. Moreover, high-performance liquid chromatography- Diode array detector analysis demonstrated that the ethanolic extract of *D. polychaetum* and *D. kotschyi* were the source of phenolic compounds such as rosmarinic acid, protocatechuic acid, naringin, apigenin, syringic acid, epicatechin, chlorogenic acid, thymol, carvacrol, rutin, p-coumaric acid, gallic acid, benzoic acid, cinnamic acid, resorcinol, quercetin, salicylic acid, 4-hydroxybenzoic acid, and ferulic acid. Rosmarinic acid and thymol were the main predominant phenolic constituents in *D. kotschyi* and *D. polychaetum* ethanolic extracts. The cytotoxicity effect of *D. kotschyi* and *D. polychaetum* ethanol extracts and the major phenolic components including rosmarinic acid, thymol, apigenin, quercetin, and nariginin has been evaluated on breast and colon cancer cells by MMT assay and results indicated IC_{50} values in the range of 90 to 140 ($\mu g.ml^{-1}$) after 48 hours of treatment with ethanol extracts. Among phenolic components, thymol caused the lowest cell viability and Narengin showed the lowest anti-proliferative activity. Both extracts also showed antioxidant activity using DPPH assay. The findings of this research suggest that the *Dracocephalum* have precious bioactive and natural compounds with significant antioxidant and *in vitro* anti-cancer activities.

***Keywords*:** Anti-cancer activity, Antioxidant activity, Essential oil, Phenolic compounds

Introduction

Medicinal plants have natural products that can be used as a source for potential drugs. Today, finding new bioactive compounds with medicinal properties has been the subject of many studies and some researchers have focused on replacing natural plant-based compounds with chemical compounds in the medical, food, and pharmaceutical industries (Kchaou et al., 2016). Essential oils (EOs) are unique and valuable resources of secondary metabolites due to their medicinal properties, such as anti-cancer, antiviral, and anti-bactericidal activities (Golkar and Moattar, 2019). In addition, phenolic compounds are another main class of secondary metabolites in plants derived from the shikimic acid pathway. They are composed of phenolic acids, flavonoids, and colored anthocyanins. The anti-inflammatory, antimicrobial, antioxidant, and antiproliferative activities of these compounds have also been reported in the literature (Apostolouet al., 2013).

Dracocephalum is a genus of flowering plants belonging to the Labiate family. *Dracocephalum* varieties are used in traditional medicine to heal many diseases. The chemical composition of *Dracocephalum* species consists of phenolic compounds, flavonoids, flavonols, terpenoids, and alkaloids. *D. polychaetum*, known as Zaroo or Mofaroo in Kerman folk medicine, is exclusively grown in a few geographical areas of Kerman province in Iran (Fallah and Hosseini Cici, 2020). *D. kotschyi*, locally known as 'Zarrin-giah' or 'Badrandjboie-Dennaie', is an aromatic and perennial herb found at an altitude of 2000-3000 metres above sea level in the central-western parts of Iran (Fattahi et al., 2013). Despite substantial information about different species in the Labiate family, research considering the phytochemical

* Corresponding author's e-mail address: *m.taghizadeh@bio.ui.ac.ir*

composition and biological activities of *D. kotschyi* and *D. polychaetum* is limited so far.

The present study aimed to determine the EOs composition, phytochemical components, total phenolic content (TFC), total flavonoids (TFD), total flavonols (TFL), and anthocyanin (Ant) of *D. polychaetum* and *D. kotschyi* by gas chromatography-mass spectrophotometry (GC-MS), and high-performance liquid chromatography-diode array detector (HPLC-DAD). Furthermore, the antioxidant activity of *D. polychaetum* and *D. kotschyi* ethanol extracts was assayed by DPPH, and the cytotoxicity activities of ethanol extracts and major phenolic components of these two plants were assayed on breast and colon cancer cells.

Materials and Methods

Plant materials

The *D. polychaetum* plants were obtained from wild-growing populations of Kerman Province (Hezar altitude of about 4000 m) in the Southeast of Iran. *D. kotschyi plants were* gathered from wild-growing populations in Isfahan Province (Fereydunshahr altitude of about 2700 m).

Volatile fraction analysis

Gas Chromatography-Mass Spectrophotometry analysis

The essential oils were extracted by the hydro-distillation method. The crushed air-dried biomass (50 g) of *D. polychaetum* and *D. kotschyi* aerial parts were hydrodistilled for 4 hours using a clevenger-type apparatus (yield 0.7 v/w %). The yields were estimated after extraction with diethyl ether. Essential oil constituents were identified by an Agilent GC7890A/MS-5975C model (Agilent Technologies, Santa Clara, CA, USA). The GC system is equipped with a HP-5MS capillary column (HP-5MS 5% Phenyl Methyl Silox: Agilent, USA, 30 m in length × 0.25 mm in diameter, flm thickness of 0.25 µm), and coupled with a mass-selective detector from the same company. The carrier gas was helium, at a flow rate of 1 mL min^{-1}. The temperature of the detector and injector was 240 °C. At first, the temperature of the oven was set at 40 °C for 3 min. Then, it was extended to 290 °C at a rate of 5 °C min^{-1}. Finally, the temperature was kept at 280°C for 15 min. The samples were injected in a pulsed split mode (the flow was 3 mL min^{-1}, split ratio 20:1). The mass-selective detector was operated at a ionization energy of 70 eV using a spectral range of 25-1000 amu. Identification of the compounds was achieved by comparing their retention indices to *n*-alkanes and their mass spectra with those recorded in the National Institute of Standard and Technology and those reported in the studies (Adams, 2007).

Nonvolatile fraction analysis

Leaf extraction procedure

Dried and powdered aerial parts of plants (300 mg DW) were homogenized with 2 mL of ethanol (Merck, Germany) and centrifuged at 10,000 rpm for 25 min. Then, the supernatant was collected and held at -20°C for further analysis.

Total Phenolic content

Total phenolic contents were mesured using the Folin-Ciocalteau method as discussed in Chua et al. (2011). The concentration of total phenol content was expressed in terms of mg equal gallic acid in 1 g of dry weight (mgGA g^{-1}DW).

Total Flavonoid and Flavonol content

Total flavonol and flavonoid contents were determined according to Miliauskas and Venskutonis (2004). The TDF and TFL were then calculated by a calibration curve method using rutin as a standard. The contents of TDF and TFL were expressed as mg rutin equivalents per gram of dry mass (mg RU g^{-1}DW).

Anthocyanin content

Total anthocyanin was estimated according to the protocol of Hara (2003). The anthocyanin content was estimated by measuring the absorbance at 511 nm using the spectrophotometer and calculated by the extinction coefficient of 33,000 M^{-1} cm^{-1}.

DPPH free radical scavenging activity

Free radical scavenging activities were measured by DPPH (1, 1-di- phenyl-2-picrylhydrazyl) assay according to Burits and Bucar protocol (2000). The reduction of DPPH absorption was read at 517 nm. Butylated hydroxytoluene (BHT) was used as the standard drug. The inhibition percentage was calculated as follows: $I\% = (A_{con} - A_{sam}) / A_{sam} \times 100$, where A_{con} and A_{sam} are the absorbance of control and sample, respectively. Radical scavenging activity was expressed as the inhibition concentration (IC_{50}), i.e., the concentration of extract necessary to decrease the initial concentration of $DPPH^{\bullet}$ by 50% (IC_{50}) under the specified experimental conditions.

Phytochemical products by HPLC analysis

Phytochemical products of plants were extracted according to Taghizadeh et al. (2019). For quantitative and qualitative measurements of phytochemicals in ethanol, an HPLC program equipped with a UV-Vis photodiode-array detector (DAD-HPLC Waters e 2695, Alliance, Milford, MA, 2489 UV-Vis detector) was applied. To confirm the peak identity, their absorption spectra and retention times were compared with those of pure (>99%) standards (syringic acid, gallic acid, protocatechuic acid, chlorogenic acid, 4-hydroxybenzoic acid, epicatechin, benzoic acid, naringin, ferulic acid, salicylic acid, rosmarinic acid, rutin, quercetin, p-coumaric acid, carvacrol and apigenin were bought from Sigma (USA), thymol and cinnamic acid were bought from Merck (Germany).

Anti-cancer analysis

Cell culture and reagent

Human breast (MCF-7) and colon (HT-29) cancer cell lines (from the Pasteur Institute of Iran, Tehran) were grown in DMED medium (Gibco, Grand Island, USA) containing 10% fetal bovine serum (FBS; Biowest, France) and 100 U mL^{-1} penicillin and streptomycin (Biowest, France) and cultured at 37°C in a humidified atmosphere with 5 % CO_2.

The rosmarinic acid, apigenin, quercetin, and naringin were purchased from Sigma-Aldrich (USA), and thymol was obtained from Merck (Germany). All phytochemical components were dissolved in ethanol.

Cytotoxic activity assay

The cytotoxic activities of rosmarinic acid, thymol, apigenin, quercetin, naringin, and ethanol extracts of *D. polychaetum* and *D. kotschyi* on MCF-7 breast and HT-29 colon cancer cell lines were measured by 3- (4,5-dimethyl thiazol-2yl) -2,5-diphenyltetrazolium bromide (MTT) assay. The cells were subcultured by trypsinization. The 5×10^3 cells were seeded in 96-well plates. After 24 h, the culture medium was changed with a medium containing increasing concentrations of samples ranging from 10 to 1280 µg mL^{-1} in each well for 48 h.

Since the solvents (DMSO and ethanol) have cytotoxic effects, the same proportion of DMSO/ethanol was added as controls. Later, 20 µL of the MTT solution (5 $mgmL^{-1}$) was added to each well, and the plate was reincubated for 3 h. Finally, the medium was removed, and 100 µL of DMSO was added to dissolve formazan crystals; absorbance was measured at 490 nm using a multi-plate reader (ELISA reader; BioTek-ELx800, USA). The ratio of the absorbance of treated cells to the absorbance of control cells was determined as cell viability (%). Half-maximal inhibitory concentration (IC_{50}) of each component was calculated using Prism 6.0 (GraphPad Software, Inc., San Diego, California, USA).

Data Presentation and Statistical Analyses

Statistical analyses were performed using the Statistical Package for the Social Sciences (SPSS) version No 19.0, Chicago, IL, USA, with three replications. The experiments followed a completely randomized design, and the values were presented as mean ± SD (standard deviation). The significant differences among treatments were evaluated using the LSD test at $P \leq 0.05$.

Results and Discussion

GC/MS of essential oil

The oxidation of fatty acids produces mainly EOs through an intracellular biogenic pathway (Golkar and Moattar, 2019). The GC-MS analysis of the EOs of *D. polychaetum* and *D. kotschyi* showed 54 compounds of the total oils. These compounds and their relative proportions in the EOs are presented in Table S1 (Supplementary file) According to the data, perillyl aldehyde and D-limonene were the main constituents of the EOs in both *Dracocephalum* species. The major components in EOs of *D. kotschyi* were perillyl aldehyde, D-limonene, p-mentha-1(7), and 8(10) -dien-9-ol. Similar to *D. kotschyi*, perillyl aldehyde, D-limonene, p-mentha-1(7), and 8(10)-dien-9-ol were identified as the main components in EOs of *D. polychaetum*. According to these data, o-cymene, ethanone, 1-(2-methylphenyl), (-)-myrtenol, trans-carveole, 2,6-octadienal, 3,7-dimethyl-, (Z)-,l-carvone, cis-geraniol,3cyclohexene1-ethanol, β,4-dimethyl, terpineol acetate, caryophyllene, cadinene, caryophyllene oxide, and carotol existed in *D. kotschyi*, but they did not exist in *D. polychaetum*. The variation in the composition of EOs of *Dracocephalum* species (type and proportion) depends on plants' genetic and environmental conditions such as humidity, temperature, altitudes, and light intensity in areas where the *Dracocephalum* species grow (Fallah et al. 2020). In another study, α-pinene, α-terpinene, p-cymene,

limonene, linalool, p-mentha-1,5-dien-8- ol, α-terpineol, trans-carveol, and caryophyllene were reported as the main components in *D. kotschyi* (Fallah et al., 2020). In a previous investigation into the EOs composition of *D. polychaetum*, the authors identified perilla aldehyde, terpinene-7-al, and limonene (Khodaei et al., 2018). Thus, the results of the EOs analysis in the present research might be used as supplementary and confirmatory data to the previous literature on *D. kotschyi* and *D. polychaetum*.

Total phenolics

Phenolic compounds are considered important secondary metabolites, possessing various roles in plants. One of these roles is the antioxidant activity in the defensive response of plants to biotic and abiotic stresses. These compounds eliminate reactive oxygen species (ROS) without causing any oxidative stress damage (Dias et al., 2016). According to this research, *D. poychaetum* exhibited a higher level of TPC as compared to *D.kotschyi* (Table 1). Previous studies have reported various contents for TPC depending on *Dracocephalum* species. Our results are consistent with other studies that reported TPC in the methanolic extract of *D. kotschyi* was 175.6 mg $GAEg^{-1}$ DW (Sharifi et al., 2017) and 188.08 mg $GAEg^{-1}$ DW (Mirzania and Farimani, 2018). Also, plant genetic and environmental conditions such as plants' geographic location and climatic factors (i.e., light intensity, photoperiod, and temperature) significantly affected the TPC. These factors also influence the biosynthesis of many secondary metabolites in many plant species (Jaakola and Hohtola, 2010).

Total Flavonoid and Flavonol

Flavonoids belong to a class of low molecular weight phenolic compounds with various functions and can be subdivided into different subgroups including flavones, flavonols, flavanones, flavanonols, flavanols or catechins, anthocyanins, and chalcones. As the main compounds of the non-antioxidant system, they act as chemical messengers and physiological regulators (Falcone Ferreyra, 2012). Flavonols are an important subgroup of flavonoids and, by their antioxidant activity, play a very significant role in causing plants to respond to environmental stresses (Golkar et al., 2019). A previous study reported the presence of many flavonoids and flavonols in different *Dracocephalum* species (Kamali et al., 2016). The findings of this research show that the TFD level is higher in *D. polychaetum* than in *D. kotschyi* Furthermore, *D. poychaetum* exhibited a higher level of TFL as compared to *D. kotschyi* (Table 1). The TFD and TFL are highly affected by circumstances like the plant's geographic location, environmental condition, and dominant climatic factors (Jaakola & Hohtola, 2010). Furthermore, different extraction methods can significantly affect the type and amount of TDF and TFL. To the best of our knowledge, this is the first report on the TFL and TDF values in *D. polychaetum.*

Anthocyanin content

Anthocyanins are a subgroup of flavonoids, a class of phytochemical compounds with antioxidant, antibacterial, antiviral, anti-cancer, and anti-inflammatory effects (Golkar et al., 2019). As presented in Table 1, the Ant contents in *D. polychaetum* and *D. kotschyi* were measured at 13.24 µmol g^{-1} DW and 12.07 µmol g^{-1} DW, respectively. A review of the previous literature revealed a lack of any studies on Ant content in the two species. In this regard, it is useful to increase Ant content because of its medicinal value and colorant properties, which make it a valuable biochemical for the food industry.

HPLC analysis

Phytochemicals are a powerful group of compounds belonging to secondary metabolites of plants that have antioxidant and anti-radical roles in the defense response of the plant to environmental stress and also have valuable pharmaceutical and medical properties.

According to the HPLC analysis in this study, chromatographic separation plants identified 18 phytochemical compounds in each species. Table 2 presents the quantitative determination of each phytochemical compound (µgg^{-1} dry weight). Our findings indicated the phytochemical compounds of both species consisted of naringin, rosmarinic acid, apigenin, epicatechin, carvacrol, rutin, thymol, 4-hydroxybenzoic acid, p-coumaric acid, benzoic acid, gallic acid, cinnamic acid, resorcinolchlorogenic acid, salicylic acid, syringic acid, quercetin, protocatechuic acid, and ferulic acid. The main differences between the two species were the quantitative amounts of each compound. Genetic and environmental factors can significantly affect the metabolism and accumulation of the phytochemicals (Dong et al., 2011). Here, different plant species can employ diverse mechanisms to distribute phytochemicals in their organs by various means. These results are in agreement with previous studies as they reported that *D. kotschyi* phytochemicals consisted of lcosmosiin, luteolin 3′-

O-β-d-glucuronide, luteolin, apigenin, cirsimaritin, isokaempferide, penduletin, xanthomicrol, calycopterin, epicatechin, chlorogenic acid, and the polyphenol rosmarinic acid (Fattahi et al., 2016, Jahaniani et al., 2005). The present results indicated that rosmarinic acid, apigenin, quercetin, naringin, thymol, and carvacrol were the predominant phytochemical compounds in *D. polychaetum* and *D. kotschyi* ethanolic extracts. In this respect, the highest amount of rosmarinic acid was observed in *D. kotschyi*. Earlier studies showed that rosmarinic acid was also the most abundant polyphenol in Iranian *D. moldavica* and *D. kotschyi* (Fattahi et al., 2013).

Moreover, monoterpenoids such as carvacrol and thymol were found for the first time in ethanolic extracts of *D. polychaetum* and *D. kotschyi*. Hence, the highest amounts of carvacrol and thymol existed in *D. polychaetum*. According to our results, the highest content of quercetin, as a flavonol compound, was found in *D. kotschyi*. This study showed no significant differences between apigenin (as a flavone compound) and naringin content of the studied species. To the best of our knowledge, there is no report in the literature demonstrating the phytochemical constituents of *D. polychaetum*. Furthermore, according to this study, resorcinol, protocatechuic acid, 4-hydroxybenzoic acid, syringic acid, ferulic acid, and naringin were identified as new phytochemical compounds in *D. kotschyi*.

Cytotoxic activity against breast and colon cancer cell proliferation

As shown in Figure. 1, the cytotoxicity assay after 48 h treatment revealed that ethanol extracts from *D. polychaetum* and *D. kotschyi* had significant cytotoxic activity on MCF-7 cancer cells with IC_{50} values of 140 μgmL^{-1} and 133 μgmL^{-1}, respectively, and significant cytotoxicity on HT29 cell line with IC_{50} values of 90 μgmL^{-1} and 126 μgmL^{-1} respectively. Among the active constituents of these extracts, thymol exhibited the highest anti-proliferative effect with IC_{50} values of 10 μgmL^{-1} for HT-29 and 23 μgmL^{-1} for MCF-7, and Naringin showed the lowest anti-proliferative activity with IC_{50} values 270 μgmL^{-1} for HT-29 and 399 μgmL^{-1} for MCF-7. Also, rosmarinic acid, apigenin, and quercetin exhibited considerable inhibitory activity against MCF-7 and HT-29 cells with IC_{50} values ranging from 35- 40 μgmL^{-1}.

In vitro cytotoxicity assay using MTT showed that both ethanol extracts and their constituents have cytotoxic activities against colon and breast cancer cell lines. These data propose that the anti-cancer potential of *D. kotschyi* and *D. polychaetum* ethanol extracts could be attributed to their main contents, including thymol, rosmarinic acid, apigenin, and quercetin. The anti-proliferative activities of thymol, rosmarinic acid, apigenin, and quercetin on the growth of various cancer cells have been reported in many studies (Zhang et al., 2018).

Despite the antioxidant, antidiabetic, anti-hyperlipidemic, and anti-lipid peroxidative properties of ethanol extract of *D. polychaetum* aerial parts (Pouraboli et al., 2016), there is no report on the anti-cancer potential of this plant. On the contrary, the anti-proliferative activity of *D. kotschyi* against several cancer cells has been indicated in several studies. For instance, it was shown that leaf extract of *D. kotschyi* could inhibit the proliferation of a number of human tumor cell lines and tumor proliferation in mice. In the reported study, xanthomicrol was recognized as an active flavone in the leaf extract of *D. kotschyi*, which is responsible for inhibiting the proliferation of malignant cells (Jahaniani et al., 2005). Furthermore, *in vitro*, cytotoxic, anti-proliferative effects of different fractions of *D. kotschyi* extract against lung cancer cell lines showed that the dichloromethane fraction and essential oil are the most effective fractions (Sani et al., 2017) for this purpose. The role of *D. kotschyi* as a promising anti-liver cancer agent was demonstrated by inducing reactive oxygen species production, cytochrome c release, and mitochondrial membrane permeabilization. These compounds start apoptosis signaling through the formation of the caspase-3 activation complex. In another research on the cytotoxicity of hexane, aqueous, chloroform, and ethanolic extracts of *D. kotschyi* aerial parts on the MDA-MB-231 breast cell line, the ethanolic extract showed the highest cytotoxicity effect (Faghihinia et al., 2015). This study confirmed the anti-cancer effect of *D. kotschyi* on breast and colon cancer cells.

DPPH scavenging activity

Bleaching the purple ethanol solution of DPPH was used to measure the DPPH scavenging activity of the ethanolic extracts of *D. polychaetum* and *D. kotschyi* and BHT as a standard compound. The concentration of the sample required to reduce the primary concentration of DPPH by 50% (IC_{50}) under the experimental situation is presented in Table 3. According to our results, the DPPH scavenging activity of *D. kotschyi* and *D. polychaetum* increased in a dose-dependent manner (Figure 2). The IC_{50} values showed the higher antioxidant activity of the *D. kotschyi* than *D. polychaetum extract*. Both

extracts showed less antioxidant activity than BHT as the standard. Other species of *Dracocephalum*, such as *D. moldavica*, also showed remarkable scavenging effects against DPPH (Fattahi et al., 2013).

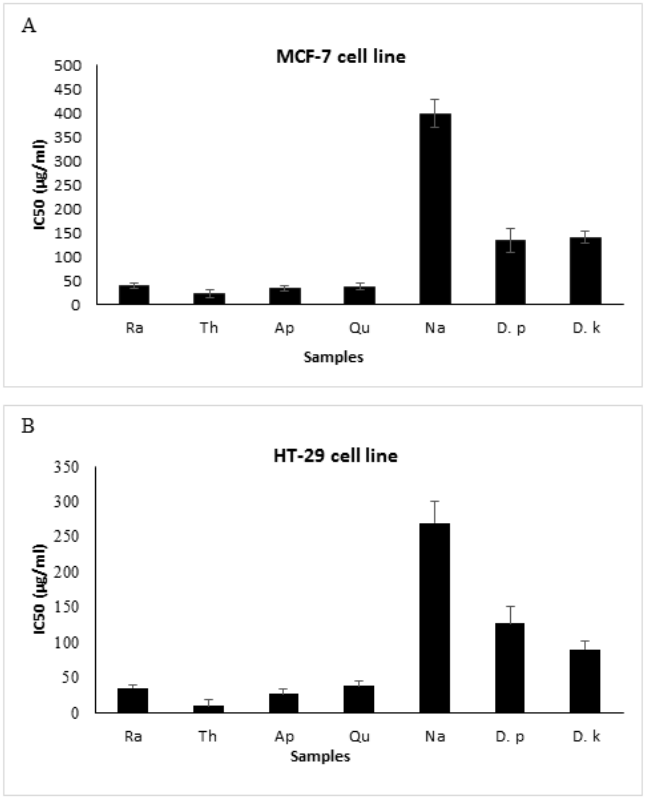

Figure 1. Anti-proliferative effects of Rosmarinic acid (Ra), Thymol (Th), Apigenin (Ap), Quercetin (Qu), Naringin (Na), *D. polychaetum* (*D. p*) and *D. kotschyi* (*D. k*) ethanolic extracts against human breast MCF-7 (A) and colon HT-29 (B) cancer cell lines. Anti-proliferative effects were determined by MTT assay. IC50 values are expressed as the mean ± SD of three independent experiments. IC50 is the drug concentration that causes a 50% decrement of cell viability.

Table 1. Contents of total phenolics, total flavonoids, total flavonols and anthocyanin in *D. kotschyi* and *D. polychaetum.*

	Studied traits			
Species	TPC[a] (mg GAE/g DW)	TFD (mg QE/g DW)	TFL (mg QE/g DW)	Ant (µg/ g DW)
D. polychaetum	209.15±1.78[a]	72.83±0.91 [a]	58.93±1.03[a]	13.24±5.3[a]
D. kotschyi	188.73±1.12 [b]	65.91±0.62 [b]	50.16±1.2[b]	12.07±3.7[b]

Data are means ± SD of three replicates. Means followed by the same letter are not significantly different at P≤0.05 according to the LSD test. [a]: TPC: Total phenolic content; TFD: Total flavonoids; TFL: Total flavonols, Ant: anthocyanin.

Conclusion

Overall, the present study was conducted to identify and quantify volatile and non-volatile fractions and evaluate the antioxidant and anti-cancer potentials of *D. kotschyi* and *D. polychaetum*, two endemic species of Iran. In this study, the antioxidant activities of the TPC, TDF, TFL, and Ant in *D. polychaetum* plants were found to be stronger than those of *D. kotschyi*. Moreover, the ethanolic extracts of *D. polychaetum* and *D. kotschyi* and the major phytochemical components such as rosmarinic acid, thymol, apigenin, quercetin, and naringin showed high cytotoxic effects on breast and colon cancer cells, as determined by MMT assay. However, further research is required to find other new natural compounds in *D. kotschyi* and *D. polychaetum*. The findings of this research suggest that the *Dracocephalum* has precious bioactive and natural compounds with significant antioxidant and *in vitro* anti-cancer activities that have promising applications in the food, pharmacological, and medicinal industries, especially in cancer therapy.

Table 2. Phytochemical compounds (µg. g^{-1} DW) in the *D. polychaetum* and *D. kotschyi* plants, identified by HPLC.

Phytochemical Compounds (µg. g^{-1} DW)	[a]RT (min)	*D. polychaetum*	*D. kotschyi*
Gallic acid	9.8	153.99±23.4[b]	189.74±36.95[a]
Resorcinol	12.3	40.05±7.8[a]	21.35±8.04[b]
Protocatechuic acid	15.5	4.25±0.89[a]	4.27±0.47[a]
4-hydroxybenzoic acid	18.5	13.85±2.23[a]	8.6±0.44[b]
Chlorogenic acid	32.5	22.44±7.5	42.3±5.7
Epicatechin	34.6	91.76±12.7	83.16±6.96
Syringic acid	36.8	14.17±2.4	8.99±1.98
Benzoic acid	40.95	19.74±2.37	9.43±0.94
p-coumaric acid	42.89	6.73±0.36	5.73±0.45
Ferulic acid	46.57	8.12±0.54	8.06±0.76
Salicylic acid	50.18	11.43±1.9	40.33±5.95
Naringin	55.2	96.48±10.53	96.54±8.64
Rosmarinic acid	57.9	2267.73±137.65	7883.06±165.17
Rutin	59.11	98.75±6.56	33.58±4.86
Cinnamic acid	61.18	42.41±4.76	53.57±5.38
Quercetin	68.15	160.02±9.54	189.65±6.52
Apigenin	76.03	3507.38±109.03	3073.39±89.76
Thymol	76.25	7771.04±197.86	1753.77±93.05

Data are means ± standard deviation (SD) of three replicates. Means followed by the same letter are not significantly different at P≤0.05 according to LSD test. [a]: RT: retention time.

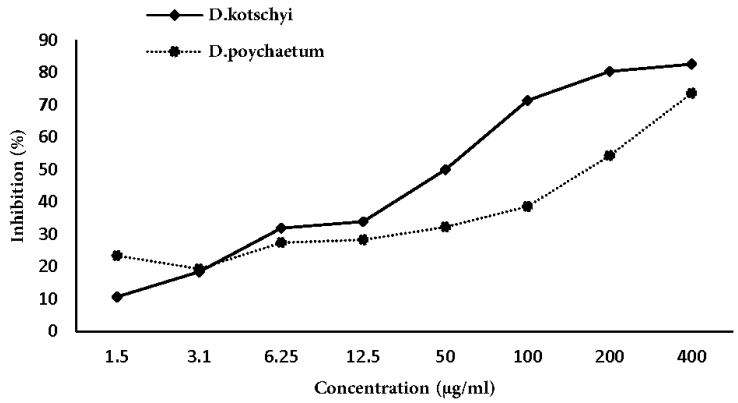

Figure 2. Graph comparing the DPPH's radical scavenging activity of different concentrations of *D. polychaetum* (*D. p*) and *D. kotschyi* (*D. k*) ethanolic extracts.

Table 3. The inhibitory concentration 50% (IC50) (µg.ml^{-1}) of ethanol extract of *D. polychaetum* and *D. kotschyi*in DPPH test.

	D. polychaetum	*D. kotschyi*	BHT
IC50	175±5.3	50±3.7	7.45 ± 1.08

Data are means ± SD of three replicates. Means followed by the same letter are not significantly different at P≤0.05 according to the LSD test.

Acknowledgments
The authors would like to extend their gratitude to the University of Isfahan, Isfahan, Iran.

Conflict of Interest
The authors declare that they have no conflicts of interest.

References

Adams RP. (2007) Identification of Essential Oil Components by Gas Chromatography/mass Spectrometry: Allured Publishing Corporation Carol Stream, IL

Apostolou A., Stagos D., Galitsiou E., Spyrou A., Haroutounian S., Portesis N., et al. (2013). Assessment of polyphenolic content, antioxidant activity, protection against ROS-induced DNA damage and anti-cancer activity of *Vitis vinifera* stem extracts. Food and chemical toxicology 61:60-68.

Burits M. and Bucar F. (2000) Antioxidant activity of *Nigella sativa* essential oil. Phytotherapy research 14:323-328.

Dias M. I., Sousa M. J., Alves R. C. and Ferreira I. C. (2016) Exploring plant tissue culture to improve the production of phenolic compounds: A review. Industrial crops and products 82:9-22.

Dong J., Ma X., Wei Q., Peng S. and Zhang S. (2011) Effects of growing location on the contents of secondary metabolites in the leaves of four selected superior clones of *Eucommia ulmoides.* Industrial Crops and Products 34:1607-1614.

Doosti M. H., Ahmadi K. and Fasihi-Ramandi M. (2018) The effect of ethanolic extract of *Thymus kotschyanus* on cancer cell growth in vitro and depression-like behavior in the mouse. Journal of traditional and complementary medicine 8:89-94.

Faghihinia L., Monajjemi R. and Ranjbar M. (2015) Cytotoxic and antioxidant effects of methanol, hexane, chloroform and aqueous extracts of *Dracocephalum kotschyi* aerial parts on MDAMB-231 cell line. Journal of Biodiversity and Environmental Sciences 6:334-340.

Falcone Ferreyra ML, Rius, S., Casati, P. 2012. Flavonoids: biosynthesis, biological functions, and biotechnological applications. Frontiers in Plant Science, 3:222

Fallah A. and Hosseini Cici S. (2020) Alteration in essential oil yield and compositions of multi-cut *Dracocephalum polychaetum* grown under different fertilization methods. International Journal of Horticultural Science and Technology 7:13-26.

Fallah S., Mouguee S., Rostaei M., Adavi Z. and Lorigooini Z. (2020) Chemical compositions and antioxidant activity of essential oil of wild and cultivated *Dracocephalum kotschyi* grown in different ecosystems: A comparative study. Industrial Crops and Products 143:111885.

Fattahi M., Bonfill M., Fattahi B., Torras-Claveria L., Sefidkon F., Cusido R. M. and Palazon J. (2016) Secondary metabolites profiling of *Dracocephalum kotschyi* Boiss at three phenological stages using uni-and multivariate methods. Journal of Applied Research on Medicinal and Aromatic Plants 3:177-185.

Fattahi M., Nazeri V., Torras-Claveria L., Sefidkon F., Cusido R. M., Zamani Z. and Palazon J. (2013) Identification and quantification of leaf surface flavonoids in wild-growing populations of *Dracocephalum kotschyi* by LC–DAD–ESI-MS. Food chemistry 141:139-146.

Golkar P. and Moattar F. (2019) Essential Oil Composition, Bioactive Compounds, and Antioxidant Activities in *Iberis amara* L. Natural Product Communications DOI: 10.1177/1934578X19846355.

Golkar P., Taghizadeh M. and Jalali S. A. H. (2019) Determination of phenolic compounds, antioxidant and anti-cancer activity of *Chrozophora tinctoria* accessions collected from different regions of Iran. Journal of food biochemistry 43:e13036.

Hara M., Oki K., Hoshino K.and Kuboi T. (2003) Enhancement of anthocyanin biosynthesis by sugar in radish (*Raphanus sativus*) hypocotyl. Plant Science 164:259-265.

Jaakola L. and Hohtola A. (2010) Effect of latitude on flavonoid biosynthesis in plants. Plant, cell & environment 33:1239-1247.

Jahaniani F., Ebrahimi S. A., Rahbar-Roshandel N, and Mahmoudian M. (2005) Xanthomicrol is the main cytotoxic component of *Dracocephalum kotschyii* and a potential anti-cancer agent. Phytochemistry 66:1581-1592.

Kamali M., Khosroyar S., Kamali H., Sani T. A and Mohammadi A. (2016) Phytochemical screening and evaluation of antioxidant activities of *Dracocephalum kotschyi* and determination of its luteolin content. Avicenna journal of phytomedicine 6:425.

Kchaou W., Abbès F., Mansour R. B., Blecker C., Attia H. and Besbes S. (2016) Phenolic profile, antibacterial and cytotoxic properties of second grade date extract from *Tunisian* cultivars (*Phoenix dactylifera* L.). Food chemistry 194:1048-1055.

Khodaei M., Amanzadeh Y., Faramarzi M. A. and Hamedani M. P. (2018) Chemical analysis and anti-bacterial effect of essential oils from three different species of *Dracocephalum* in Iran. American Journal of Essential Oils and Natural Products 6:31-34.

Miliauskas G., Venskutonis P. and Van Beek T. (2004) Screening of radical scavenging activity of some medicinal and aromatic plant extracts. Food chemistry 85:231-237.

Mirzania F. and Farimani M. M. (2018) Biochemical evaluation of antioxidant activity, phenol and flavonoid contents of *Dracocephalum kotschyi* Boiss extracts obtained with different solvents. Avicenna Journal of Phytomedicine 6(4): 425–433.

Penuelas J. and Llusià J. (1997) Effects of carbon dioxide, water supply, and seasonality on terpene content and emission by *Rosmarinus officinalis*. Journal of Chemical Ecology 23:979-993.

Pouraboli I., Nazari S., Sabet N., Sharififar F. and Jafari M. (2016) Antidiabetic, antioxidant, and antilipid peroxidative activities of *Dracocephalum polychaetum* shoot extract in streptozotocin-induced diabetic rats: In vivo and in vitro studies. Pharmaceutical biology 54:272-278.

Sani T. A., Mohammadpour E., Mohammadi A., Memariani T., Yazdi M. V., Rezaee R., et al. (2017) Cytotoxic and apoptogenic properties of *Dracocephalum kotschyi* aerial part different fractions on calu-6 and mehr-80 lung cancer cell lines. Farmacia 65:189-199.

Sharifi B., Goli S. A. H. and Maghsoudlou Y. (2017) Antioxidant activity and chemical composition of the methanolic extract and related fractions of *Dracocephalum kotschyi* leaves using liquid chromatography–tandem mass spectrometry. Industrial crops and products 104:111-119.

Sobral M. V., Xavier A. L., Lima T. C., de Sousa D. P. (2014) Antitumor activity of monoterpenes found in essential oils. The Scientific World Journal doi.org/10.1155/2014/953451.

Zhang Y., Hu M., Liu L., Cheng X-L., Cai J., Zhou J., Wang T. (2018) Anti-cancer effects of Rosmarinic acid in OVCAR-3 ovarian cancer cells are mediated via induction of apoptosis, suppression of cell migration and modulation of lncRNA MALAT-1 expression. J BUON 23:763-768.

Supplementary File:

Table S1. The GC-MS analysis indicating constituents of essential oils of *D. kotschyi* and *D. polychaetum*

Compound name [a]	**RT**	**RI**	***D. k* %** [b]	***D. p* %** [b]
α-Pinene	9.026	939	1.25	2.57
3-p-Menthene	10.148	978	0.04	-
2,3-Dehydro-1,8-cineole	10.63	995	-	0.04
Ocimene	11.04	1009	-	0.04
Terpinolene	11.407	1021	0.03	0.04
o-Cymene	11.643	1029	0.35	-
D-Limonene	11.815	1035	16.45	13.13
3-Carene	12.639	1062	0.09	0.07
cis-β-Terpineol	12.883	1070	-	0.012
cis-Linalool Oxide	13.019	1075	0.06	0.017
Linalool	13.779	1101	0.71	0.56
trans-p-Mentha-2,8-dienol	14.422	1123	0.45	0.23
±-4-Acetyl-1-methylcyclohexene	14.721	1133	0.17	0.15
cis-p-Mentha-2,8-dien-1-ol,	14.83	1137	0.46	0.26
L-Pinocarveol	14.993	1143	0.18	-
cis-Verbenol	15.138	1148	0.24	-
Ethanone, 1-(2-methylphenyl)-,	16.279	1187	0.67	-
Menthofuran	16.396	1191	1.47	0.82
Terpineol	16.487	1194	0.86	0.67
(-)-Myrtenol,	16.65	1200	0.81	-
Perillyl aldehyde	16.976	1211	27.9	56.7
Trans-Carveole	17.546	1232	1.28	-
2,6-Octadienal, 3,7-dimethyl-, (Z)-	17.809	1241	1.14	
l-carvone	17.936	1246	2.4	
cis-Geraniol	18.126	1253	1.51	
P-Menth-1-en-9-al	19.013	1285	1.5	0.4
6-Propenylbicyclo [3.1.0]hexan-2-one	19.04	1286	-	2.63
p-Mentha-1(7),8(10)-dien-9-ol	19.203	1292	11.3	10.9
3-Cyclohexene-1-ethanol, β,4-dimethyl	19.375	1298	3.43	-
Terpineol acetate	20.688	1349	0.41	-
Eugenol	20.888	1357	1.6	0.1
Copaene	21.476	1380	-	0.23
1,5,5-Trimethyl-6-methylene-cyclohexene	22.047	1402	-	0.22
Perillyl acetate	22.228	1409	0.84	2.96
Caryophyllene	22.599	1424	0.17	-
β-Ionene	24.102	1486	-	0.1
δ-Cadinene	25.026	1525	0.54	-
α-Calacorene	25.488	1545	0.03	0.03
3-Hexen-1-ol, benzoate, (Z)-	26.049	1569	0.28	-
2,4,4,6-Tetramethyl-6-phenyl-1-heptene	26.221	1576	0.03	-
Caryophyllene oxide	26.484	1587	0.89	-
Carotol	26.782	1600	0.38	-
Calarene epoxide	27.063	1613	0.23	-
Lanceol, cis	27.425	1629	-	0.49
Cyclohexene-1-acetaldehyde, α,4-dimethyl	27.778	1645	0.86	
2-Pentadecanone, 6,10,14-trimethyl	31.781	1835	0.35	
Androstan-17-one, 3-ethyl-3-hydroxy-,(5α)-	41.352	2369	-	3.1
Heptacosane	45.97	2654	0.14	-
Nonacosane	48.686	2822	0.24	-

[a] Compounds are listed in order of their retention index from a HP-5 column. RT: Retention Time, RI: Retention Index.
[b] Relative proportions of the EO components expressed as percentages obtained by GC-MS responses.

Research Article

Effect of Intramuscular and Intraperitoneal Injections of conjugated MSTN-siRNA-cholesterol on Inhibition of Myostatin Gene expression

Mitra Riasi [1], Sina Mozaffari Jovin [2,3], Ali Javadmanesh [1,4 *]

[1] *Department of Animal Science, Faculty of Agriculture, Ferdowsi University of Mashhad, Mashhad, Iran*
[2] *Department of Medical Genetics, School of Medicine, Mashhad University of Medical Sciences, Mashhad, Iran*
[3] *Medical Genetics Research Center, Mashhad University of Medical Sciences, Mashhad, Iran*
[4] *Stem Cell Biology and Regenerative Medicine Research Group, Research Institute of Biotechnology, Ferdowsi University of Mashhad, Mashhad, Iran*

Received 20 July 2022 Accepted 18 September 2022

Abstract

Myostatin (MSTN) is primarily expressed in skeletal muscle tissue and acts as a negative regulator of skeletal muscle growth by inhibiting differentiation and proliferation of myoblasts. Inhibition of MSTN expression could result in muscular hypertrophy. An effective therapeutic approach based on specific silencing of a target gene is provided by RNA interference. The distribution of biologically active small interfering RNAs (siRNAs) inside the target cells/ tissue, is a significant problem due to the limited stability and delivery of siRNAs. Strategies depending on vector delivery have also a limited clinical utility due to safety concerns. Thus direct application of active siRNAs *in vivo* is the preferred strategy. We described the efficiency of intramuscular and intraperitoneal injections of MSTN-siRNA conjugated with cholesterol into the skeletal muscle of mice. The designed siRNA molecule was complementary to the exon II of the mouse MSTN gene. Mice were injected with a weekly dose of 10 µg/kg conjucated siRNA-cholestrol intraperitoneally or intramuscularly. Our findings suggested that within a few weeks of application, siRNA-treated mice showed a significant increase in muscle mass and suppressed MSTN gene expression. Even though both types of injections increased muscle weight, intramuscular siRNA injections suppressed the MSTN gene more effectively, whereas intraperitoneal RNA injections had a more significant impact on total body weight. The cholesterol-conjugated siRNA platform discussed here may hold promise for treating several skeletal muscle-related diseases, such as atrophic muscle disease, muscular dystrophy, and type II diabetes.

***Keywords*:** Cholesterol conjunction; Gene silencing; RNA interference; Transcription regulation

Introduction

Myostatin (MSTN; formerly known as GDF-8) was discovered in a search for novel mammalian members of the TGF- β (transforming growth factor- β) group of growth and differentiation proteins (McPherron et al., 1997). It is mainly expressed in skeletal muscle and functions as a negative regulator of skeletal muscle growth by inhibiting myoblast differentiation and proliferation (Soleimani, 2019). Because of a combination of muscle fiber hypertrophy and hyperplasia , mice with knockout MSTN gene had nearly a doubling of skeletal muscle mass across the body (McPherron and Lee, 1997). Natural MSTN gene mutations have also been found in cattle (Grobet et al., 1997), dogs (Mosher et al., 2007), sheep (Clop et al., 2006), pigs (Ji et al., 1998) and humans (Schuelke et al., 2004).

RNA interference (RNAi) has already become a standard approach for gene targeting. It is becoming increasingly important for therapeutic knockdown of pathologically important genes due to its considerable effectiveness and specificity. RNA-based gene silencing techniques can be used for various purposes, from validating targets to therapeutic implementations. It offers a viable option to pharmacological drugs, which are frequently associated with toxicity and off-target effects, as well as access to genes that were previously thought to be difficult to target or "undruggable" by pharmacologists. Since the discovery in 2001 showing that small interfering RNAs (siRNA) can be utilized for specific gene downregulation in mammalian cells (Elbashir et al., 2001), numerous researchers have effectively used this technology to knock down genes *in vivo* and *in vitro* (Martin and

* Corresponding author's e-mail address: *javadmanesh@um.ac.ir*

Caplen, 2007. Scherr and Eder, 2007). In cell lines and animal models, siRNAs are considered as practical tools for gene silencing. siRNAs are double-stranded RNAs with a length of 21–23 nucleotides that cause RNA-induced silencing complex (RISC) recruitment, cleavage, and breakdown of target mRNA molecules when they engage with a RISC (Bakhtiyari et al., 2013). Because RNAi works by limiting the expression of a specific target gene, it could be a safer approach for treating a wide range of hereditary and clinical illnesses. RNA interference (RNAi) allows researchers to investigate the consequences of shutting down a gene under controlled settings. Similarly, biologists were inspired to develop plasmids expressing short hairpins to target genes because of the function and structure of miRNAs, which are naturally expressed in form of short hairpins and processed into inhibitory molecules (Zeng et al., 2002. McManus, et al., 2002). Many genes have been effectively targeted using this strategy, including those in skeletal muscle cell lines and muscle tissue (Magee et al., 2006; Payande et al., 2019. Riasi et al., 2022).

On the other hand, recent developments in chemical modification of oligonucleotides led to invention of oligos with improved nuclease resistance, pharmacokinetics, gene specificity, and reduced immunostimulatory effects (Lares et al., 2010). Despite of significant advances and a few studies demonstrating systemic and targeted siRNA delivered *in vivo*, siRNA transport to the most tissues remains a crucial hurdle. Systemic delivery of siRNA has been used for liver, tumor, spleen, and jejunum (Kawakami et al., 2011. Kinouchi et al., 2008). A crucial requirement for successful delivery of systemic RNAi *in vivo* is the introduction of "drug-like" charachteristics, such as longer half-life, tissue bioavailability and cellular delivery, into chemically synthesized siRNAs. In inspecting the potential of synthetic siRNAs to silence desired genes, chemically modified siRNAs, including cholesterol conjugated, 2'-O-methyl sugar modified and antibody-linked siRNAs, have been found to improve pharmacological properties *in vitro* and *in vivo* markedly (Morrissey et al., 2005. Song et al., 2005). Covalent conjugation of cholesterol to siRNA improves the resistant activity of free siRNA to nucleases and facilitates cellular import, which results in the efficient silencing of target genes *in vivo* (Lorenz et al., 2004. Soutschek et al., 2004).

In the current study, we tried to investigate the effect of the type of injection (intraperitoneal or intramuscular) of siRNA on the inhibitory function of MSTN gene expression in a mouse model.

Materials and Methods

Design of siRNA molecule

The mouse MSTN gene sequence with accession number NC-000067.6 was achieved from NCBI database (National Center for Biotechnology Information). The siRNA was designed using the E-RNAi program. The non-specific target was made sure of using the siRNA-Blast online program. Microsynth conjugated RNA with cholesterol in three heads to improve its stability against the endonuclease enzyme (Syntech Co., Switzerland). Myostatin gene expression inhibition was monitored and measured using a negative control (siRNA negative; Sigma, Germany) . This negative control does not complement any part of the mouse genome (Table 1).

Experiment design and tissue preparation

Twenty-four male BALB/c mice were divide into two experimental and two control groups. Animals in this experiment conformed to all relevant animal testing and ethical research requirements. Experiments were carried out with the ethical approval of Ferdowsi University of Mashhad (Approval number 3/52696). The temperature was 22±1°C, with a 12-hour light-dark cycle and free access to water and food (Roozbeh et al., 2019). The experimental group 1 (n=6) received a weekly dose of RNAi of 10 µg/kg intraperitoneally. The same dose of RNAi was administered intramuscularly to the experimental group 2 (n=6). The scramble-RNAi was given intraperitoneally and intramuscularly to the control groups (n=12). Finally, the animals were quickly killed by exposing them to an increasing CO_2 concentration. Then muscles of the right biceps were removed. The tissue was sliced, and the upper half was immediately frozen in RNA shield (Dena Zist Asia, Iran) for RNA extraction, while the lower half was fixed in 10% formaldehyde for histological investigation. Until RNA extraction, all samples were stored at -80 °C. After the tissue was fixed in paraformaldehyde 10%, the biceps muscle was embedded in paraffin. On sections (7mm) cut and mounted on silanized glass slides, hematoxylin and eosin (H&E) staining was utilized (McKinnell et al., 2008). MyoVision software was used to count the cells (Wen et al., 2018).

Table 1. siRNA sequences selected to inhibit MSTN gene

	Sequence	Strand
SiRNA	5' UCAACAGUGUUUGUGCAAAUATT 3'	Sense
SiRNA	5' AAUAUUUGCACAAACACUGUUGA 3'	Antisense

RNA extraction and quantitative PCR

In 2 ml screw-cap tubes containing ten glass beads (3mm), 20-40 mg of biceps tissue was added. The Bioprep-24 Homogenizer homogenized the samples at 3500 g for two 15-second cycles with a 15-second pause period (Allsheng, China). Then, according to the manufacturer's recommendations, total RNA extraction and cDNA synthesis were carried out with the total RNA extraction kit and Easy cDNA synthesis kit (ParsTous, Iran) utilizing oligo d(t) and random hexamers. DNase I (Thermo Fisher Scientific, Austin, TX, USA) was used to treat RNA samples before cDNA synthesis, as directed by the manufacturer. The MIQE (Minimum information for publication of qPCR experiments) guidelines were followed for all qPCR reaction settings (Bustin et al., 2009). In a BioRad CFX96 TouchTM real-time PCR instrument, 2 µl of cDNA, 10 µl of 2X SYBR Green PCR Master Mix (Ampliqon, Odense, Denmark), and 5 pM of each primer were mixed in 0.1-ml 8-strip tubes (Gunster Biotech, Viluppuram, Taiwan) in a final volume of 20 µl. (Bio-Rad Laboratories Inc., Singapore). The experiment performs under the following condition: an initial denaturation step (95°C for 3min); 45 cycles of amplification, including (95°C for 30s, 58°C for 25s, and 72°C for 20s). The specificity of amplicons was validated using melting curve analysis (60 to 95 °C). The slope of the standard curve was used to compute the reaction efficiency (efficiency = (10 (1/slope) – 1) 100). The R^2 correlation coefficients were used to make the decision. The geometric average of the GAPDH and B-actin reference genes was used to normalize the relative replication of MSTN transcript (Ruan and Lai, 2007. Ghanipour-Samami et al., 2018. Danesh Mesgaran et al., 2021). Primer sequences are shown in Table 2.

Statistical analyses

Student's t-test (SAS,v 9.4, SAS Institute Inc., Cary, USA) was used to evaluate the statistical significance of the data, and *P*-values less than 0.05 were considered statistically significant. All data were presented as mean ± standard error (SE).

Results

Relative leg weights

The results of body weight measurement in the fourth week before killing the mice in group 1 showed a 10% difference between the treatment and control groups. In contrast, intramuscular injection (group 2) had no significant effect on increasing body weight. The efficiency of the MSTN-siRNA/cholesterol conjugation molecule and its impact on increasing muscle growth was therefore assessed using the muscle weight/body index (Figure 1).

Histological analysis

Histology images were prepared as previously described. The results of myonuclear counting showed that there was a significant difference at 95% and 99% between groups which received RNAi interaperitoneally and interamuscularly in comparsion to the control group, respectively (Table 3) (Figure 2). The results demonstrated that intramuscular injection of the conjugated MSTN-siRNA/cholestrol induced muscle enlargement by suppressing the MTSN gene expression.

Table 2. Primers used in the quantitative RT-PCR experiments

Gene name	Sequence	Amplicon length (bp)	Accession number
MSTN	F:5' TCCAGAGGGATGACAGCAGT 3' R: 5' GGGCTTTTACTACTTTGTTGTACTGT 3'	177	NM_010834
GAPDH	F: 5' GAGAAACCTGCCAAGTATGATG 3' R:5' CATACCAGGAAATGAGCTTGACA 3'	196	NM_001289726
B-actin	F: 5'CTCTGGCTCCTAGCACCATGAAGA3' R: 5' GTAAAACGCAGCTCAGTAACAGTCC 3'	200	NM_028135

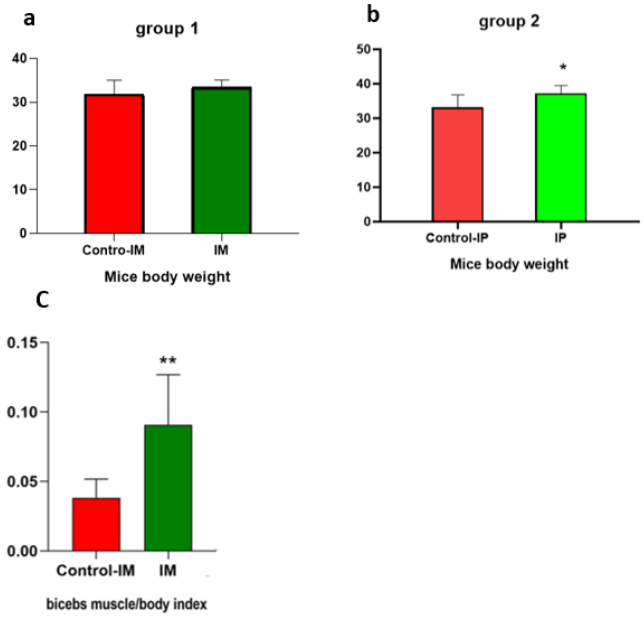

Figure 1. Intramuscular and intraperitoneal administration of the MSTN-siRNA/cholesterol conjugation induces muscle enlargement in the mouse by blocking of MSTN gene expression. After three weeks, the body weight of mice in each group was measured and compared to the control. (a) Body weight change after intramuscular injection, (b) body weight change after intraperitoneal injection, (c) comparison of muscle weight/body weight index between the MSTN-siRNA/cholesterol conjugation and control mice (group 2 0.094±0.038 versus 0.041±0.024g). Graphical representation of data uses the following convention: mean±s.d.; treated muscles in green; control muscles in red.

Figure 2. Muscle fiber density in biceps (a) control (b) right biceps muscles injected with MSTN-siRNA/cholesterol conjugation interaperitoneally (c) right biceps muscles injected with MSTN-siRNA/cholesterol conjugation intramuscularly. Serial sections (7 mm thickness) were cut and stained. (Scale bar, 100 µm)

Table 3. Results of cell counting in biceps muscle tissue of control and treated legs.

Group	mean	*P*-value
RNAi- IP	261	0.0296*
Control- IP	117	
RNAi- IM	360	0.010**
Control- IM	123	

Gene expression

The qPCR reaction results were confirmed by melt curve analysis and agarose gel electrophoresis (Supplementary Figures 1 and 2). The qPCR showed a 66% and 90% decrease in MSTN expression in muscle tissue treated with Mstn-siRNA/cholesterol conjugation interaperitoneally and interamuscular compared to the control (Figure 3). We observed a significant difference in MSTN gene expression when MSTN-siRNA was injected interamuscularlly in mice.

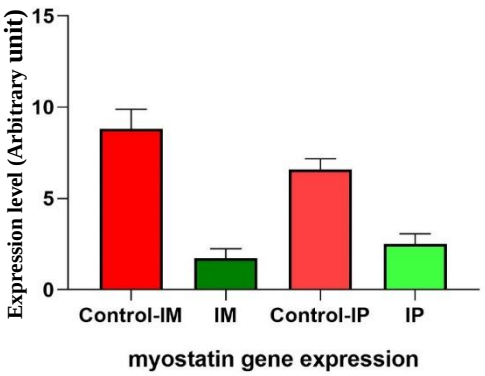

Figure 3. MSTN gene expression: MSTN mRNA expression in groups treated by MSTN-siRNA/cholesterol conjugation interaperitoneally, MSTN-siRNA/cholesterol conjugation intramuscularly and the control. MSTN expression was normalized using the geometric averages of GAPDH and b-actin. **p < 0.01

Discussion

A promising tool for the suppressing of particular disease pathways is the gene-silencing methodology based on RNAi. Due to the possibility of more excellent selectivity and decreased toxicity and side effects, it has the potential to be more effective than conventional pharmacological medications. Skeletal muscles are essential for morphofunctional function, and their atrophy results in severe illnesses like muscular dystrophy. One in every 3500 male births is affected by Duchenne muscular dystrophy (DMD), a severe condition that causes muscle atrophy (Laws et al., 2008). Although there is no treatment at the moment, gene therapy techniques are promising new directions for the creation of medications(Foster et al., 2006). Anti-myostatin-blocking antibodies are one of the therapeutic strategies used to improve muscle mass. These antibodies suppress MSTN (Bogdanovich et al., 2002). However, it requires a considerable amount of time and effort to produce antibodies against recombinant target proteins. MSTN suppression caused by overexpression of the MSTN prodomain12 in mice used as models for limb-girdle muscular dystrophy 1C was demonstrated to minimize muscle atrophy and correct intracellular MSTN signaling (Ohsawa et al., 2006). On the other hand, Magee et al. showed that increasing local skeletal muscle mass by electroporating a plasmid carrying a short-hairpin interfering RNA (shRNA) against MSTN could downregulate MSTN production (Magee et al., 2006). However, techniques based on vector administration may only have limited therapeutic utility due to safety concerns. Applying active siRNAs *in vivo* directly is the preferred strategy. We looked for a more suitable application with higher cholesterol-conjugated siRNAs effectiveness as one of the feasible platforms delivery of siRNA. Other *in vivo* investigations have used cholesterol-conjugated siRNAs to show uptake into the heart, kidney, adipose, liver, small intestine, and lung. Few published studies on the distribution of chol-siRNA to the muscle by systemic dose exist (Soutschek et al., 2004; Wolfrum et al., 2007; Soutschek et al., 2004). Therefore, in the current research, we evaluated local and systematic injections to determine whether the method of administration of DNAi could affect the efficiency of MSTN inhibition.

We made use of the siRNA sequences that were mentioned in previous research by Payande. (Payande, 2019) at Ferdowsi University in Mashhad. They transfected it into C2C12 cell line (a mouse myoblast cell line) that had been induced to express MSTN to demonstrate in that work that the present MSTN-siRNA/cholesterol conjugation could effectively downregulate the MSTN expression. The findings of this study demonstrated the remarkable efficacy of siRNA sequences in reducing gene expression while having no detrimental changes in cell morphology. Then we injected MSTN-siRNA/cholesterol conjugation in mice, as mentioned earlier.

Our weight findings validated the decrease in the muscles treated with MSTN cholesterol-conjugated siRNAs (Figure 1). The muscles in the treated legs are noticeably larger than the controls, although the body weights for the group 1 and its control were 37.20±0.7 and 33.19±0.4 g and for group 2 and its control were 33.45±0.2 and 31.85±0.5, respectively. Khan et al. conducted a study on the systemic administration of cholesterol-conjugated siRNA targeting the muscle-specific MSTN gene. They measured the expression of MSTN in several mouse muscles (Khan et al., 2016). Their findings indicate that MSTN cholesterol-conjugated siRNAs raise body weight by 10% while also increasing leg muscle size by up to 20%. When they measured the shape of the cell, they saw hypertrophy rather than hyperplasia. These confirmed all the results obtained in our research at the time of MSTN-siRNA/cholesterol conjugation intraperitoneal injection. On the other hand, no increase in body weight was seen in the treated mice in group 2, most likely, since the gain in muscle weight offset the reduction in fat formation (McPherron and Lee,

2002). When the body weight varied, we considered the muscle weight/body weight ratio to demonstrate a gain in muscle, similar to a research performed by Kinouch et al. (Kinouchi, et al., 2008). They administered the Mst-siRNA/ATCOL complex intramuscularly to 20-week-old male mdx mice, into the tibial and masseter muscles on the left side. An enormous increase in muscle mass was seen two weeks following the single injection. Morphometric measurements show both hypertrophy and hyperplasia in muscle. These findings from our investigation, comparable to those from the previous study, demonstrated the value of intramuscular injections for promoting muscle growth.

In our model, fiber size analysis and H&E staining of histological preparations reveal both hyperplasia and hypertrophy in the treatment group compared to the control group. Even though, MSTN knockout mice exhibit both muscle hypertrophy and hyperplasia, the differences between our model and the MSTN-knockout model were most likely caused by the nearly complete absence of MSTN throughout the entire development of MSTN knockout mice as opposed to "acute" MSTN inhibition in adult animals for siRNA targeting (Lee and McPherron, 2001). Our findings from siRNA injections into the intramuscular space are in line with several gene knockdown and MSTN inhibition or studies, which also demonstrate only increased muscle growth (Whittemore et al., 2003).

Gene expression data in our study showed that intramuscular injection of RNA into the target tissue was able to silence the gene with a better performance of about 80%. In comparison, intraperitoneal injection inhibited the expression with 60% efficiency. Our gene expression result of interamuscular injection of siRNA was in line with the Khan study. They observe 80-90% MSTN suppression in soleus muscle. It was possible that we would get more similar results if we used different muscle tissues in our study. Alternatively, if we used higher doses of siRNA, the rate of inhibition of gene expression in systemic injection would be higher. In Khan's study, it was noted that using higher doses of siRNA was more effective in inhibiting gene expression. On the other hand, in Kinouchi experiment, systematic delivery of siRNA knockdown MSTN gene by 25% during three weeks. Since the MSTN chol-siRNA used in the current investigation was a simple conjugate that could be injected intramuscularly and interaperitoneally, there is no need for a technically challenging delivery mechanism or complex formulations. The cholesterol conjugate can deliver to skeletal muscles and silence genes there as well. In mice, it demonstrates long-lasting silencing after a single dosage. The cholesterol-siRNA conjugates used in our study were a helpful tool for *in vivo* target validation studies. They may one day be therapeutically effective for treating some of skeletal muscle disorders.

Conclusion

Finally, the results of the current study demonsterated that the use of cholesterol-conjugated siRNA could effectively suppress the MSTN gene in mice within three weeks. However, both types of intramuscular and peritoneal injection led to an increase in skeletal muscle weight and significant inhibition of gene expression. However, it appears that future studies with greater injection doses and more frequent injections are required in order to precisely recommend one of the two methods of intramuscular and peritoneal injection.

Acknowledgments

This study was supported by the Ferdowsi University of Mashhad, grant number: 3/52696. The authors would like to thank the Kavosh Gene Sarvdasht company (Mashhad, Iran) for the technical assistance.

Conflict of Interest

The authors declare that there is no conflict of interest.

References

Bakhtiyari S., Haghani G., Basati G. and Karimfar M. H. (2013) siRNA therapeutics in the treatment of diseases. Therapeutic Delivery 4:1, 45-57.

Bogdanovich S., Krag T. O., Barton E. R., Morris L. D., Whittemore L. A., Ahima, R. S., et al. (2002) Functional improvement of dystrophic muscle by myostatin blockade. Nature 420:6914, 418-421.

Bustin S. A., Benes V., Garson J.A., Hellemans J., Huggett J., Kubista M., et al. (2009) The MIQE Guidelines: M inimum I nformation for Publication of Q uantitative Real-Time PCR E xperiments, Oxford University Press.

Clop A., Marcq F., Takeda H., Pirottin D., Tordoir X., Bibé B. and Georges M. (2006) A mutation creating a potential illegitimate microRNA target site in the myostatin gene affects muscularity in sheep. Nature Genetics 38:7, 813-818.

Danesh Mesgaran M., Kargar H., Mesgaran S. D. and Javadmanesh A. (2021) Peripartal rumen-protected L-carnitine manipulates the productive and blood metabolic responses in high producing Holstein dairy cows. Frontiers in Veterinary Science :1514.

Elbashir S. M., Lendeckel W. and Tuschl T. (2001) RNA interference is mediated by 21-and 22-nucleotide RNAs. Genes Development 15:2, 188-200.

Foster K., Foster H. and Dickson J. G. (2006) Gene therapy progress and prospects: Duchenne muscular dystrophy. Gene Therapy 13:24, 1677-1685.

Grobet L., Royo Martin L. J., Poncelet D., Pirottin D., Brouwers B., Riquet J., et al. (1997) A deletion in the bovine myostatin gene causes the double–muscled phenotype in cattle. Nature Genetics 17:1, 71-74.

Ji S., Losinski R. L., Cornelius S. G., Frank G. R., Willis G. M., Gerrard D. E., et al. (1998) Myostatin expression in porcine tissues: tissue specificity and developmental and postnatal regulation. American Journal of Physiology-Regulatory, Integrative Comparative Physiology 275:4, 65-73.

Kawakami E., Kawai N., Kinouchi N., Mori H., Ohsawa Y., Ishimaru N., et al. (2013) Local applications of myostatin-siRNA with atelocollagen increase skeletal muscle mass and recovery of muscle function. PLoS One 8:5, e64719.

Khan T., Weber H., DiMuzio J., Matter A., Dogdas B., Shah T., et al. (2016) Silencing myostatin using cholesterol-conjugated siRNAs induces muscle growth. Molecular Therapy-Nucleic Acids 5, e342.

Kinouchi N., Ohsawa Y., Ishimaru N., Ohuchi H., Sunada Y., Hayashi Y., et al. (2008) Atelocollagen-mediated local and systemic applications of myostatin-targeting siRNA increase skeletal muscle mass. Gene Therapy 15:15, 1126-1130.

Lares M. R., Rossi J. J. and Ouellet D. L. (2010) RNAi and small interfering RNAs in human disease therapeutic applications. Trends in Biotechnology 28:11, 570-579.

Laws N., Cornford-Nairn R. A., Irwin N., Johnsen R., Fletcher S., Wilton S. D., et al. (2008) Long-term administration of antisense oligonucleotides into the paraspinal muscles of mdx mice reduces kyphosis. Journal of Applied Physiology 105:2, 662-668.

Lee S. J. and McPherron A. C. (2001) Regulation of myostatin activity and muscle growth. Proceedings of the National Academy of Sciences 98:16, 9306-9311.

Lee Y., Jeon K., Lee J.T., Kim S. and Kim V. N. (2002) MicroRNA maturation: stepwise processing and subcellular localization. The EMBO Journal 21:17, 4663-4670.

Lorenz C., Hadwiger P., John M., Vornlocher H. P. and Unverzagt C. (2004) Steroid and lipid conjugates of siRNAs to enhance cellular uptake and gene silencing in liver cells. Bioorganic Medicinal Chemistry Letters 14:19, 4975-4977.

Magee T. R., Artaza J. N., Ferrini M. G., Vernet D., Zuniga F. I., Cantini L., et al. (2006) Myostatin short interfering hairpin RNA gene transfer increases skeletal muscle mass. The Journal of Gene Medicine: A cross-disciplinary journal for research on the science of gene transfer its clinical applications 8:9, 1171-1181.

Martin S. E. and Caplen N. J. (2007) Applications of RNA interference in mammalian systems. Annual Review of Genomics and Human Genetics 8:81-108.

McManus M. T., Petersen C. P., Haines B. B., Chen J. and Sharp P. A. (2002) Gene silencing using micro-RNA designed hairpins. Gene silencing using micro-RNA designed hairpins. RNA 8:6, 842-850.

McPherron A. C., Lawler A. M. and Lee S. J. (1997) Regulation of skeletal muscle mass in mice by a new TGF-p superfamily member. Nature 387:6628, 83-90.

McPherron A. C. and Lee S. J. (1997) Double muscling in cattle due to mutations in the myostatin gene. Proceedings of the National Academy of Sciences 94:23, 12457-12461.

McPherron A. C. and Lee S. J. (2002) Suppression of body fat accumulation in myostatin-deficient mice. The Journal of Clinical Investigation 109:5, 595-601.

Morrissey D. V., Lockridge J. A., Shaw L., Blanchard K., Jensen K., Breen W., et al. (2005) Potent and persistent in vivo anti-HBV activity of chemically modified siRNAs. Nature Biotechnology 23:8, 1002-1007.

Mosher D. S., Quignon P., Bustamante C. D., Sutter N. B., Mellersh C. S., Parker H. G. and Ostrander, E. A. (2007) A mutation in the myostatin gene increases muscle mass and enhances racing performance in heterozygote dogs. PLoS Genetics 3:5, e79.

Ohsawa Y., Hagiwara H., Nakatani M., Yasue A.,

Moriyama K., Murakami T. and Sunada Y. (2006) Muscular atrophy of caveolin-3–deficient mice is rescued by myostatin inhibition. The Journal of Clinical Investigation 116:11, 2924-2934.

Parise G., McKinnell I. W. and Rudnicki M. A. (2008) Muscle satellite cell and atypical myogenic progenitor response following exercise. Muscle Nerve: Official Journal of the American Association of Electrodiagnostic Medicine 37:5, 611-619.

Payande H. (2019) Inhibition of myostatin gene expression in C2C12 cells by RNAi and DNAi methods. Master of Science Thesis. Ferdowsi University of Mashhad.

Payande H., Ghahremani S. M. and Javadmanesh A. (2019) The inhibitory effect of myostatin-specific siRNA on the differentiation and growth of C2C12 cells. The Proceedings of the 3rd International and the 11th National Biotechnology Congress of Islamic Republic of Iran. 1-3 September, Tehran, Iran.

Riasi M., Javadmanesh A. and Mozaffari-Jovin S. (2022) Inhibition of myostatin gene expression using siRNA in mice. The Proceedings of the 22nd National and 10th International Congress on Biology. 31 Aug-2 Sep, Sharekord, Iran.

Roozbeh, B., Moazami, M., Rashidlamir, A., Moosavi, Z., Javadmanesh, A. (2019). The Effect of resistance training and growth hormone injection on circulating IGF-1 and IGFBP-3 levels in a rat model. Iranian Journal of Veterinary Science and Technology 11(1): 13-18.

Ruan W. and Lai M. (2007) Actin, a reliable marker of internal control? Clinica Chimica Acta 385:1-2, 1-5.

Scherr M. and Eder M. (2007). Gene silencing by small regulatory RNAs in mammalian cells. Cell cycle 6:4, 444-449.

Schuelke M., Wagner K. R., Stolz L. E., Hübner C., Riebel T., Kömen W., et al. (2004) Myostatin mutation associated with gross muscle hypertrophy in a child. New England Journal of Medicine 350:26, 2682-2688.

Soleimani S., Sekhavati M. H. and Javadmanesh A. (2019) Sequencing and Bioinformatic Investigation of Introducing a Repressive Micro-RNA Target Sites in the 3'UTR of Myostatin Gene in some Indigenous Sheep Breeds of Iran. Iranian Journal of animal science research 11: 111-119.

Song E., Zhu P., Lee S. K., Chowdhury D., Kussman S., Dykxhoorn D. M., et al. (2005) Antibody mediated in vivo delivery of small interfering RNAs via cell-surface receptors. Nature Biotechnology 23:6, 709-717.

Soutschek J., Akinc A., Bramlage B., Charisse K., Constien R., Donoghue M., et al. (2004) Therapeutic silencing of an endogenous gene by systemic administration of modified siRNAs. Nature 432:7014, 173-178.

Wen Y., Murach K. A., Vechetti Jr I. J., Fry C. S., Vickery C., Peterson C. A., et al. (2018) MyoVision: software for automated high-content analysis of skeletal muscle immunohistochemistry. Journal of Applied Physiology 124:1, 40-51.

Whittemore L. A., Song K., Li X., Aghajanian J., Davies M., Girgenrath S., et al. (2003) Inhibition of myostatin in adult mice increases skeletal muscle mass and strength. Biochemical Biophysical Research Communications 300:4, 965-971.

Wolfrum C., Shi S., Jayaprakash K. N., Jayaraman M., Wang G., Pandey R. K., et al. (2007) Mechanisms and optimization of in vivo delivery of lipophilic siRNAs. Nature Biotechnology 25:10, 1149-1157.

Zeng Y., Wagner E. J. and Cullen B. R. (2002) Both natural and designed micro RNAs can inhibit the expression of cognate mRNAs when expressed in human cells. Molecular Cell 9:6, 1327-1333.

Supplementary Files:

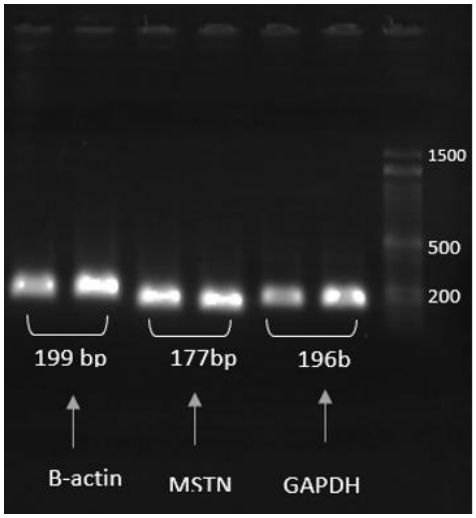

Figure S1. Agarose electrophoresis of qPCR products from GAPDH, MSTN and B-actin genes.

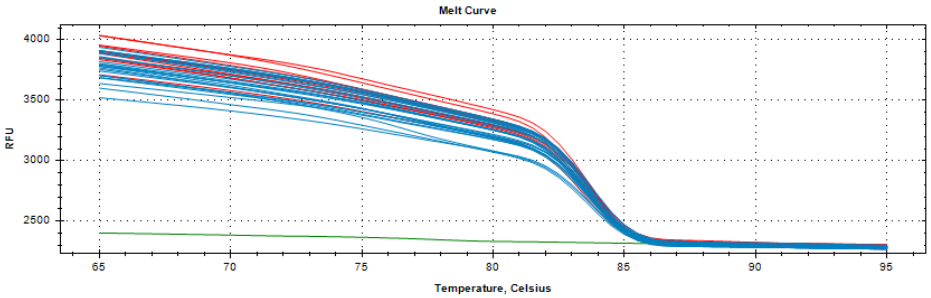

Figure S2. Melt curve analysis of mouse MSTN transcript (standard: red lines, samples: blue lines and negative control: green)

Research Article

Conversion of Membrane Lipids to Jasmonates as a Key Pathway to Develop Somatic Embryos in *Arabidopsis thaliana*

Azadeh Khadem, Nasrin Moshtaghi*, Abdolreza Bagheri

[1] Department of Biotechnology and Plant Breeding, Faculty of Agriculture, Ferdowsi University of Mashhad, Mashhad, Iran

Received 24 August 2022 Accepted 29 September 2022

Abstract

Somatic embryogenesis encompasses the same set of various developmental processes similar to zygotic embryogenesis. The conversion of somatic cells to embryos also requires stages of differentiation and reprogramming of cells. Since somatic embryogenesis is a complex process, a comprehensive investigation is required to identify the effective gene networks and their interactions with environmental factors. As part of this study, bioinformatics tools and molecular studies were used to gain a better understanding of *Arabidopsis thaliana* somatic embryogenesis. The enriched pathways of somatic embryogenesis and their core-enriched genes were identified using gene set enrichment analysis. The results indicated that significant interaction between hormones helps to induce and develop somatic embryos. The gene ontology (including biological process, molecular function and cellular compartment) of core-enriched genes revealed that lipid storage and metabolism as well as stress response are the active biological pathways during somatic embryogenesis. In the protein-protein interaction network, TIR1/AFBs as auxin receptors exhibited the greatest number of interactions and proteins involved in lipid storage and metabolism acted as mediators between auxin receptors and ethylene perception. Also, Kyoto encyclopedia of genes and genomes analysis indicated that the metabolism of membrane lipids during somatic embryogenesis of *Arabidopsis* is primarily related to the biosynthesis of jasmonates and their derivatives. This process is initiated by Lypooxygenase proteins in the chloroplast, while Acyl-CoA oxidase 1 (ACX1) and Oxophytodienoate reductase 3 (OPR3) proceed this process in the peroxisome. The qRT-PCR analysis also confirmed the role of these genes during somatic embryogenesis, as the activity of these genes decreased at the beginning of 2,4-D treatment, but it increased during somatic embryogenesis. According to these results, jasmonates play an important role during somatic embryogenesis by mediating auxin signaling and stress response.

***Keywords*:** Bioinformatics, Hormone perception, Somatic embryo, Stress-related pathways

Introduction

During embryo formation, plant cells undergo a complex process for determining the cell fate and development (Lau et al., 2012). In order to germinate an embryo and grow as a seedling, all of the stages must be progressed precisely (de Vries & Weijers, 2017; Miransari & Smith, 2014). Plant cells also have totipotency features enabling the formation of embryos from a single somatic cell (Radoeva & Weijers, 2014). The somatic embryos have a similar structure to zygotic embryos (Loyola-Vargas & Ochoa-Alejo, 2016; Winkelmann, 1996), so it can be expected that the same cell fate and other developmental processes would occur during the formation of somatic embryos. These processes are influenced by environmental inducers and alter gene activity for somatic embryogenesis (Yang & Zhang, 2010). In order to understand how somatic embryos are induced from somatic tissues, the relationship between environmental inducers and genetic pathways of differentiation needs to be understood. Plant hormones play a crucial role in interacting with and adapting to their environment (Alazem & Lin, 2015). Plants control a wide range of physiological processes in cells by changing the amount of hormone production, transmission, and accumulation. Hormones have been commonly used for induction of somatic embryogenesis (Víctor M. Jiménez & Thomas, 2005). The competitive efficiency of somatic cells in embryogenesis can be predicted by examining the extent of hormone biosynthesis and perception (Jiménez, 2001). Therefore, it is important to identify accurately the role of hormones in exploring the network of genetic and environmental inducers of somatic embryogenesis. It has been difficult to identify all of the hormonal pathways, due to their wide range of effects. Also, most researches have focused on a

* Corresponding author's e-mail address: moshtaghi@um.ac.ir

single or small number of effective factors. As a result of these restrictions, some controversial results have been reported. Therefore, it is difficult to realize somatic embryogenesis precisely. In this regard, high throughput methods such as transcriptome analysis have contributed to obtain a comprehensive view about the physiological processes (Ward et al., 2012). Further, targeted analysis of high throughput data in a specific pathway such as somatic embryogenesis helps to identify other effective environmental factors involved in somatic embryogenesis which have been neglected. Through optimizing the environmental conditions, we will be able to drive the plant cells towards a desired goal, and enhance the performance of cells during a specific pathway such as somatic embryogenesis. With progress of bioinformatics, these methods reveal more information about the plant responses to the environment. In somatic embryogenesis of *Arabidopsis*, transcriptome analysis has also provided useful information. Fold-change investigations performed on high throughput data have clarified some effective pathways in somatic embryogenesis (Gliwicka et al., 2013; Wickramasuriya & Dunwell, 2015) but some several effective genes with less expression are neglected in the fold-change studies. Further information can still be obtained using more comprehensive and precise analysis such as gene set enrichment analysis (Subramanian et al., 2005). Therefore, based on data obtained from RNA sequencing of somatic embryogenesis in a previous report (Wickramasuriya & Dunwell, 2015), this study aimed to determine the activity of plant hormones and their mechanism of action during somatic embryogenesis. For this purpose, comprehensive investigation of the available data was done by GSEA, and then the core-enriched genes were studied more precisely through identifying protein-protein interactions. Finally, the expression of some enriched genes involved in conversion of membrane lipids to jasmonates pathway were studied during somatic embryogenesis.

Materials and Methods

In silico analysis

To perform the bioinformatics analysis, the log2 FPKM values of RNA high throughput sequencing at different stages of somatic embryogenesis of *Arabidopsis* were used (Wickramasuriya & Dunwell, 2015). GSEA analysis was done through the signal-to-noise criteria via 1000 permutations using GSEA 4.3 software (Subramanian et al., 2005). Different stages of somatic embryogenesis and *Arabidopsis* leaves were considered as phenotype labels. For precise investigation of the pathways affecting somatic embryogenesis, gene ontology of core-enriched genes was determined in three groups of biological pathways, molecular function, and cellular component. Also, Kyoto encyclopedia of genes and genomes (KEGG) analysis was done to achieve the metabolic pathways affecting somatic embryogenesis. Gene ontology and KEGG analysis were performed by ClueGO plugin in Cytospscae 3.9.1 software (Bindea et al., 2009). Kappa score was considered equivalent to 0.5, and only laboratory evidence of the criterion was investigated. Protein-protein interactions of core-enriched genes were done through determining the protein network via String online software. The network type was full string network, and only the proteins whose link score was above 0.4 were examined in the protein network.

Somatic embryogenesis

Twelve days after pollination of *Arabidopsis thaliana* cv Columbia-0, the siliques were collected and disinfected by sodium hypochlorite 1%. Next, immature embryos were withdrawn from inside the embryo sacs and cultured in MS culture medium containing 1 mg/L of 2,4-D and 7 g/L of agar. Two weeks after culture, the explants were transferred to $^1/_2$ MS medium without 2,4-D to develop embryos and grow seedlings (Figure 1).

qRT-PCR analysis

Immature zygotic embryos were collected at four stages: the day of culture (control), third day (pre-somatic embryogenesis), seventh day (time of induction of somatic embryogenesis), and 10th day (post-somatic embryogenesis). It was considered that somatic embryogenesis started with the formation of callus in the regions around the shoot apical meristem (Figure 1). They were then frozen by liquid nitrogen and kept at -80°C. RNA extraction was performed by RiboEX solution according to the manufacturer's instructions. The concentration of RNAs was normalized after measuring OD using Epoch microplate spectrophotometer (Epoch, USA), and the first strand of cDNA was synthesized by cDNA synthesis kit (AddBio, Korea). To perform qRT-PCR analysis, the reaction mixture contained 1 µL of cDNA (500 $\mu g.ml^{-1}$), 1 µL of each specific primers of the studied genes (Table 1), 10 µL of qPCR master mix (Yekta Tajhiz Azma Co.), and 7 µL sterilized distilled water. qRT-PCR was done using Bio-Rad CFX96 Touch™ Real-Time PCR Detection System (Bio-Rad, USA) and the data was

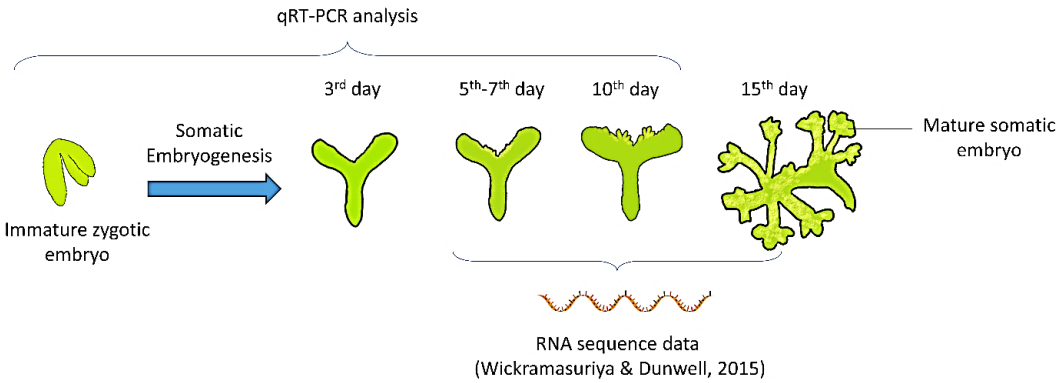

Figure 1. Stages of *Arabidopsis* somatic embryogenesis. This picture depicts the stages of somatic embryo development considered in this study.

Table 1. List of primers used in qRT-PCR analysis

Gene name	Locus ID	Sequence
β-TUBULIN	AT5G12250	Forward: 5'-TGGGAACTCTGCTCATATCT-3' Reverse: 5'-GAAAGGAATGAGGTTCACTG-3'
LOX1 (Lipoxygenase 1)	AT1G55020	Forward: 5'-TCTGTGTCTGACGAGGGTCGAATT-3' Reverse: 5'-ACTTTGCGGCAATACCTCTCTGG-3'
LOX6 (Lipoxygenase 6)	AT1G67560	Forward:5'-AGTGGAAGCGGAAGTGGAAG-3' Reverse: 5'-GAGGGCGTTGTTCTGCTAGT-3'
ACX1(Acyl-CoA oxidase 1)	AT4G16760	Forward:5'-ATCTTCGCAGAATCCCTGTGATA-3' Reverse: 5'-GCACCTAGCTTCAAGCACTTTACA-3'
OPR3 (Oxophytodienoate reductase 3)	AT2G06050	Forward: 5'-ACGGACCACTCCCGGCGGTTTTC-3' Reverse: 5'-CGTGAACTGCTTCCACAACTT-3'

analyzed with Bio-Rad CFX96 Manager and Excel software. *β-TUBULIN* was considered as the internal reference gene.

Results and Discussion

Considerable change of the activity of hormonal pathways during somatic embryogenesis

The GSEA results indicate that activity of hormones has changed mostly at the beginning and end of somatic embryogenesis. The activity of more hormonal pathways has decreased after five days of 2,4-D treatment, but it increased at the end of somatic embryogenesis. According to these data, response to auxin had considerable activity at the beginning of 2,4-D treatment, but it decreased after somatic embryo formation and during the growth of seedlings. During somatic embryogenesis, jasmonates showed the greatest change of activity, followed by gibberellin and salicylic acid (Figure S1). It is also expected from investigating different stages of somatic embryogenesis. The induction of embryonic cells in immature *Arabidopsis* embryos began on the fifth day after treatment with 2,4-D by starting formation of embryonic callus in shoot apical meristem, and on the seventh day, the entire embryo induction region around the shoot apical meristem began generating embryos. With the conversion of somatic embryos into seedlings, the activity of genes affecting differentiation and growth pathways decreased on the 15th day of 2,4-D treatment. These data indicated that somatic embryogenesis was characterized by a significant interaction between hormones. It has also been found that plant growth regulators play an important role in somatic embryogenesis, as knocking down of key genes of these pathways or using inhibitors of hormone perception causes impaired somatic embryogenesis (Bai et al., 2013; Chen & Chang, 2003; Nowak et al., 2015). Therefore, they should be examined more closely in terms of how they affect somatic embryogenesis.

Activity of biological processes under the influence of hormone perception

The gene ontology of core-enriched genes was examined in three groups of biological pathway, molecular function and cellular component. The results generally indicated that most of the proteins involved in somatic embryogenesis had either enzymatic or binding activity. Furthermore, cellular component of the genes showed that plastids, which are mostly composed of chloroplast and storage plastids, had a greater role than other intracellular organelles during somatic embryogenesis. The notable point on the 5th day compared to the control has been seed maturation as one of the active biological processes. This process associated with storage of lipids had considerable activity in the initiation of somatic embryogenesis. It suggested that after five days of the 2,4-D treatment, embryonic cells have formed, and the embryos have tended to mature. In this way, the lipid storage pathway became activated as a prerequisite for growth and maturity of the somatic embryo. Furthermore, the major activity reduction on 5th day is associated with pathways related to photosynthesis (Figure 2). It suggested that photosynthesis and lipid storage may be related to each other during the induction and growth of somatic embryos. During the maturation of zygotic embryos, lipid storage depends on light and oxygen which is released from photosynthesis. For growth and survival, zygotic embryos accumulate lipids as a source of energy when intracellular oxygen is low (Rolletschek et al., 2005). Somatic embryos are structurally and physiologically similar to zygotic embryos (Leljak-Levanić et al., 2015), therefore it is possible that they also store lipids to provide energy for growth. In addition, stress response was identified as another effective biological process during somatic embryogenesis. The response to stress decreased during the first 10 days of somatic embryogenesis. After that, in spite of removal of 2,4-D from the culture medium, the activity of genes involved in the stress response was increased. In previous studies, 2,4-D induces stress responses in plant cells, and these responses together with auxin signaling of 2,4-D affect the growth and development of somatic embryos (Philipsen & Offringa, 2017; Karami & Saidi, 2010). The results suggested that 2,4-D may indirectly affect stress induction during the maturation of somatic embryos of *Arabidopsis* by activating other physiological processes within the cells.

embryonic cells in immature *Arabidopsis* embryos began on the fifth day after treatment with 2,4-D by starting formation of embryonic callus in shoot apical meristem, and on the seventh day, the entire embryo induction region around the shoot apical meristem began generating embryos. With the conversion of somatic embryos into seedlings, the activity of genes affecting differentiation and growth pathways decreased on the 15th day of 2,4-D treatment. These data indicated that somatic embryogenesis was characterized by a significant interaction between hormones. It has also been found that plant growth regulators play an important role in somatic embryogenesis, as knocking down of key genes of these pathways or using inhibitors of hormone perception causes impaired somatic embryogenesis (Bai et al., 2013; Chen & Chang, 2003; Nowak et al., 2015). Therefore, they should be examined more closely in terms of how they affect somatic embryogenesis.

Close relationship between plant hormones and the lipid and storage proteins in the PPI network

In order to identify the relationship of biological processes involved in somatic embryogenesis, the protein-protein interaction network of core-enriched genes was determined. The PPI network was centered on genes associated with auxin signaling and transmission. Transport inhibitor response 1/Auxin signaling F-BOXs (TIR1/AFB) receptors, which possess the highest level of protein communication, bind to auxin and activate downstream pathways through ubiquitination of Auxin/Indole-3-acetic acid (AUX/IAA) proteins (Salehin et al., 2015). Close to the PPI center was another protein cluster, which is related to transcription factors associated with ethylene such as *Ethylene overproducer 1* (*ETO1*), *Ethylene response 2* (*ETR2),* and *Ethylene insensitive 4* (*EIN4)* (Figure 3). Therefore, ethylene might play a key role during somatic embryogenesis, and its downstream pathways interact closely with auxin signaling. The genes associated with lipids and storage proteins are located between these two protein clusters (Figure 3). It suggested that in addition to auxin, other plant hormones also affect lipid storage and stress induction. It has been reported that when plant cells are exposed to stress, they convert membrane lipids to produce signaling lipids such as phosphatidic acid and free fatty acids (Hou et al., 2016).

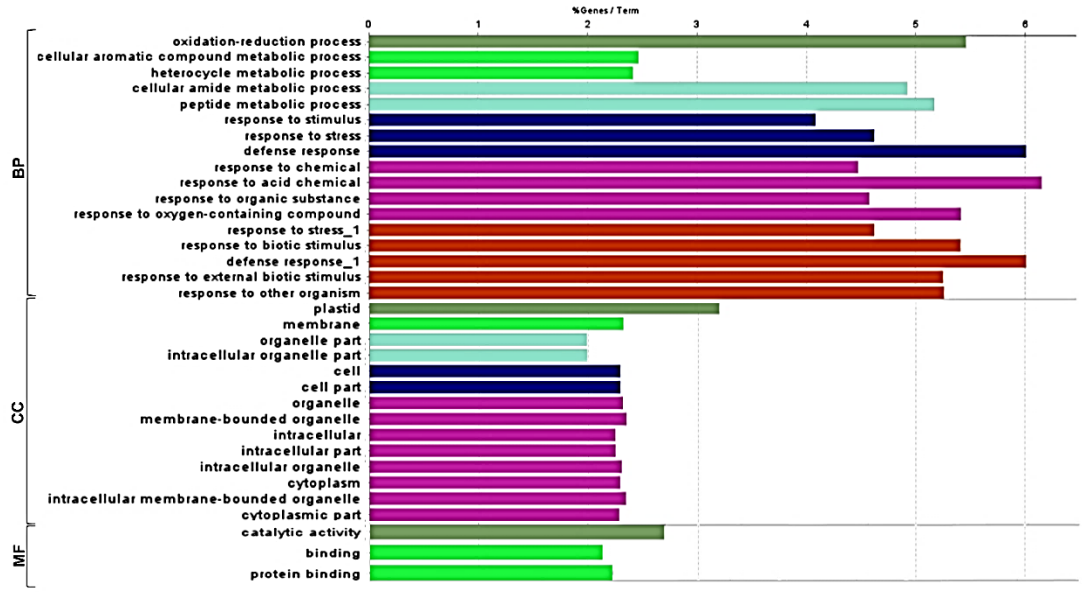

Figure 2. Gene ontology of core-enriched genes of *Arabidopsis* somatic embryogenesis. In each aspect of gene ontology, each color represents a specific gene ontology term.

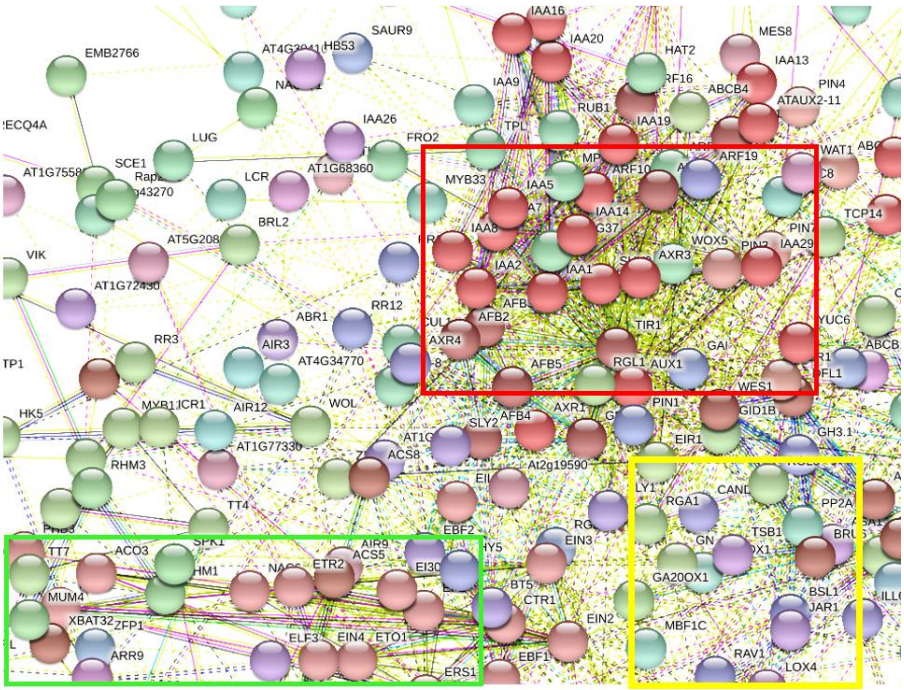

Figure 3. The central region of protein-protein interaction network of core-enriched genes. The red and green rectangles respectively represent auxin and ethylene perception. The genes associated with lipids and storage proteins are located in the yellow square.

It activates lipid-dependent signaling pathways, which results in induction of stress response (Okazaki & Saito, 2014). It has been found that any defects in function of proteins that are involved in metabolism of phospholipids impaired some biological processes such as embryogenesis and response to stress (Hou et al., 2016). Therefore, genes involved in lipid biosynthesis and metabolism may function as mediators between hormone signaling and stress induction during somatic embryogenesis.

Lipid metabolism as an active metabolic pathway during somatic embryogenesis

The KEGG analysis of metabolic pathways involved in somatic embryogenesis revealed that out

of eight active metabolic pathways in somatic embryogenesis. In this concept, four of them were involved in lipid metabolism and biosynthesis, and three of them were involved in hormone biosynthesis and signaling. The allocation of half of the active metabolic pathways to lipids in somatic embryogenesis indicated that their production and accumulation were essential for somatic embryogenesis. Also, more than half of the genes related to linoleic acid metabolism, including the *Lypooxygenase* (*LOX*) gene family, are involved in somatic embryogenesis (Table 2). Plant cells synthesize long chain fatty acids from linoleic acid and α-linolenic acid which are unsaturated fatty acids found in the cell membrane (Alché, 2019). This process is carried out by *LOX* gene family. It can be concluded that this gene family influenced the accumulation and conversion of lipids in plants. Also, these genes cooperate with *Oxophytodienoate reductase 3* (*OPR3*) and *Acyl-CoA oxidase 1* (*ACX1*) to convert α-linolenic acid to jasmonates (Zhai et al., 2017). It indicated that stress induction by 2,4-D treatment occurs gradually through lipid biosynthesis and metabolism. Since these genes play a significant role in somatic embryogenesis, changes in their activity should also be investigated during somatic embryogenesis.

Activity of the genes responsible for conversion of membrane lipids to jasmonates during somatic embryogenesis

Based on the results of bioinformatics analysis, the expression of *LOX1*, *LOX6*, *ACX1*, and *OPR3* genes was examined during the somatic embryogenesis. *LOX1* and *LOX6* are involved in the initial steps of α-linolenic acid conversion to jasmonates in the chloroplast, while *ACX1* and *OPR3* coordinate the oxidation process to produce the final compound of jasmonates in the peroxisome (Ali & Baek, 2020; Wasternack & Kombrink, 2010). The results of qRT-PCR analysis indicated that the expression of all examined genes decreased considerably after the treatment of immature embryos with 2,4-D, but increased during somatic embryogenesis. When somatic embryogenesis is induced by 2,4-D treatment, *ACX1* and *OPR3* reached their maximum expression. After that, their activity gradually decreased. However, the ascending trend of the expression of *LOX1* and *LOX6* genes persisted during the growth of seedlings (Figure 4). The results suggested that membrane lipids convert to jasmonates during somatic embryogenesis and activate downstream pathways of stress induction. Stress is one of the factors affecting reprogramming of plant cells and production of somatic embryos (Zavattieri et al., 2010). Induction of stress improved efficiency of production of somatic embryos and in some cases, induced somatic embryogenesis alone (Fehér, 2015; Ikeda-Iwai et al., 2003). Also, jasmonates has been reported as the intermediate hormone between stress and plant regeneration. Mira et al (2016) reported that jasmonates increase the expression of *JAZ1* and decrease the expression of *MYC2* which results in accumulation of IAA in plant cells. These processes have eventually resulted in successful somatic embryogenesis of *Arabidopsis* (Mira et al., 2016).

Table 2. Metabolic pathways under the influence of core-enriched genes of Arabidopsis somatic embryogenesis.

Gene Ontology ID	Gene Ontology Term	% Associated Genes	Number of Genes	Associated Genes
04016	MAPK signaling pathway	14.62	19	*ACS6, ATMPK8, EBF1, EBF2, ...*
04075	Plant hormone signal transduction	26.74	73	*ARR11, ERF1, IAA2, JAZ1, ...*
00591	Linoleic acid metabolism	55.56	5	*LOX1, LOX2, LOX3, LOX4, LOX6*
00592	alpha-Linolenic acid metabolism	41.67	15	*ACX1,LOX2, LOX3, OPR3, ...*
00901	Indole alkaloid biosynthesis	40.00	4	*ACL, MES1, MES3, MES9*
00904	Diterpenoid biosynthesis	50.00	11.00	*GA20OX2, GA20OX3, GA2OX2, ...*
00380	Tryptophan metabolism	32.65	16.00	*NIT1, SOT16, TAA1, YUC1, ...*
00966	Glucosinolate biosynthesis	26.09	6.00	*CYP79B2, CYP79B3, IMD1, ...*

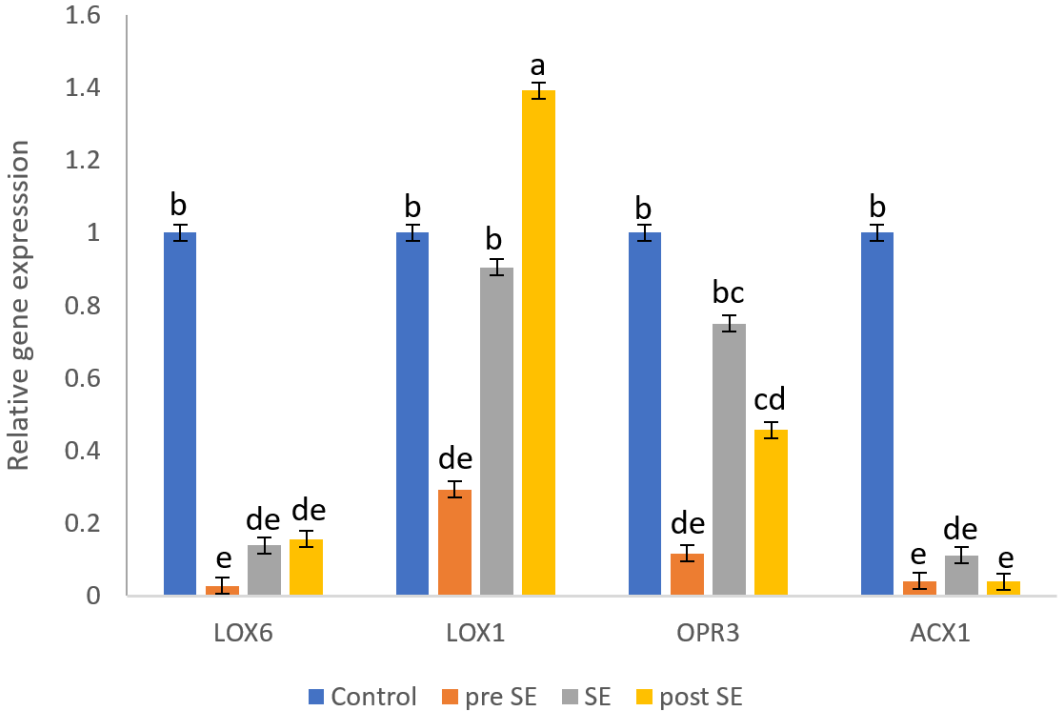

Figure 4. Relative gene expression level of some core-enriched genes involved in conversion of membrane lipids to jasmonates. *LOX6: Lypooxygenase 6*, *LOX1: Lypooxygenase 1*, *OPR3: Oxophytodienoate reductase 3*, *ACX1: Acyl-CoA oxidase 1*. Values with same letters are not significantly different at P<0.05.

Conclusion

In this experiment, it was found that somatic embryogenesis is the result of the interaction of various biological pathways involved in differentiation and development. Based on the results of this study, genes related to biosynthesis and metabolism of lipids were associated with hormones and stress signaling. In bioinformatics analysis, *LOX1*, *LOX6*, *ACX1*, and *OPR3*, which are involved in biosynthesis of jasmonates, were identified as the key genes in somatic embryogenesis of *Arabidopsis*. qRT-PCR analysis also confirmed the bioinformatic results as the expression of these genes changed during somatic embryogenesis. These results suggested that jasmonates function as one of the effective factors in somatic embryogenesis and in cooperation with other hormones, they activate downstream pathways such as stress induction. The process ultimately results in the induction and development of *Arabidopsis* somatic embryos.

A number of environmental stress factors, such as mechanical damage and pathogen attack, induce jasmonates. Therefore, the results of this study can be used in further studies to improve the efficiency of somatic embryogenesis by applying environmental stimuli or genetically modifying genes involved in jasmonates production and their downstream pathway.

Acknowledgments

This study was supported by the Ferdowsi University of Mashhad [grant number 48114 was awarded to Azadeh Khadem]. We thank Academic Center for Education, Culture and Research (ACECR) for providing laboratory and technical services.

Competing interests

The authors have no relevant financial or non-financial interests to disclose.

Abbreviations:

GSEA: Gene Set Enrichment Analysis
PPI: Protein-Protein Interaction
KEGG: Kyoto Encyclopedia of Genes and Genomes
GO: Gene Ontology

References

Alazem, M., & Lin, N. S. (2015) Roles of plant hormones in the regulation of host-virus interactions. Molecular Plant Pathology *16*: 529–540.

Alché, J. de D. (2019) A concise appraisal of lipid oxidation and lipoxidation in higher plants. Redox Biology *23*: 101136.

Ali, M. S., & Baek, K. H. (2020) Jasmonic acid signaling pathway in response to abiotic stresses in plants. International Journal of Molecular Sciences *21*(2): 124-137.

Bai, B., Su, Y. H., Yuan, J., & Zhang, X. S. (2013) Induction of somatic embryos in arabidopsis requires local *YUCCA* expression mediated by the down-regulation of ethylene biosynthesis. Molecular Plant *6*: 1247–1260.

Bindea, G., Mlecnik, B., Hackl, H., Charoentong, P., Tosolini, M., Kirilovsky, A., Fridman, W. H., Pagès, F., Trajanoski, Z., & Galon, J. (2009) ClueGO: A Cytoscape plug-in to decipher functionally grouped gene ontology and pathway annotation networks. Bioinformatics *25*: 1091–1093.

Chen, J.-T., & Chang, W.C. (2003) Effects of GA_3 , ancymidol, cycocel and paclobutrazol on direct somatic embryogenesis of *Oncidium* in vitro. Plant Cell, Tissue and Organ Culture *72*: 105–108.

de Vries, S. C., & Weijers, D. (2017) Plant embryogenesis. Current Biology *27*: 870–873.

Fehér, A. (2015). Somatic embryogenesis: stress-induced remodeling of plant cell fate. Biochimica et Biophysica Acta - Gene Regulatory Mechanisms *1849*: 385–402.

Gliwicka, M., Nowak, K., Balazadeh, S., Mueller-Roeber, B., & Gaj, M. D. (2013) Extensive modulation of the transcription factor transcriptome during somatic embryogenesis in *Arabidopsis thaliana*. PloS One *8*: e69261.

Hou, Q., Ufer, G., & Bartels, D. (2016) Lipid signalling in plant responses to abiotic stress. Plant Cell and Environment *39*: 1029–1048.

Ikeda-Iwai, M., Umehara, M., Satoh, S., & Kamada, H. (2003) Stress-induced somatic embryogenesis in vegetative tissues of *Arabidopsis thaliana*. Plant Journal *34*: 107–114.

Jiménez, V. M. (2001). Regulation of *in vitro* somatic embryogenesis with emphasis on the role of endogenous hormones. Revista Brasileira de Fisiologia Vegetal *13*: 196–223.

Jiménez, Víctor M., & Thomas, C. (2005) Participation of plant hormones in determination and progression of somatic embryogenesis. Plant Cell Monographs *2*: 103–118.

Lau, S., Slane, D., Herud, O., Kong, J., & Jürgens, G. (2012) Early embryogenesis in flowering plants: setting up the basic body pattern. Annual Review of Plant Biology *63*: 483–506.

Leljak-Levanić, D., Mihaljević, S., & Bauer, N. (2015) Somatic and zygotic embryos share common developmental features at the onset of plant embryogenesis. Acta Physiologiae Plantarum *37*: 425-439.

Loyola-Vargas, V. M., & Ochoa-Alejo, N. (2016) Somatic embryogenesis: Fundamental aspects and applications. In V. M. Loyola-Vargas & N. Ochoa-Alejo (Eds.), Somatic Embryogenesis: Fundamental Aspects and Applications. Springer International Publishing.

Karami, O. & Saidi, A. (2010). The molecular basis for stress-induced acquisition of somatic embryogenesis. Molecular Biology Reports *37*: 2493-2507.

Mira, M. M., Wally, O. S. D., Elhiti, M., El-Shanshory, A., Reddy, D. S., Hill, R. D., & Stasolla, C. (2016) Jasmonic acid is a downstream component in the modulation of somatic embryogenesis by *Arabidopsis* Class 2 phytoglobin. Journal of Experimental Botany *67*: 2231–2246.

Miransari, M., & Smith, D. L. (2014) Plant hormones and seed germination. Environmental and Experimental Botany *99*: 110–121.

Nowak, K., Wójcikowska, B., & Gaj, M. D. (2015) *ERF022* impacts the induction of somatic embryogenesis in *Arabidopsis* through the ethylene-related pathway. Planta *241*: 967–985.

Okazaki, Y., & Saito, K. (2014) Roles of lipids as signaling molecules and mitigators during stress response in plants. Plant Journal *79:* 584–596.

Philipsen, C., & Offringa, R. (2017) Unraveling the auxin mechanism in 2,4-D induced somatic embryogenesis in *Arabidopsis*. In Ph.D. Thesis.

Radoeva, T., & Weijers, D. (2014) A roadmap to embryo identity in plants. Trends in Plant Science *19*: 709–716.

Rolletschek, H., Radchuk, R., Klukas, C., Schreiber, F., Wobus, U., & Borisjuk, L. (2005) Evidence of a key role for photosynthetic oxygen release in oil storage in developing soybean seeds. New Phytologist *167*: 777–786.

Salehin, M., Bagchi, R., & Estelle, M. (2015) *SCFTIR1/AFB*-based auxin perception: mechanism and role in plant growth and development. The Plant Cell *27*: 9–19.

Subramanian, A., Tamayo, P., Mootha, V. K., Mukherjee, S., Ebert, B. L., Gillette, M. A., Paulovich, A., Pomeroy, S. L., Golub, T. R., Lander, E. S., & Mesirov, J. P. (2005) Gene set enrichment analysis: A knowledge-based approach for interpreting genome-wide expression profiles. Proceedings of the National Academy of Sciences of the United States of America *102*: 15545–15550.

Ward, J. A., Ponnala, L., & Weber, C. A. (2012)

Strategies for transcriptome analysis in nonmodel plants. American Journal of Botany *99*: 267–276.

Wasternack, C., & Kombrink, E. (2010) Jasmonates: Structural requirements for lipid-derived signals active in plant stress responses and development. ACS Chemical Biology *5*(1): 63–77.

Wickramasuriya, A. M., & Dunwell, J. M. (2015). Global scale transcriptome analysis of *Arabidopsis* embryogenesis *in vitro*. BMC Genomics *16*: 1–23.

Winkelmann, T. (1996) In Vitro Embryogenesis in Plants. Biologia plantarum 38: 616–621.

Yang, X., & Zhang, X. (2010) Regulation of somatic embryogenesis in higher plants. Critical Reviews in Plant Sciences *29*: 36–57.

Zavattieri, M. A., Frederico, A. M., Lima, M., Sabino, R., & Arnholdt-Schmitt, B. (2010) Induction of somatic embryogenesis as an example of stress-related plant reactions. Electronic Journal of Biotechnology *13*: 1–9.

Zhai, Q., Yan, C., Li, L., Xie, D., & Li, C. (2017) Jasmonates. Hormone Metabolism and Signaling in Plants, 243–272.

Research Article

Evaluation of CD86 rs17281995Gene Polymorphism in Gastric and Intestinal Cancer Subjects in Tehran and Khorramabad Cities

Masoumeh Aalipour [1], Asghar Aalipour [2], Mohammad Mousaei Ghasroldasht [1 *]

[1] *Department of Genetics, Faculty of Biological Sciences and Technology, Shahid Ashrafi Esfahani, Esfahan, Iran*
[2] *Department of Pathology, School of Medicine, Lorestan University of Medical Sciences, Khorramabad, Iran*

Received 26 May 2022 Accepted 16 October 2022

Abstract

Colorectal cancer (CRC) and gastric cancer (GC) are multifactorial diseases likely influenced by genetic susceptibility. Gastric cancer is also the fourth most common cancer in the world and the second leading cause of cancer-related mortality. CD86 (B7-2) is a costimulatory molecule found on antigen-presenting cells (APCs) that is important in autoimmune, transplantation, and tumor immunity. This protein is expressed in the immune system cells and is involved in the pathogenesis of various inflammatory disorders and inflammation. Rs17281995 polymorphism is located in section 3' UTR, and given the regulatory role of 3' UTR gene sequences, SNPs located in these regions can affect the expression and function of the corresponding protein. In the present study, the relationship between rs17281995 polymorphism located in the 3' UTR regulatory region of the CD86 gene sequence and the risk of colorectal and gastric cancer in Iranian patients was analyzed. Polymorphism was identified in 26 patients with colorectal cancer, 30 patients with gastric cancer, and 36 healthy controls using the high-resolution DNA melting curve analysis (HRM) technique. The Data was then analyzed using SPSS software. There was no significant relationship between rs17281995 polymorphism and colorectal ($P = 0.75$) and gastric cancers ($P = 0.97$) in the Iranian population. In addition, genotypic distribution analysis showed no significant difference between the patient and control groups ($P>0.05$). Among people with colorectal cancer, 0.577 had the G allele and 0.423 had the C allele. In the control group, 0.639 had the G allele and 0.361 had the C allele. In conclusion, our data indicate that the CD86 rs17281995 gene polymorphism does not seem to be a risk factor for colorectal and gastric cancers in the Iranian population.

***Keywords*:** Polymorphism, CD86, HRM, rs17281995, SNP

Introduction

Colorectal cancer (CRC) is globally the third most typical cancer (Shademan et al., 2022). Likewise, the incidence of colorectal cancer in the elderly Iranian population is lower than that of Western societies. Yet, the incidence of this type of cancer at a young age is high and rising (Arani & Kerachian, 2017). Gastric cancer (GC) is also the fourth most common cancer in the world and the second leading cause of cancer-related mortality (Jemal et al., 2011). Cancer is a multifactorial disease in which both environmental and genetic factors are involved (Poorolajal et al., 2020). The main components of cancer-causing genetic factors are mutations and polymorphisms that function by changing the proteins' expression or functioning(Landi et al., 2008). Molecular epidemiological research indicates that genetic changes such as single-nucleotide polymorphism can greatly influence the risk of developing diseases, specifically cancer(Di Pasqua et al., 2009). Given the effective role of the immune system in the fight against diseases and malignancies, today's studies utilize immune profiles and the involved genes to select the appropriate marker (Fang et al., 2014; Koido et al., 2013). The most important immunological genes expressed on the surface of colon epithelial cells are B7.2 costimulatory molecules (CD86).

CD86 (B7-2) is a costimulatory molecule found on antigen-presenting cells (APCs) that is important in autoimmune, transplantation, and tumor immunity. Through the CD28/CTLA-4 pathway, CD86 influences T-cell responses. Tumor cells deficient in B7-1 and B7-2 are unable to produce the costimulatory signals required for T-cell activation, resulting in T-cell anergy and immunological inactivity. As a result, alterations in CD86 may have an impact on how this disease develops(Hu et al., 1999; Ohtani, 2007). Eight exons make up the CD86

*Corresponding author's e-mail address: *Mghasroldasht@gmail.com*

gene on chromosome 3q21. The exon 8 and 3' untranslated region regulatory domain polymorphisms rs1129055 (+1057 G>A) and rs17281995 (+2379G>C), respectively, modulate the degree of protein kinase C phosphorylation of the CD86 cytoplasmic tail. The polymorphisms rs1129055 and rs17281995 in the CD86 gene have been extensively studied. Since then, the initial publication on the link between rs17281995 and the incidence of sporadic colorectal cancer in Caucasians was released in 2008 (Landi et al., 2008). Geng et al. (2014) demonstrated that rs17281995 and rs1129055 mononucleotide polymorphisms could cause changes in CD86 gene expression, ultimately raising the risk of malignancy and colorectal cancer in individuals (Geng et al., 2014).

Few studies have been conducted on multiple polymorphisms of CD86 and +2379 G / C genes with the risk of CRC development in the world and, moreover, little is known about the frequency of rs17281995 polymorphisms of CD86 gene in Iranian patients with gastric cancer. Research has established that single-nucleotide polymorphisms can lead to significant alteration of gene pathways within cancer cells. Consequently, early diagnosis of these polymorphisms can pave the way for early detection and prognosis of cancer. The role of the CD86 gene in various diseases and cancer occurrences has been investigated, yet accurate and comprehensive information on rs17281995 polymorphism in patients with colorectal cancer is not available. Thus, the present study tries to examine the relationship between CD86 rs17281995 gene polymorphism and its frequency distribution in target populations.

Materials and Methods

Participants

This study includes 30 (20 men and 10 women) and 26 (13 women and 13 men) formalin-fixed, paraffin-embedded (FFPE) blocks of tissue for gastric cancer and intestine cancer, that were selected from Imam Reza (AS) hospitals located in Tehran and Shahid Rahimi hospitals located in Khorramabad. Of all the FFPE blocks of tissue, those selected that were collected through biopsy or surgery, and their tumor stage was confirmed by the pathologist after histological and pathological examinations were performed. Control samples consisted of 18 (9 males and 9 females) FFPE blocks of tissue without cancer diagnosed. Healthy control samples were selected from those who experienced biopsy, and their test results were non-cancerous and negative.

DNA extraction and determination of its quality

After preparing tissue samples from healthy and sick people, genomic DNA was extracted by the Genomic DNA Extraction kit (Genet Bio) from paraffin tissue samples, according to the manufacturer's instructions. In order to evaluate the purity and concentration of the obtained DNA, absorption measurements were performed with a spectrophotometer (Eppendorf) at wavelengths of 260 and 280 nm.

Polymerase chain reaction (PCR method)

After DNA extraction, a PCR test was performed to amplify the preferred oligonucleotide sequence. To amplify the gene, the CD86 gene was first extracted by searching the NCBI-specific site. The sequence of this gene was entered into OLIGO Primer Analysis Software and a pair of specific primers were designed. In the subsequent step, to determine the specificity of the primers, their sequences were examined by NCBI Primer-BLAST. A desired 200 bp DNA fragment in the Beta actin gene was amplified by a polymerase chain reaction by a thermocycler. After the PCR reaction, the PCR products, which are 200 bp in length, were transferred to a 1.5% agarose gel along with a DNA marker with a molecular weight of 50 bp. After the electrophoresis technique was performed and the DNA bands were separated, the gel was photographed using Gel Doc.

Preparation of electrophoresis 1x TBE buffer

In this study, the buffer was employed both to create the gel and to establish the electric current in the electrophoresis tank. The buffer utilized for the agarose gel in the electrophoresis tank was buffer X1. The 1x TBE buffer (Aron Gene) has low ionic strength, which was first purchased as the 10x. To make 1000 ml 1x TBE buffer, about 100 ml 10x TBE buffer was dissolved in 900 ml of distilled water and diluted to make 1x TBE buffer. In this study, 1.5% gel electrophoresis was utilized. After the electrophoresis technique was performed and DNA bands were separated, the gel was photographed using Gel Doc (Compact, ATP).

Performing the melting curve analysis (HRM Method) on the sample of patients in the Study

Primer Design

In this study, CD86 gene polymorphism was assessed. In order to design a specific primer, the

nucleotide sequence of the CD86 gene was first collected from the NCBI site. Then it was checked if the two sequences were matched using the BLAST server in NCBI. The required primer design to amplify the region around the target SNP was first developed by OLIGO Primer Analysis Software. Additionally, to ensure that only the desired fragment was amplified, not attached elsewhere in the genome, their accuracy and uniqueness were confirmed using Primer 3 and Primer BLAST. Table 1 indicates the primer sequence used in the PCR reaction.

Primer Preparation

The primers were collected by Pishgam Company and received as lyophilized. According to the manufacturer's protocol, adding distilled water increased the primer's concentration to 100 pmd / ml. Stock and working solutions were both kept at -20 ° C.

HRM Test

This method is a homogeneous and new method after PCR amplification that is performed in a closed tube. The HRM technique enables the analysis of genetic changes (SNPs, mutations, and methylations) in PCR products. HRM differentiates nucleic acid samples based on GC sequence, length, and volume. HRM analysis includes the amplification of the desired gene in 80-250 bp fragments in a reaction that contains a dye that binds to fluorescent double-stranded DNA.

After distributing the mixture to the strip, the required amount of DNA was added to each strip from different samples. Each time an HRM was performed, a strip was considered as a negative control, implying that the DNA sample was not contaminated. The final volume of the reaction mixture in each strip was considered to be 25µl. After mixing the ingredients, including Eva Green (5 µl), DNA (18/57µl), Primer Forward, and Reverse (1/67 pmol/µlit) in the microtube, the microtube was placed in the Rotor-Gene Q device. According to the following program, firstly the samples were exposed to 95 °C for 15 min and then 45 cycles with 95 °C for 15 seconds and 60 °C for 20 seconds. Finally, the graphs were illustrated in temperatures ranging from 65 to 95 °C with a decreased temperature of 0.1 °C.

Statistical Analysis

SPSS software was employed to perform statistical analysis on the data when p-values of less than 0.05 were considered significant. It should be noted that the tests performed for this project were conducted in two independent experiments.

Results

Characteristics of Colorectal Cancer Specimens

In this study, a total of 44 people were studied, of whom 26 (13 men and 13 women) had colorectal cancer and 18 (nine men and nine women) were healthy individuals who were considered as controls. The subjects' ages ranged from 31 to 93 years. Most people with colorectal cancer were over 62 years old, and most of the subjects had moderate differentiation with PT between 3 and 4.

Characteristics of Gastric Cancer Specimens

In this study, a total of 48 people were studied, of which 30 (20 men and 10 women) had gastric cancer and 18 (nine men and nine women) were healthy individuals who were considered controls. The subjects' ages ranged from 44 to 85 years. Most people with gastric cancer were over 58 years old. Most patients had moderate differentiation and showed PT between 3 and 4. The results of the genotypic CD86 gene (rs17281995 polymorphism) in colorectal cancer patients and the control group are shown in Table 2.

After performing electrophoresis and separating the DNA bands from each other, the gel was photographed using the Gel Doc device. According to Figure 1, it is clear that the bright single bands of DNA, with a length of 200 bp, indicate the quality of the PCR product.

Statistical analysis of genotypic data revealed that the p-value was equal to 0.75. Thus, no significant difference was observed in the genotypic distribution of the patient and control groups (P>0.05). After the genotypic analysis was performed, allelic abundance was also discussed. Among people with colorectal cancer, 0.577 had the G allele and 0.423 had the C allele. In the control group, 0.639 had the G allele and 0.361 had the C allele. The bar graph of rs17281995 allelic frequency distribution in patients with colorectal and a control cancer is shown in Figure 2.

The p-value was equal to 0.55; hence, there was no significant difference in the allelic distribution of the patient and control groups (P>0.05). The results of genotypic polymorphism rs17281995 of CD86 gene in gastric cancer patients and the control group are examined in Table 3.

As shown by the table above, the p-value was equal to 0.97. Thus, no significant difference was observed in the genotypic distribution of the patient and control groups (P>0.05). After genotypic analysis, allelic distribution was also discussed. Among patients with gastric cancer, 0.533 had the G allele and 0.467 had the C allele. In the control group,

0.528 had the G allele and 0.472 had the C allele. The bar graph of rs17281995 allelic distribution in patients with gastric and control cancers is shown in Figure 3.

The p-value was equal to 0.95, so there was no significant difference in the allelic distribution of patients and controls (P>0.05).

Table 1. Sequence and characteristics of the primer used to amplify the studied gene polymorphism.

Product Length (PCR)	Primer Sequence	Annealing Temperature	SNP ID
162	F:CCTACAGATGTCCTACGGGAA R:TAGTGATCCCACCTTAGAGCC	60 ℃	rs17281995

Table 2. Genotype and allele frequency of the rs17281995 polymorphism in patients with colorectal cancer and the control group.

			SNP			P-value
			CC	GC	GG	0.75
Group	Control	**Count**	1	11	6	
		% Within group	5.6%	61.1%	33.3%	
	Case	**Count**	3	16	7	
		% Within group	11.5%	61.5%	29.6%	

Discussion

Nowadays, gastrointestinal cancers, particularly gastric cancer and colorectal cancer are the leading causes of cancer-related death globally (Forat-Yazdi et al., 2015; Namazi et al., 2018; Namazi et al., 2017). The CRC and GC can be developed and progress in complex ways through the interaction of multiple genetic and environmental factors. The aim of this study was to determine the CD86 rs17281995 gene polymorphism in gastric and intestinal cancer subjects in the Iranian population. The results indicated that the frequency of G and C alleles did not differ between patients with colorectal cancer and that it is not a risk factor. Regarding the genotypic frequency of CD86, the results showed that the frequency of GG, GC, and CC genotypes differed between people with colorectal cancer and the control group, but it was not significant (p=0.75). This could be due to the small population of our study. Inconsistent with the results of the present study is a study performed in Iran, showing that the CC genotype and C allele in rs17281995 polymorphism are associated with the risk of intestinal cancer. This study revealed that CC genotype and C allele occur more often in female patients based on gender status (Azimzadeh et al., 2013). The reason for the difference between the results in this study and those of the present study could be due to the small population of our study. A meta-analysis by War et al. showed that the rs17281995 polymorphism was significantly associated with an increased risk of cancer, particularly colorectal cancer, in the Caucasus population, yet no significant association was observed in other Asian populations. A valid reason for this discrepancy could be the significantly different sizes of the studies (2075 vs. 781) because one of the conditions needed for the results of the sample size to be real is that the larger the sample size is, the more generalizable it is to the whole population(Geng et al., 2014). The most important genes expressed on the surface of the epithelial cells of the gastrointestinal tract are CD80 and CD86, co-stimulatory molecules of the B7 family, i.e., membrane-bound molecules that play an important role in activating the immune system, especially T lymphocytes. Lack of B7 molecules leads to decreased stimulation of T lymphocytes, especially $CD4^+$. It is important when cancer cells can escape the attacks by the immune system and T lymphocytes, which are responsible for destroying cancer cells, fail to be stimulated by them (Lenschow et al., 1996; van der Merwe et al., 1997). The results of the rs17281995 polymorphism in patients with gastric cancer are as follows: the frequency of G and C alleles is not different between patients with gastric cancer and those in the control group, thus it

is not a risk factor. As regards the genotypic frequency of CD86, the results indicated that the frequency of GG, GC, and CC genotypes did not differ between gastric cancer and control subjects. A meta-analysis by Zhuang et al. suggests that polymorphism of 592C> A in the interleukin 10 (IL-10) promoter may be associated with an increased risk of GC among Asians(Zhuang et al., 2010). Yet in another study, an association was seen between the IL-17F A7488G polymorphism and gastric cancer (Wu et al., 2010). IL-17F 7488 polymorphism has previously been indicated to be associated with increased inflammation in Helicobacter pylori infection(Arisawa et al., 2007). Saeki et al. explained that the rs4072037 polymorphism of mucin 1 (MUC1) increases the risk of GC, primarily the diffuse type (Saeki et al., 2011). The authors established that rs4072037 plays an important role in regulating transcription as well as selecting the MUC1 split site. However, no study has been conducted thus far to investigate the association of the rs17281995 polymorphism with gastric cancer. Hence, this study was the first to do so. Molecular epidemiological studies have described some relatively common genetic variations, namely single nucleotide polymorphism (SNP), as biomarkers for genetic susceptibility to GC progression (Canedo et al., 2008; Milne et al., 2009; Yin et al., 2009). These genetic variations may modulate the effects of exposure to environmental factors by regulating several biological pathways during gastric cancer. Genetic variations in inflammation-related genes, particularly cytokines and their receptors, are thought to play an important role in tumor development and progression (Canedo et al., 2008; González et al., 2002; Machado et al., 2003). Therefore, the role of genetic polymorphisms in the risk of GC has led to an increase in studies in recent years.

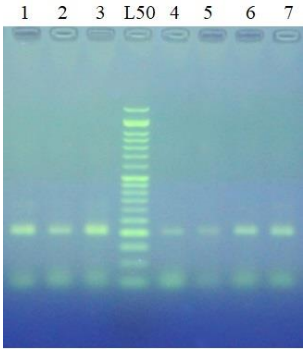

Figure 1. The electrophoresis PCR products of CD86 (200 pb) on 1.5% agarose gel. Column L50: marker 50bp, columns 1-7: PCR product.

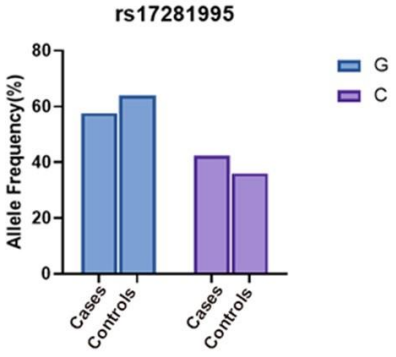

Figure2. Bar graph for allelic distribution of rs17281995 in colorectal cancer patients and controls.

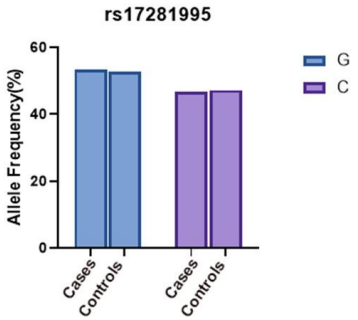

Figure 3. Bar graph for allelic distribution of rs17281995 in patients with gastric cancer and controls.

Table 3. Genotype and allele frequency of rs17281995 polymorphism in patients with gastric cancer and the control group.

			SNP			P-value
			CC	GC	GG	0.97
Group	Control	Count	4	9	5	
		% Within group	22%	50%	27%	
	Case	Count	7	14	9	
		% Within group	23.3%	46.7%	30%	

Conclusion

In the present study, it was discovered that there is no association between the frequency of alleles and genotypes of rs17281995 polymorphism in terms of colorectal and gastric cancer.

Conflict of Interests

The authors declare that there is no conflict of interest in this study.

References

Arani, S.H. and Kerachian, M.A. (2017) Rising rates of colorectal cancer among younger Iranians: is diet to blame?. Current Oncololgy 24(2):131-137.

Arisawa, T., Tahara, T., Shibata, T., Nagasaka, M., Nakamura, M., Kamiya, Y., et al. (2007) Genetic polymorphisms of molecules associated with inflammation and immune response in Japanese subjects with functional dyspepsia. International journal of molecular medicine 20(5): 717-723.

Azimzadeh, P., Romani, S., Mirtalebi, H., Fatemi, S.R., Kazemian, S., Khanyaghma, M., et al. (2013) Association of co-stimulatory human B-lymphocyte antigen B7-2 (CD86) gene polymorphism with colorectal cancer risk. Gastroenterology and Hepatology from Bed to Bench 6(2): 86.

Canedo, P., Durães, C., Pereira, F., Regalo, G., Lunet, N., Barros, H., et al. (2008) Tumor necrosis factor alpha extended haplotypes and risk of gastric carcinoma. Cancer Epidemiology, Biomarkers & Prevvention 17(9): 2416-2420.

Di Pasqua, A.J., Wallner, S., Kerwood, D.J. and Dabrowiak, J.C. (2009) Adsorption of the PtII anticancer drug carboplatin by mesoporous silica. Chemistry & Biodiversity 6(9): 1343-1349.

Fang, S.H., Efron, J.E., Berho, M.E. and Wexner, S.D., (2014) Dilemma of stage II colon cancer and decision making for adjuvant chemotherapy. Journal of the American College of Surgeons 219(5): 1056-1069.

Forat-Yazdi, M., Gholi-Nataj, M., Neamatzadeh, H., Nourbakhsh, P. and Shaker-Ardakani, H. (2015) Association of XRCC1 Arg399Gln polymorphism with colorectal cancer risk: a HuGE meta analysis of 35 studies. Asian Pacific Journal of Cancer Prevention 16(8): 3285-3291.

Geng, P., Zhao, X., Xiang, L., Liao, Y., Wang, N., Ou, J., et al. (2014) Distinct role of CD86 polymorphisms (rs1129055, rs17281995) in risk of cancer: evidence from a meta-analysis. Plos one 9(11): e109131.

González, C.A., Sala, N. and Capellá, G. (2002) Genetic susceptibility and gastric cancer risk. International Journal of Cancer 100(3): 249-260.

Hu, J.Y., Wang, S., Zhu, J.G., Zhou, G.H. and Sun, Q.B. (1999) Expression of B7 costimulation molecules by colorectal cancer cells reducestumorigenicity and induces anti-tumor immunity. World Journal of Gastroenterology 5(2): 147.

Jemal, A., Bray, F., Center, M.M., Ferlay, J., Ward, E. and Forman, D. (2011) Global cancer statistics. A Cancer Journal for Clinicians 61(2):69-90.

Koido, S., Ohkusa, T., Homma, S., Namiki, Y., Takakura, K., Saito, K., et al. (2013) Immunotherapy for colorectal cancer. World journal of gastroenterology: World Journal of Gastroenterology 19(46): 8531.

Landi, D., Gemignani, F., Naccarati, A., Pardini, B., Vodicka, P., Vodickova, L., et al. (2008) Polymorphisms within micro-RNA-binding sites and risk of sporadic colorectal cancer. Carcinogenesis 29(3): 579-584.

Lenschow, D.J., Walunas, T.L. and Bluestone, J.A. (1996) CD28/B7 system of T cell costimulation. Annul Review of Immunology 14(1): 233-258.

Machado, J.C., Figueiredo, C., Canedo, P., Pharoah, P., Carvalho, R., Nabais, S., et al. (2003) A proinflammatory genetic profile increases the risk for chronic atrophic gastritis and gastric carcinoma. Gastroenterology 125(2): 364-371.

Milne, A.N., Carneiro, F., O'morain, C. and Offerhaus, G.J.A. (2009) Nature meets nurture: molecular genetics of gastric cancer. Human Genetic 126(5): 615-628.

Namazi, A., Forat-Yazdi, M., Jafari, M.A., Foroughi, E., Farahnak, S., Nasiri, R., et al. (2017) Association between polymorphisms of ERCC5 gene and susceptibility to gastric cancer: A systematic review and meta-analysis. Asian Pacific Journal of Cancer Prevention 18(10): 2611.

Namazi, A., Forat-Yazdi, M., Jafari, M., Farahnak, S., Nasiri, R., Foroughi, E., et al. (2018) Association of interleukin-10-1082 A/G (rs1800896) polymorphism with susceptibility to gastric cancer: meta-analysis of 6,101 cases and 8,557 controls. Arq Gastroenterol 55: 33-40.

Ohtani, H. (2007) Focus on TILs: prognostic significance of tumor infiltrating lymphocytes in human colorectal cancer. Cancer immunology 7(1).

Poorolajal, J., Moradi, L., Mohammadi, Y., Cheraghi, Z. and Gohari-Ensaf, F. (2020) Risk factors for stomach cancer: a systematic review and meta-analysis. Epidemiology and health 42.

Saeki, N., Saito, A., Choi, I.J., Matsuo, K., Ohnami, S., Totsuka, H., et al. (2011) A functional single nucleotide polymorphism in mucin 1, at chromosome 1q22, determines susceptibility to diffuse-type gastric cancer. Gastroenterology 140(3): 892-902.

Shademan, B., Masjedi, S., Karamad, V., Isazadeh, A., Sogutlu, F. and Nourazarian, A. (2022) CRISPR Technology in Cancer Diagnosis and Treatment: Opportunities and Challenges. Biochemical Genetics 1-25.

van der Merwe, P.A., Bodian, D.L., Daenke, S., Linsley, P. and Davis, S.J. (1997) CD80 (B7-1) binds both CD28 and CTLA-4 with a low affinity and very fast kinetics. Journal of Experimental Medicine 185(3) : 393-404.

Wu, X., Zeng, Z., Chen, B., Yu, J., Xue, L., Hao, Y., et al. (2010) Association between polymorphisms in interleukin-17A and interleukin-17F genes and risks of gastric cancer. International Journal of Cancer 127(1): 86-92.

Yin, M., Hu, Z., Tan, D., Ajani, J.A. and Wei, Q. (2009) Molecular epidemiology of genetic susceptibility to gastric cancer: focus on single nucleotide polymorphisms in gastric carcinogenesis. American Journal of Translational Research 1(1): 44.

Zhuang, W., Wu, X.T., Zhou, Y., Liu, L., Liu, G.J., Wu, T.X., et al. (2010) Interleukin10-592 promoter polymorphism associated with gastric cancer among Asians: a meta-analysis of epidemiologic studies. Digestive Diseases and Sciences 55(6): 1525-1532.

Research Article

Comparative Transcriptome Analyses of a Transgenic Sugar Beet Resistant to *Beet Necrotic Yellow Vein Virus*

Mahdieh Yousefiara [1], Mohammad Ali Malboobi [2 *], Abdolreza Bagheri [1 *], Nasrin Moshtaghi [1]

[1] *Biotechnology and Plant Breeding Department, Faculty of Agriculture, Ferdowsi University of Mashhad, Mashhad, Iran*
[2] *Institute of Agricultural Biotechnology, National Institute of Genetic Engineering and Biotechnology, Tehran, Iran*

Received 1 September 2022 Accepted 28 October 2022

Abstract

Genetic engineering is a powerful technology of the present century that has revolutionized the agricultural, health, pharmaceutical and food industries worldwide. It is important to identify changes caused by transgenes that may be attributed to unintended traits in the risk assessment of genetically modified (GM) crops. Rhizomania, which is caused by *beet necrotic yellow vein virus* (BNYVV) infection, is considered to be a significant constraint in order to produce sugar beet worldwide. The resistance of transgenic sugar beet plants to the BNYVV was previously developed through RNA silencing by expression of hairpin RNA (hpRNA) structures. In the present study, the RNA sequencing (RNA-seq) analysis was performed in order to evaluate the transcriptional changes of an event of transgenic sugar beet plants, named 219-T3:S3-13.2 (S3), with the non-transgenic parental plants grown in virus-infected soil. The results of the present study indicate that there are only 0.9% differentially expressed genes (DEGs) at significant levels. The functional analysis shows alterations of transcription in lipids, amino acids, and carbohydrates metabolisms, cellular processes (autophagy), hormone signal transduction, and biosynthesis of secondary metabolites in the transgenic event, which are related to stress-adaption for which most of the genes were up-regulated. All in all, we conclude that the presence of the transgenes does not have substantial effects on the plant gene expression patterns. This work also indicates that RNA-seq analysis can be useful to evaluate the unintended effects and risk assessment of GM sugar beet plants.

***Keywords*:** Safety assessment, RNA silencing, differentially expressed genes

Introduction

Widely acceptance and cultivation of genetically modified (GM) crops have made it the fastest-growing agricultural technology in the world. Cultivation of GM crops that are resistant to biotic and abiotic stress has benefits such as increasing farm income and crop production, as well as reducing the use of pesticides and greenhouse gas emissions (Liu and Stewart Jr, 2019). These complementary breeding techniques provide solutions for food security and climate change, and possibly introduce more desirable and wider range of food products to the market. The application of genetic engineering is only one part of agricultural innovation that contributes to the success of modern agriculture. However, like any new technology, possible risks must be assessed and managed, a task that has been left to legislators for the past 30 to 40 years (Turnbull et al., 2021).

The safety assessment of GM crops is considered based on the principle of substantial equivalence and also the analysis of comparative safety (Co-operation and Development, 1993; Kok and Kuiper, 2003; Organisms, 2011; Organization, 1996). This principle is based on the notion that a typical, almost non-GM near- isogenic type, as well as a history of safe usage can be considered as a comparator for the safety assessment of new GM crops (Benevenuto et al., 2022).

Agrobacterium-mediated transformation is one of the most common methods used to create GM crops. In the method mentioned above, transfer-DNA (T-DNA) from *Agrobacterium tumefactions* is inserted into the plant nuclear genome (Gelvin, 2017). Because of the stochastic nature of plant transformation mechanisms with *Agrobacterium*, transgenic cassettes can be integrated into genomic sites that may have unintended effects on the gene (Barros et al., 2010).

*Corresponding authors' e-mail addresses:
alimalboobi@gmail.com, abagheri@um.ac.ir,

In the recent decade, the roles of emerging "omics" technologies in the assessment of unintended transgene effects have been commonly proposed. In this regard, transcriptomics, proteomics and metabolomics are common technologies used to determine the molecular composition of a system as a measure of equivalence (Fu et al., 2021). With the advent of the next generation of sequencing and the increasing power of computing platforms, RNA sequencing (RNA-Seq or whole transcriptome shotgun sequencing) was developed and quickly replaced microarrays as the method of choice for transcriptomics with almost no bias (Almeida-Silva et al., 2021). The RNA-seq method usually involves identifying suitable biological samples (and replicates), isolating the whole RNA, enrichment of non-ribosomal RNAs, converting RNA to cDNA, building a fragmented library, sequencing on a high-throughput sequencing platform, generating single or paired-end reads with a length of 30-300 base, alignment or assembly of these reads and downstream analysis. In addition to whole transcriptome analysis, there are several ways of downstream analyses including transcript discovery and annotation, the possible gene regulation mechanisms, differential gene expression patterns, identification of alternative splicing products, allele-specific expression examination, RNA editing detection, viral detection, gene fusion detection, and other types of variant detection (Griffith et al., 2015). In particular, the RNA-Seq method facilitates the evaluation and analysis of genetic changes, mutations, and variations or differences in gene expression of different groups or treatments such as transgenic plants versus conventional plants (Matsaunyane and Dubery, 2018).

Recent advances on the next-generation of sequencing technologies along the releases of the sugar beet genome (Dohm et al., 2014) have made it possible to access more detailed information, as well as refined tools, in which they were not available before. So that, it can result in more accurate identifications of differentially expressed genes. Sugar beet (*Beta vulgaris* L. var. Saccharifera) is one of two main sugar crops worldwide that has a broad range of cultivation and significant economic values. The root is used to produce sugar, whereas the stem and leaf are used to feed and produce ethanol and biofuels (Dohm et al., 2014; Finkenstadt, 2014). Rhizomania, which is derived from the *beet necrotic yellow vein virus* (BNYVV), is considered one of the main restraints of sugar beet production in the world, so that it causes a severe reduction in sugar by 80 percent (Galein et al., 2018). The BNYVV is a member of the genus *Benyvirus* within the family *Benyviridae* (Liebe et al., 2020), a soil-borne virus transmitted by the plasmodiophorid *Polymyxa beta*. It has a multi-part genome that contains 4 or 5 positive single-stranded RNAs. Subsequently, Zare et al. (2015) have developed the BNYVV-resistant transgenic sugar beet plants and S3 event using the promoted RNA silencing versus the BNYVV by expressing the hairpin RNA (hpRNA) structures (Zare et al., 2015).

Transcriptomics approach has an important role in the assessment of potential differences between two genotypes due to the extensive coverage of plant pathways and metabolic networks compared to other "omics" approaches (Barros et al., 2010). This study focused on the transcriptomics approach of the RNA sequencing (RNA-seq) in order to identification of possible unintended effects in transgenic events. Since rhizomania virus disease significantly reduces the amount of sugar extracted from sugar beet roots and RNA silencing gets more active after soil-borne virus infection, we compared the root transcriptome profiles of wild-type (WT) sugar beet genotype 9597 (non-transgenic counterpart), as a controlling factor, with a transgenic event, which is named 219-T3:S3-13.2 (S3).

In the present study, the main hypothesis was defined that T-DNA insertion has no unintended effect on transgenic sugar beet plan. We considered probable tiny differences between transgenic sugar beet plants and their non-transgenic counterparts. The crucial question in this research is whether any difference in the transcriptome or not?

Materials and Methods

Plant Materials and Growth Conditions

The transgenic sugar beet (*Beta vulgaris* L.) event, i.e. 219-T3: S3-13.2 or IHP-P (S3), which was previously developed at the National Institute of Genetics Engineering and Biotechnology and has been performed in the present study. IHP-P carrying two copies of 5′-UTR of RNA2 with the gene sequence encoding P21 coat protein, so that they were placed in the sense and antisense connected by an intron expressing hpRNAs (Zare et al., 2015). Wild-type parental plants Var. 9597 (WT) was kindly provided by the Sugar Beet Seed Institute. Homozygous transgenic sugar beet seeds derived from the third generation and Var. 9597 (WT) seeds were planted in small pots consisting of equal amounts of autoclaved sand and garden soil at phytotron (i.e. under conditions of 16/8h light/dark, photoperiod 25/20°Cday/night and relative humidity

of 60%) in. After eight weeks of doing that step, each plant was transferred to the 1-L pot containing soil infested with the BNYVV collected from a farm around Shiraz city, Iran. All contaminated soils were diluted one to one with a 1:1:1 (v/v/v) sterilized mixture of peat, perlite, and vermiculite. Plants grew in a growing room with a light cycle of 16/8 hours of light/darkness at temperature of 25-30°C. After 3 months, the roots of plants were harvested and washed to remove the soil. The roots of plants were immediately frozen by liquid nitrogen and stored at temperature of -80°C for the RNA extraction.

RNA extraction and sequencing

The total RNA was derived from the roots of four samples including WT1 and WT2 for non-transgenic counterparts, and S31, S33 for S3 events, using the RNX plus solution according to the manufactur's instructions (SINACLON, Iran). RNA pellets were dissolved in water DEPC treated water. The total RNA was treated with DNAaseI (SINACLON, Tehran, Iran) to eliminate possible contamination of genomic DNA and then heat treatment (55°C for 10 minutes) to inactivate the enzyme and stored at temperature of -80°C. The quality of RNA was determined by the optical density (OD) ration values of OD260: OD280 and OD260: OD230, and also integrity was evaluated by 1% agarose gel electrophoresis. The RNA library and sequencing were built by the Novogene Corporation (Beijing). In summary, poly (A) $^{+}$RNA was enriched with the total RNA by oligo(dT) beads. Then, the mRNA was randomly fragmented by the Novogene Corporation (Beijing), furthermore, the cDNA was synthesized using random hexamers. The library construction includes the A-tailing, terminal repair, size selection, ligation of sequencing adapters and PCR enrichment. Paired sequencing was performed on the HiSeq 5000 Illumina platform.

RNA sequence analysis

The software "FastQC" (version 0.11.5) was utilized to control the RNA-seq data quality. Reads were cleaned using the software "Trimmomatic" (version 0.39; http://www.usadellab.org/cms/?page=trimmomatic) . Then, the clean reads were mapped to the reference genome sequence of the Sugar beet (GeneBank assembly accession, RefBeet-1.2.2) using the software "Hisat2" (version 2.2.1; http://daehwankimlab.github.io/hisat2/download/) with the default parameters. Sorting of reads was done using the software "Samtools" (www.htslib.org/download/), and subsequently the assembly of reads was performed using the software "StringTie" (https://ccb.jhu.edu/software/stringtie/). The software "Cuffdiff" (http://cole-trapnell-lab.github.io/cufflinks/) was used to identify genes, in which they were differentially expressed between every pair of samples. The q-value were considered as differentially expressed genes when gene expression is less than 0.05, and also their expression as an up-regulated or down-regulated was determined by the factor $\log_2$ fold change (FC), $+2 \leq \log_2 FC \leq -2$, respectively. We performed the enrichment analysis to evaluate the function and biological pathways of the differentially expressed genes (DEGs) by the software "KOBAS" (http://kobas.cbi.pku.edu.cn/home.do) using databases like the gene ontology (GO), encyclopedia of Kyoto genes, and genomes (KEGG). DEGs were significantly enriched in metabolic pathways when their Benjamini and Hochberg's-corrected *P*-values are less than 0.05. The volcano plot, heatmap, and Venn diagrams of the GO analysis were produced using the R package ggplots (https://www.rstudio.com).

Results

Assessment of RNA-seq data and mapping

The Illumina cDNA sequencing was conducted on libraries prepared from roots of two transgenic events, as well as two non-transgenic counterparts (WT). The RNA sequencing results of sugar beet roots were calculated through about 20.8 GB of data consisting of between 41 and 50 million of 150-bp paired-end raw reads for each library with Q20 above 97% and Q30 above 92%. These results indicate that the quality of RNA-seq data is adequate for the subsequent analysis. After trimming the reads, clean reads were mapped to the sugar beet reference genome (Accession No. RefBeet-1.2.2, Table 1).

Table 1. Statistics of the RNA sequencing results of sugar beet roots infested by the BNYVV.

Sample	Raw reads	Clean reads	Alignment rates (%)	Q20[a](%)	Q30[b](%)	GC(%)
WT1	43527574	43094660	69.34	97.47	92.69	43.00
WT2	45655544	45175322	68.54	97.44	92.65	42.64
S31	48711000	48154782	87.04	97.32	92.47	43.28
S33	41409562	40832888	66.46	97.47	92.97	43.26

[a,b]Q_{phred}, the base quality values; Q_{phred}=-10$\log_{10}$(e); Q20, error rate 1/100; Q30, error rate 1/1000.

Analysis of differentially expressed genes

The software "Cufflinks" was utilized to detect DEGs using a q-value<0.05 for reporting up- and down-regulated genes between S3 and WT. Overall, the expression of 37447 genes are compared between S3 and WT, out of which 343 genes were found as DEGs. This result corresponds to the difference in expression of about 0.9% of genes (310 upregulated; 33 downregulated) (Supplementary data file 1). In the present study, we focused on the most important genes and further narrowed down the number of DEGs. It was done by applying a stringent threshold for the log2-fold change or higher, so that it resulted in 308 DEGs within the S3_WT DEGs dataset (277 upregulated; 31 downregulated).

To illustrate the difference between plants, a heat map was provided using the R software for high differentially expressed genes in the S3 event versus WT (Figure 1). A volcano plot is also constructed using data shown in Figure 2. The volcano plot illustrates the relationship between FC and the statistical significance of DEGs.

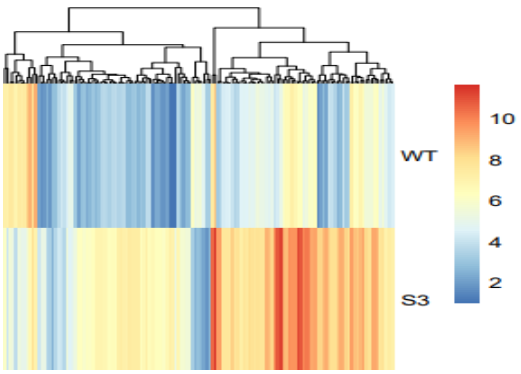

Figure 1. Heatmap generated for the differentially expressed genes of sugar beet roots infested by the BNYVV, which is reported by cufflinks analyses. Genes are arranged in descending order based on FC. Red and blue colors, respectively, represent higher and lower levels of gene expression.

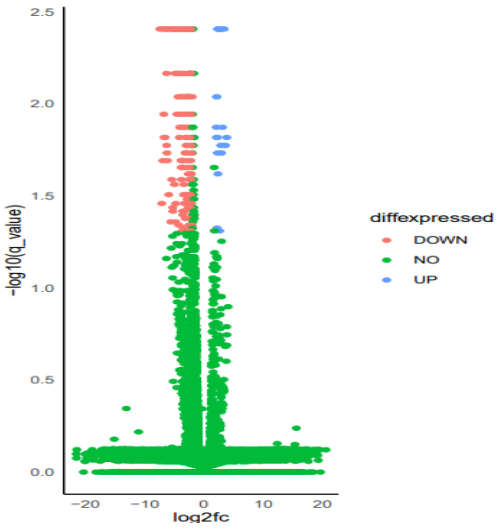

Figure 2. A volcano plot for the differentially expressed genes of sugar beet roots infested by the BNYVV. Each plotted dot indicates an individual gene. Green dots represent genes with no significant differentially expressed, whereas red and blue dots represent significant DEGs.

GO annotation and enrichment analysis of differentially expressed genes

In order to elucidate the possible changes in biological pathways, we performed a functional enrichment analysis of the DEGs based on the KEGG data using the software "KOBAS" (version 3.0). As shown in Figure 3, most of the changes occurred in metabolic pathways when comparing the infected transgenic event and WT transcriptomes. The increased ratios led to a health of the transgenic event despite of the BNYVV infestation.

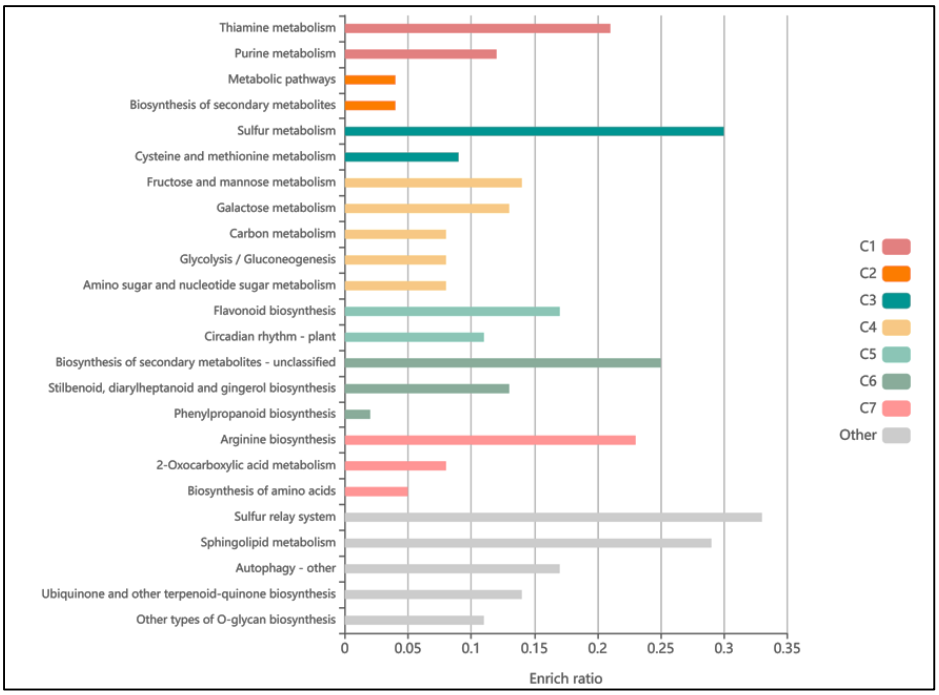

Figure 3. A bar plot showing the KEGG pathway enrichment of DEGs in S3_WT dataset for sugar beets infested by the BNYVV. S3_WT are up-regulated. In this bar plot, each row indicates an enriched function, and the bar length represents the enrichment ratio. The enrichment ratio is calculated as the "number of input genes"/"number of background genes".

The GO classification resulted in 66 terms for the identified genes with increased expression levels within the S3_WT dataset comparison. Overexpressions are considerable in 19 terms and 4 main biochemical pathways. These four major pathways are metabolism, environmental signal processing, genetic information processing and cellular processes. No pathway was found for genes with the reduced expression levels within the S3_WT dataset (Figure 3 and Supplementary data file 2).

According to analyses of the GO and KEGG pathway, 11 pathways including cellular processes, environmental information processing, genetic information processing, energy metabolism, organismal systems, lipid metabolism, amino acid metabolism, carbohydrate metabolism, metabolism of cofactors and vitamins, biosynthesis of secondary metabolites and nucleotide metabolism have shown significant enrichment ratios (Table 2). Such pathways are calculated as the "number of input genes"/"number of background genes". In a comparison between the transgenic S3 event and WT, the enriched GO terms were shown in 19 terms including sulfur relay system (3 out of 9 genes , 33.33 %), sulfur metabolism (7 out of 23 genes, 30.43%), sphingolipid metabolism (6 out of 21 genes, 28.57 %), biosynthesis of secondary metabolites – unclassified (3 out of 12 genes , 25 %), arginine biosynthesis (7 out of 31 genes , 22.58 %), thiamine metabolism (5 out of 24 genes , 20.83 %), flavonoid biosynthesis (9 out of 52 genes , 17.3 %), autophagy – other (5 out of 29 genes , 17.24 %), ubiquinone and other terpenoid-quinone biosynthesis (5 out of 36 genes , 13.88 %), fructose and mannose metabolism (7 out of 51 genes , 13.72 %), galactose metabolism (6 out of 48 genes , 12.5 %), purine metabolism (9 out of 77 genes , 11.68 %), cysteine and methionine metabolism (7 out of 79 genes , 8.86 %), carbon metabolism (17 out of 207 genes , 8.21 %), plant hormone signal transduction (15 out of 187 genes , 8.02 %), glycolysis / gluconeogenesis (8 out of 104 genes , 7.69 %), amino sugar and nucleotide sugar metabolism (8 out of 105 genes , 7.61 %), metabolic pathways (85 out of 1940 genes , 4.38 %) and biosynthesis of secondary metabolites (41 out of 974 genes , 4.20 %) were differentially expressed, so that all terms have been described as being up-regulated (Figure 3 and Supplementary data file 2). In summary, the

transgenic plants (S3) have revealed by up-regulation in some genes involved in the main pathways related to secondary metabolites, cellular processes, lipid metabolism, carbohydrate metabolism and amino acid metabolism (Table 2). Therefore, they are well-known defense responses of plants under a variety of stress conditions. As expected, plant hormone signal transduction, which is responsible for the plant-pathogen interactions, was also significantly up- regulated for the S3.

Discussion

Engineering of the virus-resistant transgenic crops by RNA silencing uses naturally defense mechanism of plants against viruses (Giudice et al., 2021). Moreover, a rapid cleavage of RNA transcripts up to the undetectable level and also lack of protein production reduce the safety risks related to toxic and allergenic compounds. These benefits make it a promising, sustainable, and environmentally friendly tool for the commercial release of virus-resistant transgenic products (Zare et al., 2015).

However, the main concern for transgenic crops is the public acceptance of this technology. Utilizing of exogenous DNA sequences into the plant genome may cause adverse effects such as silencing and/or modification of active genes, physical disruption, activation of silent genes, inactivation of endogenous genes, regulation of other genes through influencing biochemical pathways, and fusion protein formation (Jiang et al., 2017). The process of obtaining transgenic plants may affect the host plant genome. These concerns promoted the use of the unbiased high-throughput "omics" technologies to validate the substantial equivalence.

In the present study, we utilized the RNA-seq technique to investigate the possibility of detecting differentially expressed genes, which are derived from T-DNA insertion in the root of a transgenic sugar beet plants, S3-219 event. Our results show a differential expression of about 0.9% in the analyzed transcripts between S3 and WT.

Several studies used the RNA-seq technique to compare transcriptomes of transgenic plants with their non-transgenic counterpart to find possible changes in metabolism of papaya (*Coat protein of papaya ring spot virus* (PRSV) for resistance against the virus), wheat (*Glycine max* drought-responsive element-binding factor (GmDREB1) for drought- and salt-tolerant), *Bt* rice and maize (EPSPS and *Cry*1Ab genes) (Fu et al., 2019; Fu et al., 2021)(Fang et al., 2016; Jiang et al., 2017. Furthermore, several previous works that used microarray to investigate the transcriptome profile have reported similar results for wheat plants producing high level of gluten subunits (Baudo et al., 2006), rice plants that produce CsFv antibodies (Batista et al., 2008), glyphosate-resistant soybeans (Cheng et al., 2008), MON810 (insect-resistant maize), in which very limited transcriptional and diversity-dependent transcriptional regulations (Coll et al., 2008), this event, as well as glyphosate-tolerant NK603 maize, had fewer transcriptional differences than changes resulted from conventional breeding and environmental factors (Barros et al., 2010), rice plants that produce antifungal proteins (Montero et al., 2011) and barley plants that produce endo-chitinase involved in defense against stresses (Kogel et al., 2010).

However, a few studies have reported significant differences between transcripts of transgenic plants and their isogenic counterparts (Ben Ali et al., 2020; Ko et al., 2018; Lambirth et al., 2015). Schnell et al. (2015) indicated that the effects of insertion are inevitable results of genetic engineering, however, the introduction of unwanted traits is not. They also showed that genetic changes, such as the movement of transposable elements, the non-homologous end-binding process applied on double-stranded fractures and the intracellular transfer of organelle DNA, are comparable to the effects of insertion occurrence in plants. Thus, the effects of genetic engineering-related insertions are comparable to the genetic changes in naturally grown plants too. In light of this conclusion, a more extensive study of how genetic changes occur indicates plant genomes are constantly changing and, therefore, the effects of insertion have a relatively small contribution to the final genetic composition of plant species (Schnell et al., 2015).

The GO annotation and enrichment analysis of differently expressed genes exhibited the S3 event is shows by more changes in biological pathways than its non-transgenic counterparts. Some genes were all up-regulated in 11 biological pathways (Table 2) that can be due to resistance to the viral propagation.

Given that the study samples were taken from plants challenged with the virus, the difference in gene expression is not far-fetched. As a result of viral infections, plants can show changes in several metabolic pathways (Weiland et al, 2020). Carbohydrate metabolism changes in response to viral infections, which can be seen as changes in glucose levels and the expression of genes involved in glucose metabolism. Plants can also react to viral infections by altering the production of amino acids

which are required for plant defense responses and the multiplication of viruses (Kogovšek et al., 2016). When plants are exposed to pathogens, they produce secondary metabolites and pathogen-related proteins which are involved in plant defense (Kogovšek et al., 2016). It has also been suggested that differences between transgenic and non-transgenic materials may be observed under stress conditions. These findings indicate that the environment play an effective role on gene expression than gene modification as shown by previous publications, for instance in maize (Barros et al., 2010; Fu et al., 2021), rice (Batista et al., 2008; Fu et al., 2019), wheat (Baudo et al., 2006; Jiang et al., 2017), barley (Kogel et al., 2010), papaya (Fang et al., 2016) and soybean (Cheng et al., 2008). In addition, some studies have shown that inserting transgenes is very similar to the process of stress exposure, which triggers the expression of defense genes for adaptation and increased stress tolerance of transgenic plants (Fu et al., 2019; Montero et al., 2011; Jiang et al., 2017).

In the present study, patterns of variable expression of genes involved in biological pathways including lipids, amino acids, and carbohydrates metabolisms, cellular processes, biosynthesis of secondary metabolites and plant hormone signal transduction in S3 reflect significant gene expression changes, which occurred after gene insertion and may has an important role in plant resistance to the virus. In a previous study, it was also showed that alterations in the root protein profiles of transgenic plants were less than 8% compared to their non-transgenic counterparts. Different proteins are most likely related to the metabolism and defense/stress response (Hejri et al., 2021).

Conclusion

In this study, transcriptome analysis of silencing-induced transgenic sugar beet plants and non-transgenic counterparts were conducted while being exposed to the BNYVV. Our results show that there are slight differences in transcript, so that DEGs at significant levels consist of just 0.9% of transcriptomes of the parental wild-type plants versus the transgenic event. A number of DEGs are characterized as up-regulated genes, which is mainly related to pathogen resistance and stress tolerance, involved in carbohydrate, lipid, and amino acid metabolism, cellular processes, biosynthesis of secondary metabolites and hormone signaling pathways. These findings show that the T-DNA insertion does not activate unintended adverse effects following to gene expression in the roots of transgenic sugar beet. Many differentially expressed genes can be due to the enhanced pathogen resistance of transgenic sugar beet and well-being status of it. In our future study, we will survey the content of small-RNA produced through RNA silencing technique in transgenic plants. We will also investigate the presence of other viruses in the field-grown sugar beet plants which affects the severity of rhizomania disease.

Table 2. Significantly enriched KEGG pathways of sugar beet roots S3 _ WT infested by the BNYVV.

Main Pathway[a]	Pathway category	Enrich ratio
Environmental Information Processing	plant hormone signal transduction	8.02 %
Cellular Processes	Autophagy – other	17.24 %
Genetic Information Processing	Sulfur relay system	33.33 %
Organismal Systems	Circadian rhythm - plant	10.52 %
Energy metabolism	Sulfur metabolism	30.43 %
Lipid metabolism	Sphingolipid metabolism	28.57 %
Amino acid metabolism	Arginine biosynthesis; Cysteine and methionine metabolism	22.58 % 8.86 %
Metabolism of cofactors and vitamins	Thiamine metabolism; Ubiquinone and other terpenoid-quinone biosynthesis	20.83 % 13.88 %
Carbohydrate metabolism	Fructose and mannose metabolism;	13.72 %

	Galactose metabolism; Glycolysis	12.5 %
	Gluconeogenesis; Amino sugar and nucleotide	7.69 %
	sugar metabolism	7.61 %
Nucleotide metabolism	Purine metabolism	11.68 %
Biosynthesis of secondary metabolites	Flavonoid biosynthesis	17.30 %

[a] Only pathways with a p value of <0.05 were considered significantly enriched in this table.

Supplementary data

Supplementary data file 1. DEGs S3_WT dataset (XLS).

Supplementary data file 2. Function enrichment S3_WT up-regulated (XLS).

Acknowledgment

The financial support from the National Institute of Genetic Engineering and Biotechnology through grant No.102M and the Ferdowsi University of Mashhad through the Project No. 37010 are gratefully acknowledged.

Conflict of Interest

No conflict of interest was reported by the author(s).

References

Almeida-Silva F., Moharana K. C. and Venancio T. M. (2021) The state of the art in soybean transcriptomics resources and gene coexpression networks. in silico Plants 3: https://doi.org/10.1093/insilicoplants/diab005.

Barros E., Lezar S., Anttonen M. J., Van Dijk J. P., Röhlig R. M., Kok E. J. and Engel K. H. (2010) Comparison of two GM maize varieties with a near-isogenic non-GM variety using transcriptomics, proteomics and metabolomics. Plant Biotechnology Journal 8:436-451.

Batista R., Saibo N., Lourenço T. and Oliveira M. M. (2008) Microarray analyses reveal that plant mutagenesis may induce more transcriptomic changes than transgene insertion. Proceedings of the National Academy of Sciences 105:3640-3645.

Baudo M. M., Lyons R., Powers S., Pastori G. M., Edwards K. J., Holdsworth M. J. and Shewry P. R. (2006) Transgenesis has less impact on the transcriptome of wheat grain than conventional breeding. Plant Biotechnology Journal 4:369-380.

Ben Ali S.-E., Draxler A., Poelzl D., Agapito-Tenfen S., Hochegger R., Haslberger A. G. and Brandes C. (2020) Analysis of transcriptomic differences between NK603 maize and near-isogenic varieties using RNA sequencing and RT-qPCR. Environmental Sciences Europe 32:1-23.

Benevenuto R. F., Venter H. J., Zanatta C. B., Nodari R. O. and Agapito-Tenfen S. Z. (2022) Alterations in genetically modified crops assessed by omics studies: Systematic review and meta-analysis. Trends in Food Science & Technology 120: 325-337.

Cheng K. C., Beaulieu J., Iquira E., Belzile F., Fortin M. and Strömvik M. (2008) Effect of transgenes on global gene expression in soybean is within the natural range of variation of conventional cultivars. Journal of Agricultural and Food Chemistry 56:3057-3067.

Coll A., Nadal A., Palaudelmas M., Messeguer J., Melé E., Puigdomenech P. and Pla M. (2008) Lack of repeatable differential expression patterns between MON810 and comparable commercial varieties of maize. Plant Molecular Biology 68:105-117.

Dohm J. C., Minoche A. E., Holtgräwe D., Capella-Gutiérrez S., Zakrzewski F., Tafer H., Rupp O., Sörensen T. R., Stracke R. and Reinhardt R. (2014) The genome of the recently domesticated crop plant sugar beet (Beta vulgaris). Nature 505:546-549.

EFSA (2011) Panel on Genetically Modified Organisms (GMO)—Guidance for risk assessment of food and feed from genetically modified plants. EFSA J., 9, 2150.

Fang, J., Lin, A., Qiu, W., Cai, H., Umar, M., Chen, R., & Ming, R. (2016). Transcriptome profiling revealed stress-induced and disease resistance genes up-regulated in PRSV resistant transgenic papaya. Frontiers in Plant Science, 7, 855.

FAO; WHO (1996) Biotechnology and Food Safety. In Report of a Joint FAO/WHO Consultation; FAO Food and nutrition paper 61; Food and Agriculture Organization: Rome, Italy, ISBN 92-5-103911-9.

Finkenstadt V. L. (2014) A review on the complete utilization of the sugarbeet. Sugar Tech 16:339-346.

Fu W., Wang C., Xu W., Zhu P., Lu Y., Wei S., Wu X., Wu Y., Zhao Y. and Zhu S. (2019) Unintended effects of transgenic rice revealed by transcriptome and metabolism. GM Crops & Food 10:20-34.

Fu W., Zhu P., Qu M., Zhi W., Zhang Y., Li F. and Zhu S. (2021) Evaluation on reprogramed biological processes in transgenic maize varieties using transcriptomics and metabolomics. Scientific Reports 11:1-13.

Galein Y., Legrève A. and Bragard C. (2018) Long term management of rhizomania disease—Insight into the changes of the beet necrotic yellow vein virus RNA-3 observed under resistant and non-resistant sugar beet fields. Frontiers in Plant Science 9:795.

Gelvin S. B. (2017) Integration of Agrobacterium T-DNA into the plant genome. Annual Review of Genetics 51:195-217.

Giudice G., Moffa L., Varotto S., Cardone M. F., Bergamini C., De Lorenzis G., Velasco R., Nerva L. and Chitarra W. (2021) Novel and emerging biotechnological crop protection approaches. Plant Biotechnology Journal 19:1495-1510.

Griffith M., Walker J. R., Spies N. C., Ainscough B. J. and Griffith O. L. (2015) Informatics for RNA sequencing: a web resource for analysis on the cloud. PLoS Computational Biology 11:e1004393.

Hejri S., Salimi A., Malboobi M. A. and Fatehi F. (2021) Comparative proteome analyses of rhizomania resistant transgenic sugar beets based on RNA silencing mechanism. GM Crops & Food 12:419-433.

Jiang Q., Niu F., Sun X., Hu Z., Li X., Ma Y. and Zhang H. (2017) RNA-seq analysis of unintended effects in transgenic wheat overexpressing the transcription factor GmDREB1. The Crop Journal 5:207-218.

Ko D. K., Nadakuduti S. S., Douches D. S. and Buell C. R. (2018) Transcriptome profiling of transgenic potato plants provides insights into variability caused by plant transformation. PLoS One 13:e0206055.

Kogel K.-H., Voll L. M., Schäfer P., Jansen C., Wu Y., Langen G., Imani J., Hofmann J., Schmiedl A. and Sonnewald S. (2010) Transcriptome and metabolome profiling of field-grown transgenic barley lack induced differences but show cultivar-specific variances. Proceedings of the National Academy of Sciences 107:6198-6203.

Kogovšek P., Pompe-Novak M., Petek M., Fragner L., Weckwerth W. and Gruden K. (2016) Primary metabolism, phenylpropanoids and antioxidant pathways are regulated in potato as a response to Potato virus Y infection. PLoS One 11:e0146135.

Kok E. J. and Kuiper H. A. (2003) Comparative safety assessment for biotech crops. TRENDS in Biotechnology 21:439-444.

Lambirth K. C., Whaley A. M., Blakley I. C., Schlueter J. A., Bost K. L., Loraine A. E. and Piller K. J. (2015) A comparison of transgenic and wild type soybean seeds: analysis of transcriptome profiles using RNA-Seq. BMC Biotechnology 15:1-17.

Liebe S., Wibberg D., Maiss E. and Varrelmann M. (2020) Application of a reverse genetic system for beet necrotic yellow vein virus to study Rz1 resistance response in sugar beet. Frontiers in Plant Science 10:1703.

Liu Y. and Stewart Jr C. N. (2019) An exposure pathway-based risk assessment system for GM plants. Plant Biotechnology Journal 17:1859.

Matsaunyane L. B. and Dubery I. A. (2018) Molecular Approaches to Address Intended and Unintended Effects and Substantial Equivalence of Genetically Modified Crops. *In* Transgenic Crops-Emerging Trends and Future Perspectives. IntechOpen London.

Montero M., Coll A., Nadal A., Messeguer J. and Pla M. (2011) Only half the transcriptomic differences between resistant genetically modified and conventional rice are associated with the transgene. Plant Biotechnology Journal 9:693-702.

OECD (1993) Safety Evaluation of Foods Derived by Modern Biotechnology, Concepts and Principles; Organization for Economic Cooperation and Development: Paris, France.

Schnell J., Steele M., Bean J., Neuspiel M., Girard C., Dormann N., Pearson C., Savoie A., Bourbonniere L. and Macdonald P. (2015) A comparative analysis of insertional effects in genetically engineered plants: considerations for pre-market assessments. Transgenic Research 24:1-17.

Turnbull C., Lillemo M. and Hvoslef-Eide T. A. (2021) Global regulation of genetically modified crops amid the gene edited crop boom–a review. Frontiers in Plant Science 12:630396.

Weiland, J. J., Sharma Poudel, R., Flobinus, A., Cook, D. E., Secor, G. A., & Bolton, M. D. (2020). RNAseq analysis of rhizomania-infected sugar beet provides the first genome sequence of beet necrotic yellow vein virus from the USA and identifies a novel alphanecrovirus and putative satellite viruses. Viruses, 12(6), 626.

Zare B., Niazi A., Sattari R., Aghelpasand H., Zamani K., Sabet M., Moshiri F., Darabie S., Daneshvar M. and Norouzi P. (2015) Resistance against rhizomania disease via RNA silencing in sugar beet. Plant Pathology 64:35-42.

Journal of Cell and Molecular Research (2022) 14 (1), 54-62 DOI: 10.22067/jcmr.2022.78495.1047

Research Article

Investigating the Effect of Stable Glutamine on the Neuronal Differentiation of PC-12 Cells in 2D- and 3D-Culture Media

Seyed Majid Jalalian Hosseini [1], Javad Baharara [2 *], Shahrbanoo Oryan [3], Mohammad Amin Kerachian [4,5]

[1] *Department of Biology, Science and Research Branch, Islamic Azad University, Tehran, Iran*
[2] *Department of Biology and Research Center for Animal Development Applied Biology, Mashhad Branch, Islamic Azad University, Mashhad, Iran*
[3] *Department of Zoology, Faculty of Biological Sciences, Kharazmi University, Tehran, Iran*
[4] *Medical Genetics Research Center, Mashhad University of Medical Sciences, Mashhad, Iran*
[5] *Department of Medical Genetics, Faculty of Medicine, University of Medical Sciences, Mashhad, Iran*

Received 29 August 2022 Accepted 28 October 2022

Abstract

Glutamine (Gln) is an essential amino acid with a wide range of cellular functions and is necessary for cell proliferation. It is usually added to the culture media in the form of L-glutamine, which is highly unstable and degrades in a temperature-dependent manner during the culture period. Although, Gln is beneficial for the cells, its degradation produces ammonia which is toxic and negatively affect cell culture. Pheochromocytoma cells (PC-12), originating from cancerous cells of the rat adrenal gland, are considered as a suitable model to study the differentiating effects of different factors. Previous studies showed the importance of Gln in the normal growth and differentiation of the cells. Alginate, is one of the biomaterials currently used as a natural scaffold for the induction of neuronal differentiation. In the present experimental research, the effect of stable and elevated levels of Gln on the growth and neuronal differentiation of PC-12 cells was compared under 2D- and 3D- (sodium alginate hydrogel beads) culture conditions. The cells' viabilities were determined and compared between experimental groups using live/dead cell staining by Acridine orange/Propidium iodide (AO/PI), and the 3-(4,5-dimethylthiazol-2-yl)-2,5-diphenyltetrazolium bromide (MTT) test. Furthermore, cells were stained using cresyl violet to detect neuronal Nissl bodies. The induction of differentiation was confirmed using immunocytochemical analysis of Nestin and β-tubulin III proteins and Cells' nuclei were counterstained with 4′,6-diamidino-2-phenylindole (DAPI). Results showed that high concentration of Gln can induce neuronal differentiation in PC-12 cells under both 2D- and 3D- culture conditions and increases the expression of progenitor and mature neuronal markers Nestin and β-tubulin III, respectively.

Keywords*: *Neural differentiation, Glutamine, PC-12 cells, Alginate

Introduction

Glutamine (Gln) is a conditionally essential amino acid in animals and is the most abundant free amino acid in the body. Gln has a wide range of cellular and physiological functions, including protein synthesis, lipid metabolism, and cell growth. Since Gln is involved in the nucleic acid biosynthesis it is essential for cell proliferation (Sarkadi et al., 2020; Suh et al., 2022). Furthermore, it is the main energy supply substance of mitochondria. The oxidation of Gln can eliminate some strong oxidizing substances in cells. (Zhao et al., 2019). Both intracellular and extracellular (free) Gln are essential for neuronal health considering their significant neuroprotective effects (Wang et al., 2019).

It was determined that Gln has different effects on gene expression profile of intestinal cells based on its concentration (Ban& Kozar, 2010). Many studies showed the impact of Gln on the growth, proliferation, and differentiation of different cell types during tissue engineering studies (Ban& Kozar, 2010; Yousefi Taemeh et al., 2021; Brose et al., 2014). For instance, in a previous study it was confirmed that Gln improves intestinal cell proliferation and stem cell differentiation in mice (Chen et al., 2018). Moreover, it can reduce muscle cells damage and inflammation (Raizel & Tirapegui, 2018).

* Corresponding author's e-mail addresses:
baharara@yahoo.com, *baharara@mshdiau.ac.ir*

Gln is usually added to the culture media in the form of L-glutamine and at the concentration of 2mM. It is highly unstable and degrades in a temperature-dependent manner during the culture period. Although Gln is yet effective at very low concentrations, differentiated cells require much higher concentrations of Gln to survive (Rubin et al., 2019). The degradation of Gln produces ammonia which is toxic for the cells in the culture. Glutamine dipeptides, such as GlutaMAX (Glx), which is commercially available, are more stable and are resistant to the degradation. Hence, Glx can be used at higher concentrations and for long-term culture conditions (Yousefi Taemeh et al., 2021). Despite the numerous studies in the field, the application of the stable form of Gln at high concentrations still requires more research.

Pheochromocytoma cells (PC-12) are originated from rat neuroendocrine tumor pheochromocytoma, which is the tumor of the chromaffin cells of the adrenal medulla. These cells are considered as a suitable model cell line to study the differentiation induction potential of different compounds. When these cells are exposed with proper concentrations of nerve growth factor (NGF), their proliferation slows down, and they adopt the appearance of neurons (Darbinian et al., 2013; Gordon et al., 2013). Alginate, alginic acid, is a polysaccharide obtained from the cell wall of brown algae (Mobini et al., 2019). Alginate is one of the biomaterials with high biocompatibility, high degradability, and non-antigenic properties which is currently used as a natural scaffold for neuro-regeneration (Yi et al., 2019). Alginate can promote the survival and growth of Schwann cells and neurite outgrowth in nerve cells. It was shown that alginate increases axon elongation in the nervous system of mice (Akter et al., 2016).

The present study evaluated the capabilities of PC-12 cells under 2D- and 3D- culture conditions to simulate *in vivo* conditions for the induction of neural differentiation at a high concentration of Gln. Our results showed that high concentration of Gln under both 2D- and 3D- culture conditions can induce neuronal differentiation in PC-12 cells as well as the expression of neuronal markers Nestin (a marker of neural progenitors) and β-tubulin III (a marker of mature neurons). Hence, it could be a novel strategy to generate neural cells for *in vitro* and *in vivo* experiments.

Materials and Methods

Experimental groups

2D-culture; PC-12 cells were cultured in the polystyrene flasks (3×10^4 cell/ml). In the treatment group, cells received Gln at a concentration of 40mM for 7d (GLN), while in the control group they received no Gln (PC-12) (stable glutamine;GlutaMAX, Gibco-USA).

3D culture; Alginate-encapsulated PC-12 cells cultured in a six-well plates containing Gln (40Mm) for 7d (from day 8 to14) (ALG+GLN). No Gln was added to the beads' culture media at control groups (ALGINATE).

PC-12 cell line

PC-12 cell line was purchased from Pasteur Institute cell bank, Tehran, Iran. The Roswell Park Memorial Institute (RPMI1640; Gibco-USA) medium supplemented with 10% fetal bovine serum (FBS; Gibco-USA), 5% horse serum (HS; Sigma-USA), and 1% penicillin/streptomycin (PS; Sigma-USA), was applied as the culture media. Cells were incubated in the presence of 5% carbon dioxide (CO_2), 90% humidity, and a temperature of 37°C (Memmert; Germany). Upon reaching 80% confluency, cells were sub-cultured, and applied for downstream assays (Abe et al., 2015).

Encapsulation of PC-12 cells in sodium alginate hydrogel

To prepare alginate hydrogel, sodium alginic acid (Sigma-USA) (0.3gr) was dissolved in 10ml of deionized water (3% v/w), and sterilized (autoclave; 121°C for 15min). 1ml of cell suspension, containing 3×10^6 cells, was considered per ml of alginate. Alginate beads were prepared by dripping the mixture onto a 6-well plates containing 102mM calcium chloride (Sigma-USA) using a 21-gauge syringe. They were incubated at RT under sterile conditions for 20min. Then, solution was removed from each well and remained beads were washed with Phosphate Buffered Saline (PBS; 3 times) and RPMI1640 culture medium (1 time). Following the washing steps, beads were transferred to another plate with complete RPMI1640 culture medium. To induce neuronal differentiation, the medium was exchanged with the freshly prepared differentiation medium every other day for 14d (Razavi et al., 2015).

Morphological observations

2D- and 3D-cultures were carefully observed by an inverted microscope (Olympus, IX70-Japan) with 200X magnification. Features such as cell appearances, growth rate of the colonies, neurite

formation, and the appearance of alginate beads were monitored.

Cell viability (MTT) assay

PC-12 cells encapsulated in alginate beads were kept inside 6-well plates (CO_2 incubator; 37°C, 14d). After draining the culture medium 10 beads were broken in a microtube and transferred to the 96-well plates on 10 and 14d; Then, MTT solution (Sigma, USA;100µl of 1µg/ml solution) was added per well (dark (CO_2) incubation; 37°C). 3h later, upon the appearance of formazan crystals the supernatant was replaced with 80µl of dimethyl sulfoxide (DMSO, Sigma-USA) (Abnosiet al., 2010). Remained samples were completely removed from DMSO after 30min, and absorbances were measured (wavelength of 570nm) (EPOCH spectrophotometer; Epoch-USA)).

Cell survival evaluation (acridine orange/propidium iodide) staining

To compare the survival of the cells encapsulated in hydrogel scaffolds qualitatively, acridine orange/propidium iodide (AO/PI) staining (Sigma, USA) was performed. In this method, live cells are detected with their green fluorescent, while dead cells are seen in yellow, orange, or red colors (Kim et al., 2017). Beads were exposed with acridine orange solution for 15min at room temperature on day 14. The cells were then washed 3 times with PBS 1X before the addition of PI (Incubation time, 30sec). Samples were rinsed (PBS 1X, 3 times) and subsequent fluorescent microscopy was performed (Olympus-Japan).

Cresyl violet staining

Cresyl violet staining (Sigma Aldrich, USA) of neuronal Nissl bodies was done on 7 and 14d for 2D- and 3D-cultures, respectively. Following one round of washing with PBS 1X, cells were fixed using 70% ethanol for 10min at room temperature, and then incubated in cresyl violet solution (0.25% cresyl violet, 0.8% glacial acetic acid, 0.6mM sodium acetate, 100cm^3 distilled water) for 3 to 10min (light microscopy, Olympus IX70, Japan).

Immunocytochemistry

The supernatant of 2D- and 3D- cultures was removed and the samples were fixed with 4% paraformaldehyde (PFA; Sigma, USA) for 20min after washing with PBS 1X, followed by washing steps (3 times, with a 5-minute interval). Then, cell membranes were permeabilized with 0.3% Triton X-100 (Sigma, USA) for 30min, plus another round of washing with PBS 1X. Afterward, to block the secondary antibody reaction, 10% goat serum (Sigma, USA) was added to the samples for 45min. After removing the goat serum, samples were stained with the primary antibodies Nestin (1:100) (Biorbyt, UK), and β-tubulin III (1:100) (Biorbyt-UK), and were kept in the refrigerator (2-8°C, 24h). Later, washed samples (4times with PBS 1X) were incubated with goat anti-rabbit IgG (H+L) antibody (FITC; 1:150; dark incubation, 37°C, 1.5h) (Biorbyt-UK). At the final step, samples were transferred to the dark room, washed (3times), and stained with DAPI (DAPI (4′,6-diamidino-2-phenylindole; Sigma, USA) just before the fluorescence imaging (Olympus, IX70-Japan) based on the previous protocols (Aamodt and Grainger, 2016; Agarwal et al., 2022; Bernal and Arranz, 2018).

Data analysis

The percentage of visual expression of desired differentiation markers was measured using ImageJ software, version 1.51 and averages were expressed as Mean ± SD. Further statistical analyses were carried out using ANOVA and Tukey's tests (GraphPad PRISM, version 9.4.1., *p*-value <0.05).

Results

Morphological evaluation of PC-12 cells

Preliminary examination of PC-12 cells (2D-culture) showed a round morphology for these cells. Successive divisions were observed with 24-48h intervals. Each individual cell began to form a colony with a low adhesiveness (Figure 1A), whereas in the presence of glutamine (40mM), cells showed cytoplasmic retraction, changes in their spherical morphology, and the appearance of short neurites (Figure 1B). In 3D culture PC-12 cells retained their round appearance and formed colonies. Transparent appearance of colonies indicates the growth and proliferation of PC-12 cells in Glutamine-free 3D cultures (Figure 2C), and culture supplemented with Gln (40Mm) (Figure 2D).

Evaluation of 3D-cultured cell viabilities

The viability of alginate-encapsulated PC-12 cells (in the presence and absence of Gln) was measured on 10 and 14d post encapsulation through MTT assay. As it is shown in Figure 3, although minor increase was observed regarding the viability of the cells from 3D culture groups at 10 and 14d (ALGINATE and ALG+GLN), these changes were not statistically significant. Thus, our results demonstrated that encapsulation the PC-12 cells with alginate does not exert remarkable toxicity (Figure 3).

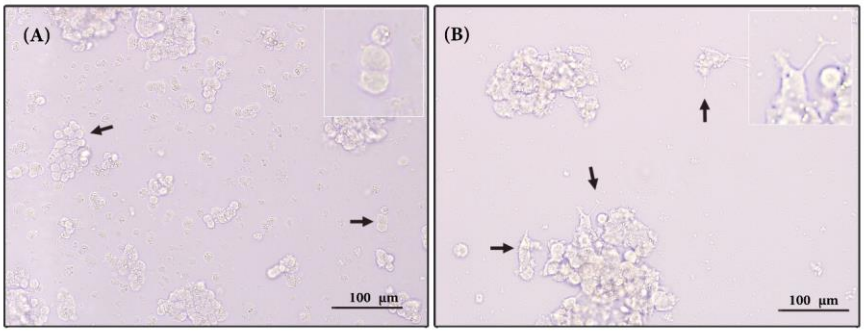

Figure 1. The morphology of PC-12 cells under 2D-culture condition (5d). (A) PC-12 cells' morphologies are shown for Gln-free cultures (arrows indicate dividing rounded cells), and (B) cultures supplemented with Gln (40Mm). Arrows show cytoplasmic retraction and neurite formation (Scale bar 100µm, light microscopy, Olympus IX70, Japan).

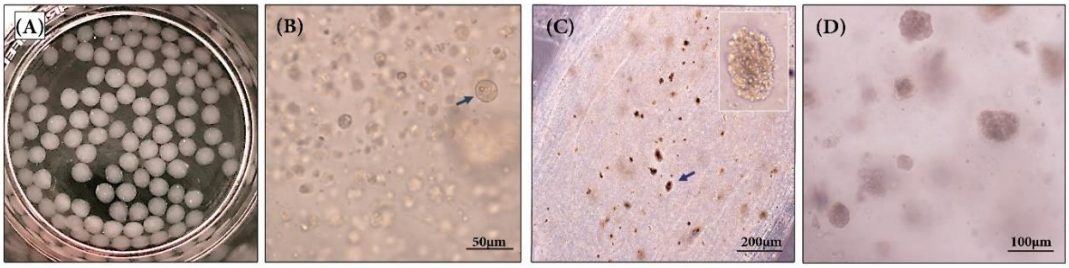

Figure 2. Light microscopy of PC-12 cells encapsulated with alginate beads. (A) Alginate beads, established in the calcium chloride solution, are shown. (B) PC-12 cells (arrows) encapsulated in alginate beads before they start any division or proliferation (1d), (C) following the formation of transparent cell colonies inside the beads in Gln-free culture (6d), and (D) culture supplemented with 40Mm Gln (1d after treatment) (Scale bars=50µm (B), 200µm (C), 100µm(D)).

PC-12 cell survival in alginate beads

Live-dead cell staining of PC-12 cells in alginate beads, indicated their proper survival 2 weeks post encapsulation. Live cells were detected in green (acridine orange dye), while dead ones were observed as red entities (PI dye) (Figure 4).

Cresyl body staining of Nissl bodies

Nissl bodies are rough endoplasmic reticulum (with ribosomes) and are the sites of protein synthesis. The detection of purple Nissl bodies in PC-12 cells indicated their neural differentiation in all investigated groups (Figure 5A). Quantified results showed that the mean number of encapsulated cells differentiated into neuron-like cells (ALG+GLN; 14d, 7d with 40mM Gln) was significantly increased in comparison to the control ALGINATE group. No significant difference was observed for PC-12 cells in 2D-culture in the presence and absence of Gln (7d, 40mM) (Figure 5B).

Immunocytochemistry reveals neuronal differentiation biomarkers in 2D- and 3D cultures of PC-12 cells

To determine the neuronal differentiation potential of PC-12 cells, the protein expression of 2 specific neural markers Nestin (neural progenitor cells) and β-tubulin III (neural mature cells) was investigated via immunohistochemistry analysis. Results from 2D-cultures showed that the mean percentage of Nestin and β-tubulin III in the presence of Gln (7d, 40mM) was increased (31.39 ± 2.71%; 32.83 ± 3.36%) in comparison to the control group (11.87 ± 2.28%;12.88 ± 3.43%) (Figures 6 and 8A).

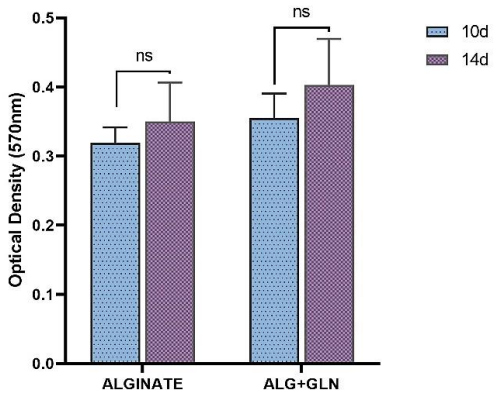

Figure 3. PC-12 cell survival under 3D cultures, obtained by MTT assay. Mean optical densities (570nm) are shown at two investigated time points (10, 14d). Differences were not significant between days 10 and 14 for 2D-cultured PC-12 cells (Gln-free

as control group) (P=0.2195), 3D-cultured cells in the absence [ALGINATE (P=0.8699)], and presence [ALG+GLN (P=0.8951)] of glutamine (Gln). Results are shown as Mean of 3 independent replicates ± SD (p<0.05).

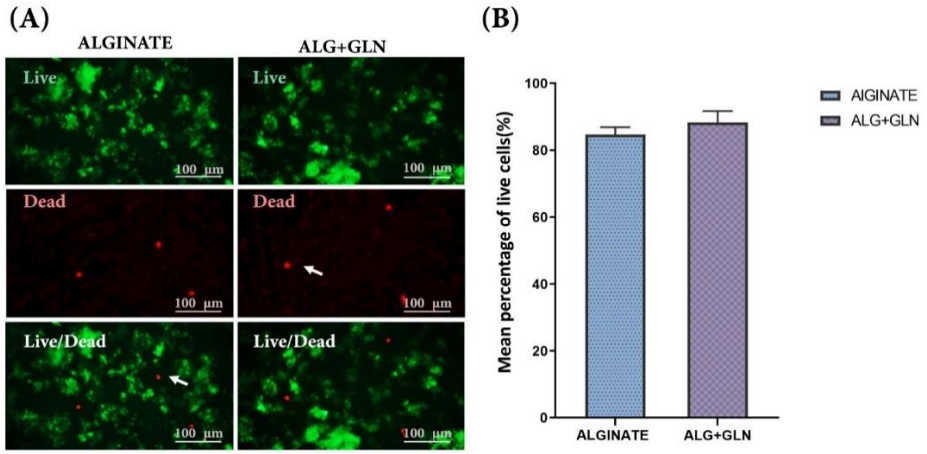

Figure 4. PC-12 cell survival under 3D-culture condition in the absence and presence of Gln (40mM). (A) Acridine orange (AO)/propidium iodide (PI) staining of PC-12 cells in 3D- cultures confirmed proper survival of the cells. It is clear that most of the cells are remained alive (green) 2 weeks following the encapsulation. (B) Images from AO/PI staining of the cells were quantified and reported as the mean percentage of live cells. There was no significant difference between the viability of the cells from ALGINATE (84.67±2.18) and ALG+GLN groups (89.67±2.08) (p<0.05; 3 independent replicates).

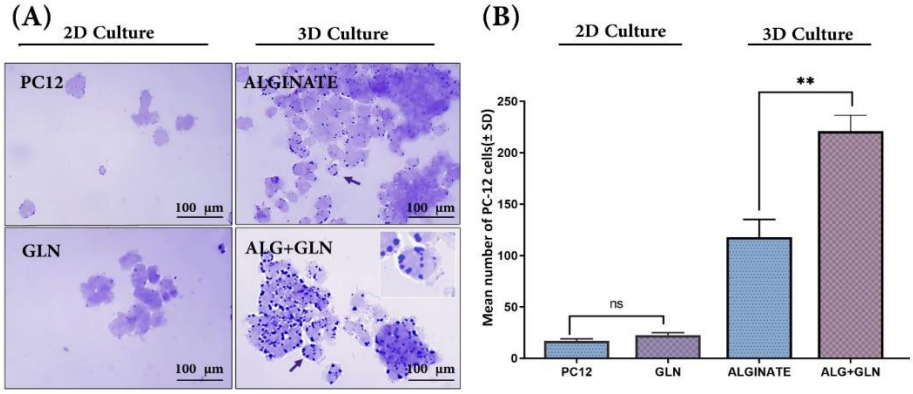

Figure 5. Cresyl violet staining confirmed Nissl bodies' formation. (A) Light microscopic images of Cresyl violet stained PC-12 cells from 2D- and 3D-groups (arrows) (3 replicates, scale bar=100µm). (B) Mean number (±SD) of PC-12 cells, which were positive for Nissl bodies 7d after treatment with 40mM glutamine are shown under 2D- and 3D-culture conditions (p<0.05; 3 replicates).

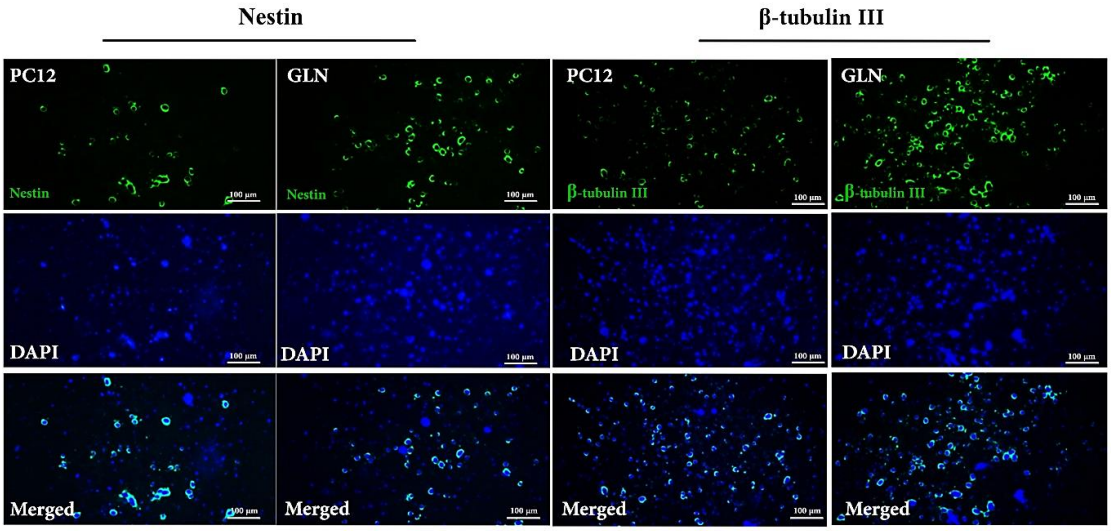

Figure 6. Immunocytochemistry staining for neural markers Nestin and β-tubulin III of PC-12 cells in 2D culture (7d, 40mM Gln). Cells' nuclei were counterstained with 4′,6-diamidino-2-phenylindole (DAPI). PC12, control; GLN, the presence of 40mM glutamine (Scale bar=100µm, 3 replicates).

For 3D cultures, immunocytochemistry analysis on 14d (7d after treatment with 40mM Gln) demonstrated the remarkable increase of Nestin (38.40 ± 2.60%) and β-tubulin III (47.68 ± 2.23%) in comparison to the controls (24.67 ± 2.08%; 29.74 ± 2.27%, respectively). Also, a higher level of Nestin and β-tubulin III protein expression was detected for the cells in 3D-culture vs. 2D-cultures (Figures 7 and 8B).

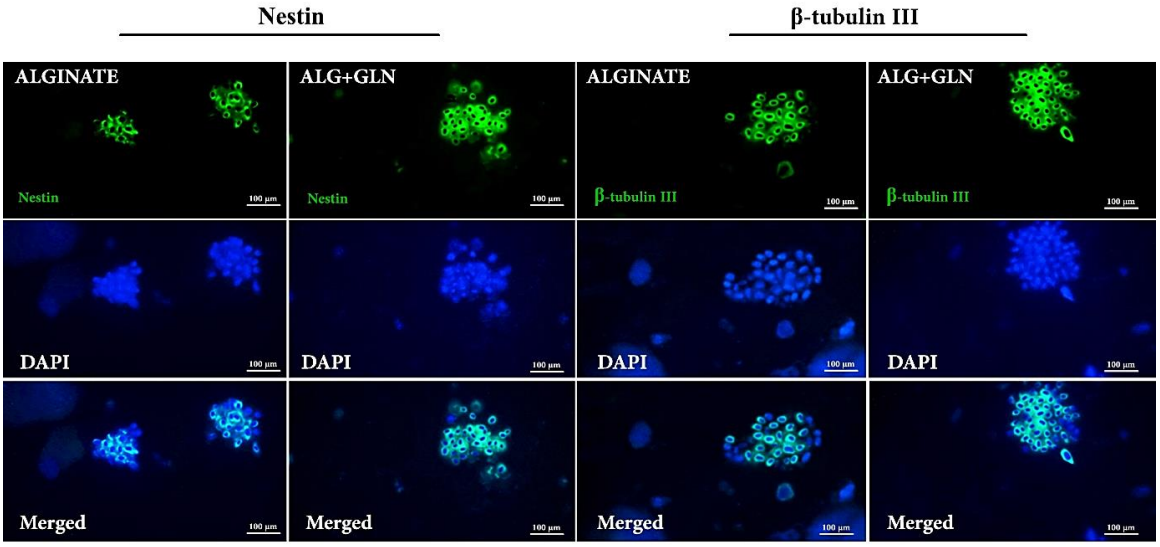

Figure 7. Immunocytochemistry staining for neural markers Nestin and β-tubulin III of PC-12 cells in 3D culture 7d after the treatment (on 14d) in the absence (ALGINATE) or presence (ALG+GLN) of 40mM glutamine. All nuclei are counterstained with 4′,6-diamidino-2-phenylindole (DAPI) (Scale bar=100µm, 3 replicates).

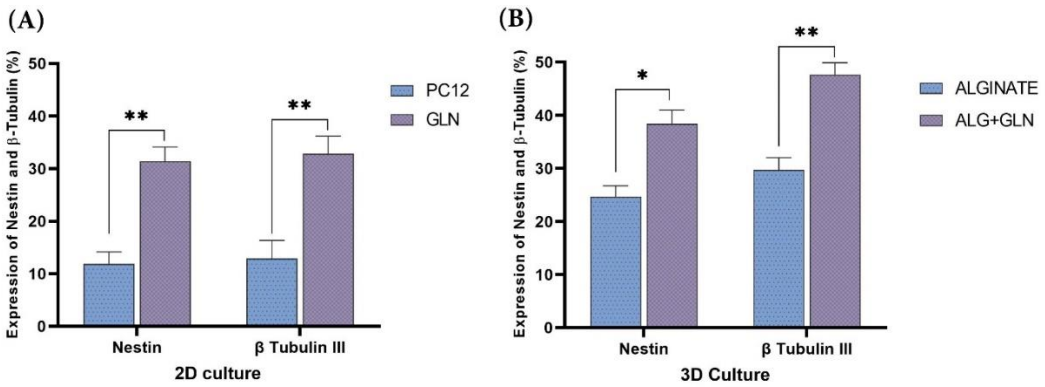

Figure 8. Comparing mean percentages of neuronal markers protein expression 7d after treatment with 40mM glutamine under 2D- and 3D culture conditions (p<0.05; 3 independent replicates). (A) The mean percentage of Nestin and β-tubulin III protein expression in 2D-culture showed a significant increase in GLN group in comparison to the PC-12 group for both markers. (B) The mean percentage of Nestin and β-tubulin III protein expression in 3D-culture showed a significant increase for both markers in ALG+GLN group vs. ALGINATE.

Discussion

The effect of stable Gln on the growth and neuronal differentiation of PC-12 cells in 2D polystyrene culture flasks and 3D alginate hydrogel beads was studied. Morphological changes of neuronal cell lines following the treatment with different chemicals have been the subject of many studies in the field of developmental neurotoxicity. Assessment of neurite growth and density could be considered as an accurate factor (Geranmayeh et al., 2015) and is regarded as an indicator of neuronal differentiation in PC-12 cells (Wiatrak et al., 2020). Our results from 2D-cultures indicated clear cytoplasmic condensation and morphological change of the cells, as well as limited neurite outgrowth with short length.

It was shown in the present study that Gln can increase the survival of PC-12 cells. It may be due to the protective role of Gln against the oxidative stress and its inhibitory effect on the activation of PI3K/Akt signaling pathway (Zhao et al., 2019). It was found that a high concentration of Gln (500mg/kg) can heal hippocampal injuries in rats by the inhibition of apoptosis (Wang et al., 2019). Another *in vitro* study based on pH and ammonia values showed that Gln (2% and 3%) is not toxic (Suh et al., 2022). In various studies, the effects of high concentrations of Gln were studied in the range of 20 to 80 mM (Ban & Kozar, 2010). Results showed that stable Gln (40mM) can act as a differentiation factor for PC-12 cells as it was evidenced by the increased expression of Nestin and β-tubulin III protein markers. This capacity for inducing the neural differentiation of the cells was further confirmed by comparative and quantitative staining of Nissl bodies from PC-12 cells.

It was also shown that Gln concentrations higher than 10mM can significantly increase the mRNA and protein levels of Hsp70 (Wang et al., 2017). Alginate plays a significant role in supporting the proliferation and differentiation of neural/-like cells. Cell encapsulation with alginate-based hydrogels is a rapid, non-toxic, and complete method to immobilized the cells (Andersen et al., 2015). Alginate hydrogel provides a suitable 3D platform for neural cultures and their proper differentiation (Cheravi et al., 2022; Razavi et al., 2015). The present study showed a significant difference (p<0.05) among alginate-encapsulated cells in the presence of a high concentration of Gln in comparison to the control group, based on the increased protein expression of Nestin and β-tubulin III .These differences were also significant for 3D-cultured cells in comparison to the cells in 2D culture, which could be attributed to the beneficial characteristics of alginate, such as supporting the proper cell adhesion and differentiation (Martins et al., 2018). Also, the results of investigating cell survival in 3D-culture showed that there was no significant difference between days 10 and 14, which is consistent with the results of similar studies (Razavi et al., 2015).

In summary, results from the present study, confirmed that supplementing 2D- and 3D- cultures of PC-12 cells with a high concentration of the stable form of glutamine can induce their differentiation and the acquisition of neuronal-like phenotype, which could be a promising approach in neural tissue engineering and regenerative medicine studies aimed to treat neuronal injuries.

Acknowledgement

This study was part of the Ph.D. thesis of Seyed Majid Jalalian Hosseini, Islamic Azad University,

Tehran, Iran. The authors would like to express their thanks to the Research Center for Applied Biology of Animal Development, Islamic Azad University of Mashhad, as well as, the Stem Cells and Regenerative Medicine Research group, Academic Center for Education, Culture and Research (ACECR)- Khorasan Razavi for their sincere help.

Conflict of interest

The authors declare that they have no conflict of interest.

References

Aamodt J. M. aznd Grainger D. W. (2016) Extracellular matrix-based biomaterial scaffolds and the host response. Biomaterials 86:68-82.

Abe H., Ino K., Li C.-Z., Kanno Y., Inoue K. Y., Suda A., Kunikata R., Matsudaira M., Takahashi Y. and Shiku H. (2015) Electrochemical imaging of dopamine release from three-dimensional-cultured PC12 cells using large-scale integration-based amperometric sensors. Analytical chemistry 87:6364-6370.

Abnosi M., Najafabadi M., Soleimani Mehranjani M., Momeni H. and Safarabadi F. (2010) Preparation of Natural Scaffold from Sciatic Nerve and Viability Evaluation of Seeded Rat Bone Marrow Mesenchymal Stem Cells. Journal of Cell & Tissue 1.43-52

Agarwal G., Roy A., Kumar H. and Srivastava A. (2022) Graphene-collagen cryogel controls neuroinflammation and fosters accelerated axonal regeneration in spinal cord injury. Biomaterials Advances:212971.1-12.

Akter F. 2016. Principles of tissue engineering. In Tissue engineering made easy. Elsevier. 3-16.

Andersen T., Auk-Emblem P .and Dornish M. (2015) 3D cell culture in alginate hydrogels. Microarrays 4:133-161.

Baiguera S., Del Gaudio C., Lucatelli E., Kuevda E., Boieri M., Mazzanti B., Bianco A. and Macchiarini P. (2014) Electrospun gelatin scaffolds incorporating rat decellularized brain extracellular matrix for neural tissue engineering. Biomaterials 35:1205-1214.

Ban K. and Kozar R. A. (2010) Glutamine protects against apoptosis via downregulation of Sp3 in intestinal epithelial cells. American Journal of Physiology-Gastrointestinal and Liver Physiology 299:G1344-G1353

Bernal A. and Arranz L. (2018) Nestin-expressing progenitor cells: function, identity and therapeutic implications. Cellular and Molecular Life Sciences 75:2177-2195.

Brose S. A., Marquardt A. L .and Golovko M. Y. (2014) Fatty acid biosynthesis from glutamate and glutamine is specifically induced in neuronal cells under hypoxia. Journal of neurochemistry 129:400-412.

Chen S., Xia Y., Zhu G., Yan J., Tan C., Deng B., Deng J., Yin Y. and Ren W .(2018) Glutamine supplementation improves intestinal cell proliferation and stem cell differentiation in weanling mice. Food & nutrition research 62.1-9.

Cheravi M., Baharara J., Yaghmaei P. and Roudbari N. H. (2022) The effect of cerebrospinal fluid-derived exosomes on neural differentiation of adipose mesenchymal stem cells in alginate hydrogel scaffold. Nova Biologica Reperta 8:265-278.

Darbinian N. 2013. Cultured Cell Line Models of Neuronal Differentiation: NT2, PC12. In Neuronal Cell Culture .Springer. 23-33

Geranmayeh M., Baghbanzadeh A., Barin A., Salar-Amoli J. and Dehghan M. (2015) Effects of different culture media on optimization of primary neuronal cell culture for in vitro models assay. Iranian Journal of Veterinary Medicine 9:163-170.

Gordon J., Amini S. and White M. K. 2013. General overview of neuronal cell culture. In Neuronal Cell Culture. Springer. 1-8.

Katebi S., Esmaeili A., Ghaedi K. and Zarrabi A. (2019) Superparamagnetic iron oxide nanoparticles combined with NGF and quercetin promote neuronal branching morphogenesis of PC12 cells. International journal of nanomedicine 14:2157.-2169

Kim Y., Kang K., Jeong J., Paik S. S., Kim J. S., Park S. A., Kim W. D., Park J. and Choi D. (2017) Three-dimensional (3D) printing of mouse primary hepatocytes to generate 3D hepatic structure. Annals of surgical treatment and research 92:67-72.

Li J., Ghazwani M., Liu K., Huang Y., Chang N., Fan J., He F., Li L., Bu S. and Xie W. (2017) Regulation of hepatic stellate cell proliferation and activation by glutamine metabolism. PLoS One 12:e0182679.1-17.

Martins J. P., Ferreira M. P., Ezazi N. Z., Hirvonen J. T., Santos H. A., Thrivikraman G., França C. M.,

Athirasala A., Tahayeri A. and Bertassoni L .E. (2018) 3D printing: Prospects and challenges. Nanotechnologies in Preventive and Regenerative Medicine:299-379.

Mobini S., Song Y. H., McCrary M. W. and Schmidt C. E. (2019) Advances in ex vivo models and lab-on-a-chip devices for neural tissue engineering. Biomaterials 198:146-166.

Raizel R. and Tirapegui J. (2018) Role of glutamine, as free or dipeptide form, on muscle recovery from resistance training: A review study. Nutrire 43:1-10.

Razavi S., Khosravizadeh Z., Bahramian H. and Kazemi M. (2015) Time-Dependent Effect of Encapsulating Alginate Hydrogel on Neurogenic Potential. Cell Journal (Yakhteh) 17:304-311.

Rubin H. (2019) Deprivation of glutamine in cell culture reveals its potential for treating cancer. Proceedings of the National Academy of Sciences 116:6964-6968.

Sarkadi B., Meszaros K., Krencz I., Canu L., Krokker L., Zakarias S., Barna G., Sebestyen A., Papay J. and Hujber Z. (2020) Glutaminases as a novel target for SDHB-associated pheochromocytomas /paragangliomas. Cancers 12:599.1-25.

Suh J.-K., Nejad J. G., Lee Y.-S ,.Kong H.-S., Lee J.-S. and Lee H.-G. (2022) Effects of L-glutamine supplementation on degradation rate and rumen fermentation characteristics in vitro. Animal bioscience 35:422-433.

Wang H., Tang C., Jiang Z., Zhou X., Chen J., Na M., Shen H. and Lin Z.(2017) Glutamine promotes Hsp70 and inhibits α-Synuclein accumulation in pheochromocytoma PC12 cells. Experimental and Therapeutic Medicine 14:1253-1259.

Wang Q., Zhang C., Zhang L., Guo W., Feng G., Zhou S., Zhang Y., Tian T., Li Z. and Huang F. (2014) The preparation and comparison of decellularized nerve scaffold of tissue engineering. J Biomed Mater Res A 102:4301-4308.

Wiatrak B., Kubis-Kubiak A., Piwowar A. and Barg E. (2020) PC12 cell line: cell types, coating of culture vessels, differentiation and other culture conditions. Cells 9:9581-15..

Yi S., Xu L. and Gu X. (2019) Scaffolds for peripheral nerve repair and reconstruction. Experimental neurology 319:112761.1-11.

Yousefi Taemeh S., Mehrzad J. and Dehghani H. (2021) Effect of glutamine stability on the long-term culture and line establishment of chicken primordial germ cells. Journal of Cell and Molecular Research 13:44-53.

Zhao Y., Wang Q., Wang Y., Li J., Lu G. and Liu Z. (2019) Glutamine protects against oxidative stress injury through inhibiting the activation of PI3K/Akt signaling pathway in parkinsonian cell model. Environmental health and preventive medicine 24:1-7.

Journal of Cell and Molecular Research (2022) 14 (1), 63-70 DOI: 10.22067/jcmr.2022.76959.1041

Research Article

Study of lncRNA *NEAT1* Gene Expression in Ovarian Cancer

Amin Moqadami, Mohammad Khalaj-Kondori *

Department of Animal Biology, Faculty of Natural Sciences, University of Tabriz, Tabriz, Iran

Received 31 May 2022 Accepted 31 October 2022

Abstract

Long non-coding RNAs (lncRNAs) have recently emerged as effective regulatory agents in biological processes as well as in the formation of tumors. LncRNAs are important regulators of cell transformation and cancer progression. LncRNA *NEAT1* is one of the most important lncRNAs, and its deregulation has been reported in a variety of human cancers. Ovarian cancer has an inverse relationship with the number of reported pregnancies and deliveries, while it has a direct relationship with infertility. This study aimed to investigate *NEAT1* expression in ovarian cancer. A total of 140 tissue samples, including 70 ovarian tumors and 70 marginal samples, were included in the study. Total RNA was extracted using the RNXplus solution. The quality and quantity of the extracted RNAs were determined using gel electrophoresis and a NanoDrop device. The complementary DNA was synthesized by the reverse transcriptase enzyme, and quantitative reverse transcriptase PCR was used to quantify the expression of *NEAT1*. A comparison between the mean expression of *NEAT1* in ovarian tumors and marginal samples showed an increase in *NEAT1* expression in tumor tissue that was not statistically significant (P-value = 0.2). ROC curve analysis also showed that *NEAT1* expression level might not be an informative biomarker for ovarian cancer.

***Keywords*:** NEAT1, Ovarian Cancer, qRT-PCR, Biomarker

Introduction

Cancer is caused by unregulated cell division affected by environmental factors and genetic abnormalities. Recent research suggests that the extracellular matrix plays an essential role in the development of cancer (Motofei, 2021). Oncogenes, tumor suppressor genes, DNA repair genes, and programmed death genes are the main genes, and their deregulation results in cell transformation into a cancerous state (Basu, 2018). Today, one of the most prevalent and deadly diseases is cancer. According to statistics, the number of new cancer cases worldwide is anticipated to be 19.3 million, while the number of cancer fatalities is close to 10.0 million (9.9 million excluding nonmelanoma skin cancer) and adds more than 10% to the overall cost of healthcare in industrialized nations (Sung et al., 2021; Zaorsky et al., 2021).

Ovarian cancer is the seventh most prevalent malignancy among women and the eighth most common cause of cancer death. It is so lethal among female cancers that it is estimated to kill more than 140,000 people worldwide each year. (Torre et al., 2018). In the United States, approximately 19,880 new cases and 12,810 deaths of ovarian cancer were predicted in 2022 (Siegel et al., 2022). Due to its late diagnosis, it is one of the deadliest types of gynecological cancers. It is usually diagnosed in these cases when the disease has reached advanced stages and is mostly incurable (Matulonis et al., 2016). There are several types of ovarian cancer, but the most well-known type is epithelial ovarian cancer (Momenimovahed et al., 2019). Women are more likely to develop cancer, especially ovarian cancer, after menopause as a result of age-related risk factors that may raise their risk of cancer. (Koshiyama et al., 2014). A woman's lifetime risk of developing ovarian cancer is 1–1.5 percent, and the resulting death rate is approximately 50 percent. Ovarian cancer is closely related to infertility while having an inverse relationship with the number of reported pregnancies and deliveries. Ovarian cancer risk is also increased by late menopause and early puberty (Torre et al., 2018).

Non-coding RNAs are a new group of genes known in the human genome that regulate various biological processes (Ghasemi et al., 2020; Khajehdehi et al., 2021). Recently, much attention has been paid to the role of these RNAs in complex

* Corresponding author's e-mail address: khalaj@tabrizu.ac.ir

human diseases, including cancer (Ghasemi et al., 2021a; Khajehdehi et al., 2022; Ostovarpour et al., 2021) and neurological diseases (Khodayi-Shahrak et al., 2022; Khodayi et al., 2022). In recent years, many ncRNA genes have been identified through several different screening schemes (Khajehdehi et al., 2022; Zhang et al., 2019). They have demonstrated their capacity to be both diagnostic and therapeutic for different cancers (Fotuhi et al., 2021; Ghasemi et al., 2021a; Ghasemi et al., 2021b). Every year, increasing numbers of lncRNAs are evaluated as biomarkers for prognosis and diagnosis; a number of these have even received clinical application approval (Jarroux et al., 2017).

Nuclear Enriched Abundant Transcript 1 (*NEAT1*) is a structural component of paraspeckles that controls several genes' expression via nuclear retention (Liu et al., 2020). NEAT1 is transcribed from locus type 1 multiple endocrine neoplasms of familial tumor syndrome and is located on chromosome 11. This gene has two short (NEAT1_S) and long (NEAT1_L) isoforms that are transcribed from the same promoter and differ in their 3' end processes (West et al., 2014). It acts as a gene regulator in various cancers (Chakravarty et al., 2014; Zhen et al., 2016). Changes in expression levels of *NEAT1* have recently been reported in various human cancers, including leukemia, colorectal cancer, glioma, hepatocellular carcinoma, lung cancer, breast cancer, and prostate cancer (Dong et al., 2018). *NEAT1*'s pathogenic impact on human malignancies is attributed to the Akt and Wnt signaling pathways (Li et al., 2018; Lo et al., 2016). *NEAT1* can regulate STAT3 signaling activity via molecular processes, including microRNA sponges, transcriptional activation or inhibition, and epigenetic modifications. (ZadehRashki et al., 2022). NEAT1 also functions as a ceRNA and suppresses several tumor-suppressor miRNAs. This lncRNA is thought to be a therapeutic target and a potential biomarker in several cancer types (Ghafouri-Fard and Taheri, 2019). Cancer stem cells (CSC) generated from non-small cell lung cancer (NSCLC) had elevated *NEAT1* expression. BRCA1 may bind to the upstream region of the *NEAT1* gene to decrease *NEAT1* expression in breast tissue. *NEAT1* overexpression due to BRCA1 deficiency dramatically accelerates the formation of breast tumors (Lo et al., 2016). In contrast to most of the literature, scientists observed *NEAT1* down-regulation in invasive breast cancer, esophageal carcinomas, pheochromocytomas, and paragangliomas (Hu et al., 2018). Liu et al. examined the expression and role of *NEAT1* in the metastasis of OC cells and found that *NEAT1* was elevated in both OC tissue samples and cell lines. They also found that the knockdown of *NEAT1* prevented metastasis of OC cells via the downregulation of Rho-associated coiled-coil containing protein kinase 1 (*ROCK1*) (Liu et al., 2018). Chai et al. reported that the high expression of *NEAT1* in ovarian cancer is due to an RNA-binding protein called HUR, which increases the level of *NEAT1*. In contrast, a small non-coding RNA called miR-124-3p directly targets *NEAT1* and reduces its expression in ovarian cancer (Chai et al., 2016).

In this study, we compared expression levels of the lncRNA *NEAT1* between OC tumoral and corresponding marginal tissues and evaluated its potential as a biomarker for OC development.

Materials and Methods

Sample Collection

140 samples collected by a gynecologist, including 70 ovarian cancer and 70 marginal tissue samples, from patients referred to AL-Zahra Hospital in Tabriz. These samples were promptly frozen in liquid nitrogen, transported to the lab, and stored there until RNA extraction. The Clinical Research Ethics Committee accepted the research plan, and all individuals completed informed consent forms following AL-Zahra Hospital's standards. Clinical data were gathered both from hospital records and from interviewing patients.

RNA extraction, cDNA synthesis, and quantitative reverse transcriptase PCR

Total RNA was isolated using the RNX Plus solution (Cinnagen, Tehran, Iran) according to the manufacturer's protocol. DNase I (GeneAll, Seoul, Korea) was used to remove DNA contamination. Nanodrop (Thermo Fisher Scientific NanoDrop 2000, CA, USA) and 2% agarose gel electrophoresis (v/w) were used to evaluate the quantity and quality of RNA samples, respectively. To make cDNA, 1 µl of DNase I, 1.32 µl of DNase I buffer, equivalent to 800 ng of RNA, and water were poured into the microtube and placed in a thermocycler for 30 minutes at 37°C. 1 µl of EDTA was added and placed in the thermocycler at 65 °C for 10 minutes. 0.5 µl of Oligo dT, 0.5 µl of Random Hexamer, 0.5 µl of RT enzyme, and RT buffer were added and kept at 37 °C for 25 minutes. The reverse transcriptase enzyme was incubated for 5 minutes at 85 °C in the machine. Gene Runner software was used to design the primer. For the *NEAT1* gene, the forward primer was designed as F: CTGCCTTCTTGTGCGTTTCT,

and the reverse primer was designed as R: GACCAACTTGTACCCTCCCA. For the internal control gene, *GAPDH*, the primers were designed as F: GAGAAGTATGACAACACGCTC and R: TGAGTCCTTCCACGATAC. The real-time quantitative PCR (qPCR) assays were performed using the StepOnePlus™ Real-Time PCR System (Applied Biosystems). For both *NEAT1* and *GAPDH* genes: Master Mix SYBR Green (Amplicon Company) 5 µl, primer F 0.12 µl, primer R 0.12 µl, cDNA 4 µl (dilution 1:100), water 0.76 µl in final volume 10 µl were used. The $2^{-\Delta\Delta Ct}$ method was used to evaluate the expression level.

Statistical Analysis

The normality of the data was assessed by the Kolmogorov–Smirnov test. The Mann-Whitney test was used to evaluate differences in *NEAT1* expression between tumor and non-tumor samples. The Mann–Whitney test was also used to investigate the relationship between *NEAT1* expression and clinicopathologic characteristics. SPSS version 24, and GraphPad Prism 8 were used for statistical analysis, and P-values less than 0.05 were considered significant. The ROC curve analysis was done to assess the sensitivity and specificity of *NEAT1* as a diagnostic biomarker.

Results

Population Study

The clinicopathologic data of the patients are shown in Table 1. A total number of seventy ovarian cancer patients were enrolled in the research. Sixty-two percent (44/70) were below 55 years and 38% (26/70) were older than 55. 70% (49/70) of patients had stage I/II and the other 30% (21/70) had stage III/IV ovarian cancer. The majority of patients (54%) were nonsmokers and 46% were smokers. 70% of patients had stage I/II and the other 30% had stage III/IV ovarian cancer. Thirty-six percent (25/70) of patients had lymph metastasis and 64% (45/70) had no lymph metastasis in their tumor. Regarding invasion, 83% (58/70) of patients had invasion and the remaining had no invasion (Table 1).

Table 1. Association between lncRNA *NEAT1* expression and clinicopathological characteristics in ovarian cancer patients.

Clinical parameters	No. of cases (%)	P-value
Age		**0.16**
≤55	44 (62)	
>55	26 (38)	
TNM (Tumor stage I vs. Margins)		**0.16**
Stage I	29 (50)	
Margins	29 (50)	
TNM (Tumor stages I&II vs. margins)		**0.27**
Stages I&II	49 (50)	
Margins	49 (50)	
TNM (Tumor stages III&IV vs. margins)		**0.6**
Stage III&IV	21 (50)	
Margins	21 (50)	
TNM (Tumor stage I&II vs. III & IV)		**0.38**
Stage I&II	49 (70)	
Stage III&IV	21 (30)	
Smoking		**0.34**
No	38 (54)	
Yes	32 (46)	
Lymph		**0.78**

No	45 (64)	
Yes	25 (36)	
Invasion		**0.19**
No	12 (17)	
Yes	58 (83)	

Expression of lncRNA *NEAT1* in ovarian cancer

NEAT1 and *GAPDH* amplicons were amplified by PCR and confirmed by 2% agarose gel electrophoresis (Figure 1). The expression of *NEAT1* was quantified by qRT-PCR and compared between ovarian tumors and marginal groups. The results showed that *NEAT1* expression was high in tumor samples compared to tumor margins, but the increase was not statistically significant (p-value = 0.25) (Figure 2).

The ROC curve was also plotted by GraphPad Prism v8.0 software (Figure 3) to evaluate its potential as a biomarker for ovarian cancer. The results showed an area under the curve of 0.56, which indicates a poor potential for *NEAT1* expression level as a biomarker for ovarian cancer.

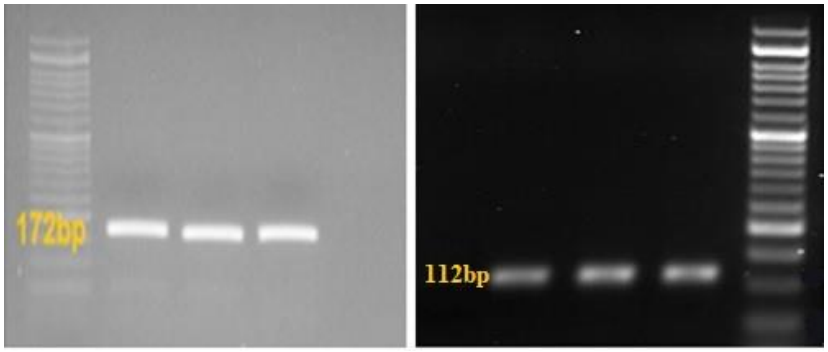

Figure 1. Gel electrophoresis of the PCR products of *GAPDH* (112 bp) and *NEAT1* (172 bp)

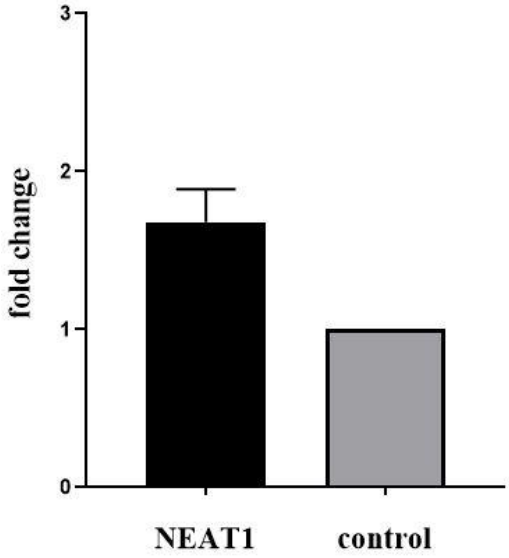

Figure 2. Fold change of *NEAT1* gene expression in tumor samples compared to the tumor margins.

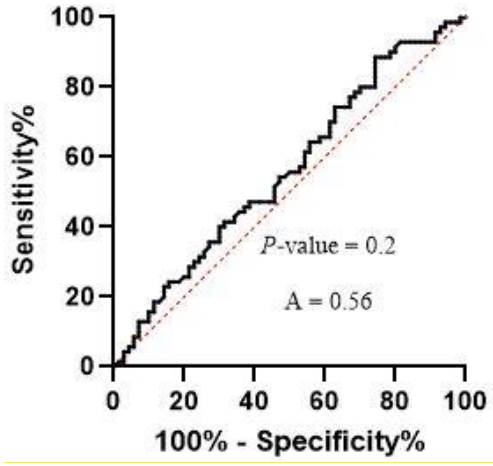

Figure 3. ROC curve analysis to evaluate the biomarker potency of *NEAT1*.

Discussion

In the present study, we examined lncRNA *NEAT1* expression in ovarian cancer. As compared to marginal tissue, the expression of lncRNA *NEAT1* was higher in ovarian tumor tissue, although the difference was not statistically significant.

One of the three forms of malignant tumors in the female reproductive system is ovarian cancer. Ovarian cancer metastases are a major cause of death, and this cancer has the highest mortality rate of any gynecological tumor. (Chen et al., 2019). Ovarian cancer patients have a poor overall survival rate despite improvements in surgery and treatment. Only 25% to 35% of women with advanced ovarian cancer survive for five years, and the prognosis is often relatively poor because of late diagnosis. More than 70% of those diagnosed with this cancer have progressed to the last stage, in which the disease has migrated past the ovaries. Understanding the molecular mechanisms involved in ovarian cancer is necessary to prevent, diagnose, and treat ovarian cancer because there is no reliable early-stage diagnostic tool, which contributes to this high death rate (Karnezis et al., 2017).

Long non-coding RNAs have recently emerged as effective regulators in biological processes as well as in the formation of tumors (Ghasemi et al., 2020; Khajehdehi et al., 2021). These are longer than 200 nucleotides and have been linked to a variety of disorders, making them prospective therapeutic targets (Nandwani et al., 2021). Multiple lncRNAs have recently been shown to be dysregulated in OC and to play key roles in tumor growth, including proliferation, apoptosis, cell cycle, migration, invasion, metastases, and pharmaceutical resistance, via a wide range of molecular processes (Fotuhi et al., 2021; Wang et al., 2019). For example, SRY-related high-mobility-group box 4 (*SOX4*), a member of the Sox family of transcription factors, showed high expression levels and caused OC cells to proliferate (Xi et al., 2017). Additionally, lncRNA *TP73-AS1* was discovered to be elevated in both OC tissues and cells by Wang, X., et al. Matrix metalloproteinase 2 (*MMP2*) and *MMP9* were primarily altered by LncRNA *TP73-AS1* to increase OC cell growth (Wang et al., 2018). Further investigations revealed that lncRNAs, including *HOXD-AS1* and *EBIC*, increased OC cell proliferation by stimulating the Wnt/beta-catenin signaling pathway (Shu et al., 2018; Xu et al., 2018; Zhang et al., 2017). Furthermore, it was shown that lncRNA *MALAT1* suppression significantly reduced the proliferation of OC cells via the PI3K-AKT pathway (Jin et al., 2017).

Recently, many studies have shown that *NEAT1* plays an important role in tumor progression (West et al., 2014). *NEAT1* expression was found to be significantly higher in prostate adenocarcinoma, stomach adenocarcinoma, liver hepatocellular carcinoma, kidney papillary cell carcinoma, and kidney clear cell carcinoma compared to normal tissues in one study of *NEAT1*. Remarkably, *NEAT1* expression was low in invasive breast carcinoma, esophageal carcinoma, and pheochromocytoma & paraganglioma compared to normal tissues. (Hu et al., 2018). Guo et al. demonstrated that *NEAT1* plays an essential role in the tumorigenesis and metastasis of hepatocellular carcinoma. (Guo et al., 2015). A study by Ma et al. showed that *NEAT1* lncRNA expression is increased in gastric adenocarcinoma. *NEAT1* may affect the progression of gastric adenocarcinoma by increasing tumor growth (Ma et al., 2016). Tankachan et al. showed that *NEAT1* is a significant biomarker with a promising future that can be used to treat breast and gynecologic cancers (Thankachan et al., 2021). Furthermore, Xu et al. reported that knocking down *NEAT1* has been shown to inhibit ovarian cancer cell proliferation, colony formation, migration, and invasion while increasing cell death (Xu et al., 2020). According to recent research by Yang et al. it was shown that NEAT1-containing paraspeckles could be produced by p53, which regulates replication stress and chemosensitivity in cancer cells (Yang et al., 2017). Knowing the functional nature of *NEAT1* in various cancers, we decided to investigate its role in ovarian cancer. This study has shown that *NEAT1* expression is increased in ovarian cancer tumor tissue compared to healthy tumor margin tissue; however, this increase was not significant.

Conclusion

The expression of *NEAT1* lncRNA in ovarian cancer tumor tissue was increased insignificantly compared to healthy tumor margin tissue, so it might not be considered a biomarker for the diagnosis and prognosis of ovarian cancer.

Acknowledgment
We appreciate the Research Deputy of the University of Tabriz and all participants involved in this study.

Conflict of Interest
None.

References

Basu A. K. (2018) DNA Damage, Mutagenesis and Cancer. International Journal of Molecular Sciences 19:970.

Chai Y., Liu J., Zhang Z. and Liu L. (2016) HuR-regulated lncRNA NEAT1 stability in tumorigenesis and progression of ovarian cancer. Cancer Med 5:1588-1598.

Chakravarty D., Sboner A., Nair S. S., Giannopoulou E., Li R., Hennig S., et al. (2014) The oestrogen receptor alpha-regulated lncRNA NEAT1 is a critical modulator of prostate cancer. Nat Commun 5:5383.

Chen S.-N., Chang R., Lin L.-T., Chern C.-U., Tsai H.-W., Wen Z.-H., et al. (2019) MicroRNA in Ovarian Cancer: Biology, Pathogenesis, and Therapeutic Opportunities. International Journal of Environmental Research and Public Health 16:1510.

Dong P., Xiong Y., Yue J., Hanley S. J. B., Kobayashi N., Todo Y., et al (2018) Long Non-coding RNA NEAT1: A Novel Target for Diagnosis and Therapy in Human Tumors. Front Genet 9:471.

Fotuhi S. N., Khalaj-Kondori M. and Karimi H. (2021) LncRNA HOXD-AS1 Is Upregulated in Ovarian Cancer. Journal of Cell and Molecular Research 12:49-55.

Ghafouri-Fard S. and Taheri M. (2019) Nuclear Enriched Abundant Transcript 1 (NEAT1): A long non-coding RNA with diverse functions in tumorigenesis. Biomedicine & Pharmacotherapy 111:51-59.

Ghasemi T., Khalaj-Kondori M., Hosseinpour Feizi M. A. and Asadi P. (2020) lncRNA-miRNA-mRNA interaction network for colorectal cancer; An in silico analysis. Comput Biol Chem 89:107370.

Ghasemi T., Khalaj-Kondori M., Hosseinpour Feizi M. A. and Asadi P. (2021a) Aberrant expression of lncRNAs SNHG6, TRPM2-AS1, MIR4435-2HG, and hypomethylation of TRPM2-AS1 promoter in colorectal cancer. Cell Biol Int 45:2464-2478.

Ghasemi T., Khalaj-Kondori M., Hosseinpour Feizi M. A. and Asadi P. (2021b) Long non-coding RNA AGAP2-AS1 is up regulated in colorectal cancer. Nucleosides Nucleotides Nucleic Acids 40:829-844.

Hu J., He G., Lan X., Zeng Z., Guan J., Ding Y., et al. (2018) Inhibition of ATG12-mediated autophagy by miR-214 enhances radiosensitivity in colorectal cancer. Oncogenesis 7:1-12.

Jarroux J., Morillon A. and Pinskaya M. 2017. History, Discovery, and Classification of lncRNAs. *In* Long Non Coding RNA Biology. M.R.S. Rao, editor. Springer Singapore, Singapore. 1-46.

Jin Y., Feng S. J., Qiu S., Shao N. and Zheng J. H. (2017) LncRNA MALAT1 promotes proliferation and metastasis in epithelial ovarian cancer via the PI3K-AKT pathway. Eur Rev Med Pharmacol Sci 21:3176-3184.

Karnezis A. N., Cho K. R., Gilks C. B., Pearce C. L. and Huntsman D. G. (2017) The disparate origins of ovarian cancers: pathogenesis and prevention strategies. Nature Reviews Cancer 17:65-74.

Khajehdehi M., Khalaj-Kondori M., Ghasemi T., Jahanghiri B. and Damaghi M. (2021) Long Noncoding RNAs in Gastrointestinal Cancer: Tumor Suppression Versus Tumor Promotion. Dig Dis Sci 66:381-397.

Khajehdehi M., Khalaj-Kondori M. and Hosseinpour Feizi M. A. (2022) Expression profiling of cancer-related long non-coding RNAs revealed upregulation and biomarker potential of HAR1B and JPX in colorectal cancer. Mol Biol Rep 49:6075-6084.

Khodayi-Shahrak M., Khalaj-Kondori M., Hosseinpour Feizi M. A. and Talebi M. (2022) Insights into the mechanisms of non-coding RNAs' implication in the pathogenesis of Alzheimer's disease. Excli j 21:921-940.

Khodayi M., Khalaj-Kondori M., Hoseinpour Feizi M. A., Jabarpour Bonyadi M. and Talebi M. (2022) Plasma lncRNA profiling identified BC200 and NEAT1 lncRNAs as potential blood-based biomarkers for late-onset Alzheimer's disease. Excli j 21:772-785.

Koshiyama M., Matsumura N. and Konishi I. (2014) Recent concepts of ovarian carcinogenesis: type I and type II. Biomed Res Int 2014:934261.

Li S., Li J., Chen C., Zhang R. and Wang K. (2018) Pan-cancer analysis of long non-coding RNA NEAT1 in various cancers. Genes & diseases 5:27-35.

Liu H., Yan X. and Yu J. (2020) Long noncoding RNA NEAT1/microRNA-125a axis predicts increased major adverse cardiac and cerebrovascular event risk independently in patients with unprotected left main coronary artery disease underwent coronary artery bypass grafting. J Clin Lab Anal 34:e23299.

Liu Y., Wang Y., Fu X. and Lu Z. (2018) Long non-coding RNA NEAT1 promoted ovarian cancer cells' metastasis through regulation of miR-382-3p/ROCK1 axial. Cancer Sci 109:2188-2198.

Lo P.-K., Zhang Y., Wolfson B., Gernapudi R., Yao Y., Duru N., et al. (2016) Dysregulation of the BRCA1/long non-coding RNA NEAT1 signaling axis contributes to breast tumorigenesis. Oncotarget 7:65067.

Matulonis U. A., Sood A. K., Fallowfield L., Howitt B. E., Sehouli J. and Karlan B. Y. (2016) Ovarian cancer. Nat Rev Dis Primers 2:16061.

Momenimovahed Z., Tiznobaik A., Taheri S. and Salehiniya H. (2019) Ovarian cancer in the world: epidemiology and risk factors. Int J Womens Health 11:287-299.

Motofei I. G. (2021) Biology of cancer; from cellular and molecular mechanisms to developmental processes and adaptation. Seminars in Cancer Biology.

Nandwani A., Rathore S. and Datta M. (2021) LncRNAs in cancer: Regulatory and therapeutic implications. Cancer Letters 501:162-171.

Ostovarpour M., Khalaj-Kondori M. and Ghasemi T. (2021) Correlation between expression levels of lncRNA FER1L4 and RB1 in patients with colorectal cancer. Mol Biol Rep 48:4581-4589.

Shu C., Yan D., Mo Y., Gu J., Shah N. and He J. (2018) Long noncoding RNA lncARSR promotes epithelial ovarian cancer cell proliferation and invasion by association with HuR and miR-200 family. Am J Cancer Res 8:981-992.

Siegel R. L., Miller K. D., Fuchs H. E. and Jemal A. (2022) Cancer statistics, 2022. CA: A Cancer Journal for Clinicians 72:7-33.

Sung H., Ferlay J., Siegel R. L., Laversanne M., Soerjomataram I., Jemal A., et al. (2021) Global Cancer Statistics 2020: GLOBOCAN Estimates of Incidence and Mortality Worldwide for 36 Cancers in 185 Countries. CA: A Cancer Journal for Clinicians 71:209-249.

Thankachan S., Bhardwaj B. K., Venkatesh T. and Suresh P. S. (2021) Long Non-coding RNA NEAT1 as an Emerging Biomarker in Breast and Gynecologic Cancers: a Systematic Overview. Reproductive Sciences 28:2436-2447.

Torre L. A., Trabert B., DeSantis C. E., Miller K. D., Samimi G., Runowicz C. D., et al. (2018) Ovarian cancer statistics, 2018. CA Cancer J Clin 68:284-296.

34- Wang J.-y., Lu A.-q. and Chen L.-j. (2019) LncRNAs in ovarian cancer. Clinica Chimica Acta 490:17-27.

Wang X., Yang B., She Y. and Ye Y. (2018) The lncRNA TP73-AS1 promotes ovarian cancer cell proliferation and metastasis via modulation of MMP2 and MMP9. Journal of cellular biochemistry 119:7790-7799.

West J. A., Davis C. P., Sunwoo H., Simon M. D., Sadreyev R. I., Wang P. I., Tolstorukov M. Y. and Kingston R. E. (2014) The long noncoding RNAs NEAT1 and MALAT1 bind active chromatin sites. Mol Cell 55:791-802.

Xi J., Feng J. and Zeng S. (2017) Long noncoding RNA lncBRM facilitates the proliferation, migration and invasion of ovarian cancer cells via upregulation of Sox4. American Journal of Cancer Research 7:2180.

Xu H., Sun X., Huang Y., Si Q. and Li M. (2020) Long non-coding RNA NEAT1 modifies cell proliferation, colony formation, apoptosis, migration and invasion via the miR-4500/BZW1 axis in ovarian cancer. Mol Med Rep 22:3347-3357.

Xu Q. F., Tang Y. X. and Wang X. (2018) LncRNA EBIC promoted proliferation, metastasis and cisplatin resistance of ovarian cancer cells and predicted poor survival in ovarian cancer patients. Eur Rev Med Pharmacol Sci 22:4440-4447.

Yang C., Li Z., Li Y., Xu R., Wang Y., Tian Y. and Chen W. (2017) Long non-coding RNA NEAT1 overexpression is associated with poor prognosis in cancer patients: a systematic review and meta-analysis. Oncotarget 8:2672-2680.

ZadehRashki N., Shahmohammadi Z., Damrodi Z., Boozarpour S., Negahdari A., Mansour Moshtaghi N., et al. (2022) LncRNAs as Regulators of the STAT3 Signaling Pathway in Cancer. Journal of Cell and Molecular Research 13:137-150.

Zaorsky N. G., Khunsriraksakul C., Acri S. L., Liu D. J., Ba D. M., Lin J. L., et al. (2021) Medical Service Use and Charges for Cancer Care in 2018 for Privately Insured Patients Younger Than 65 Years in the US. JAMA Network Open 4:e2127784-e2127784.

Zhang P., Wu W., Chen Q. and Chen M. (2019) Non-Coding RNAs and their Integrated Networks. J Integr Bioinform 16.

Zhang Y., Dun Y., Zhou S. and Huang X. H. (2017) LncRNA HOXD-AS1 promotes epithelial ovarian cancer cells proliferation and invasion by targeting miR-133a-3p and activating Wnt/β-catenin signaling pathway. Biomed Pharmacother 96:1216-1221.

Zhen L., Yun-Hui L., Hong-Yu D., Jun M. and Yi-Long Y. (2016) Long noncoding RNA NEAT1 promotes glioma pathogenesis by regulating miR-449b-5p/c-Met axis. Tumour Biol 37:673-683.

Scientific Reviewers

MANUSCRIPT PREPARATION

Manuscripts should be prepared in accordance with the uniform requirements for Manuscript's Submission to **"Journal of Cell and Molecular Research".**

Language: Papers should be in English (either British or American spelling). The past tense should be used throughout the results description, and the present tense in referring to previously established and generally accepted results. Authors who are unsure of correct English usage should have their manuscript checked by somebody who is proficient in the language; manuscripts that are deficient in this respect may be returned to the author for revision before scientific review.

Typing: Manuscripts must be typewritten in a font size of at least 12 points, double-spaced (including References, Tables and Figure legends) with wide margins (2.5 cm from all sides) on one side of the paper. The beginning of each new paragraph must be clearly indicated by indentation. All pages should be numbered consecutively at the bottom starting with the title page.

Length: The length of research articles should be restricted to ten printed pages. Short communication should not exceed five pages of manuscript, including references, figures and tables. Letters should be 400-500 words having 7-10 references, one figure or table if necessary. Commentaries and news should also be 800-1000 words having 7-10 references and one figure or table if necessary.

Types of Manuscript: JCMR is accepting original research paper, short communication reports, invited reviews, letters to editor, biographies of scientific reviewers, commentaries and news.

Statement of Human and Animal Rights: Author's should declare regulatory statement regarding the experiments using animals, human cells/tissues that all in vivo experiments have been performed according to the guidelines (explained by WHO, international animal rights federations or your respective institute) to use animals in their research work.

Conflict of Interest Statement: Authors or corresponding author should declare statement of conflict of interest at the last of manuscript.

Manuscript Evaluation Time: All submitted manuscripts will be evaluated and reviewed according to following evaluation schedule. Pre-Editorial Evaluation: All submitted manuscripts, right after their submission to JCMR will be evaluation by Editors for being according to the journal scope and format. This evaluation can take 2-7 days of submission. Reviewer's Evaluation: Selected manuscripts after pre-editorial evaluation will be sent to minimum two blind reviewers assigned by Editor-in-Chief. This process may take 21-27 days. Post Editorial Evaluation: After receiving reviewer's comments, editors evaluate the manuscripts considering the comments and decide their first decision. This process takes 3-5 days and then authors are informed regarding the editorial decision.

GENERAL ARRANGEMENT OF PAPERS

Title: In the first page, papers should be headed by a concise and informative title. The title should be followed by the authors' full first names, middle initials and last names and by names and addresses of laboratories where the work was carried out. Identify the affiliations of all authors and their institutions, departments or organization by use of Arabic numbers (1, 2, 3, etc.).

Footnotes: The name and full postal address, telephone, fax and E-mail number of corresponding author should be provided in a footnote.

Abbreviations: The Journal publishes a standard abbreviation list at the front of every issue. These standard abbreviations do not need to be spelled out within paper. However, non-standard and undefined abbreviations used five or more times should be listed in the footnote. Abbreviations should be defined where first mentioned in the text. Do not use abbreviations in the title or in the Abstract. However, they can be used in Figures and Tables with explanation in the Figure legend or in a footnote to the Table.

Abstract: In second page, abstract should follow the title (no authors' name) in structured format of not more than 250 words and must be able to stand independently and should state the Background, Methods, Results and Conclusion. Write the abstract in third person. References should not be cited and abbreviations should be avoided.

Keywords: A list of three to five keywords for indexing should be included at bottom of the abstract. Introduction should contain a description of the problem under investigation and a brief survey of the existing literature on the subject.

Materials and Methods: Sufficient details must be provided to allow the work to be repeated. Correct chemical names should be given and strains of organisms should be specified. Suppliers of materials need only be mentioned if this may affect the results. Use System International (SI) units and symbols.

Results: This section should describe concisely the rationale of the investigation and its outcomes. Data should not be repeated in both a Table and a Figure. Tables and Figures should be selected to illustrate specific points. Do not tabulate or illustrate points that can be adequately and concisely described in the text.

Discussion: This should not simply recapitulate the Results. It should relate results to previous work and interpret them. Combined Results and Discussion sections are encouraged when appropriate.

Acknowledgments: This optional part should include a statement thanking those who assisted substantially with work relevant to the study. Grant support should be included in this section.

References: References should be numbered and written in alphabetical order. Only published, "in press" papers, and books may be cited in the reference list (see the examples below). References to work "in press" must be accompanied by a copy of acceptance letter from the journal. References should not be given to personal communications, unpublished data, manuscripts in preparation, letters, company publications, patents pending, and URLs for websites. Abstracts of papers presented at meetings are not permissible. These references should appear as parenthetical expressions in the text, e.g. (unpublished data). Few example of referencing patterns are given as follows:

Examples of text references:

Cite a source written by one author: (Kikuchi, 2014)

Cite a source written by two authors: (Rinn and Chang, 2012)

Cite a source written by three or more authors: (Mead et al., 2015)

Examples of end references:

>>> Kikuchi K. (2014) Advances in understanding the mechanism of zebrafish heart regeneration. Stem Cell Research 13:542-555.

>>> Irfan-Maqsood M. (2013) Stem Cells of Epidermis: A Critical Introduction. Journal of Cell and Molecular Research 5:1, 1-2.

>>> Rinn J. L. and Chang H. Y. (2012) Genome regulation by long noncoding RNAs. Annual Review of Biochemistry 81:1-9.

>>> Bongso A., Lee E. H. and Brenner S. (2005) Stem cells from bench to bedside. World Scientific Publishing Co. Singapore, 38-55 pp.

(6 authors:) Mead B., Berry M., Logan A., Scott R. A., Leadbeater W. and Scheven B. A. (2015) Stem cell treatment of degenerative eye disease. Stem Cell Research 14:243-257.

Note: When citing more than six authors, give the name of the first author and abbreviate the others to et al.

(more than 6 authors:) Vaculik C., Schuster C., Bauer W., Iram N., Pfisterer K., Kramer G., et al. (2012) Human dermis harbors distinct mesenchymal stromal cell subsets. Journal of Investigative Dermatology 132:563-574.

Note: All the reference should be in EndNote format (JCMR EndNote Style is available on JCMR's web site, Author's Guideline)

Tables and Figures: Tables and Figures should be numbered (1, 2, 3, etc.) as they appear in the text. Figures should preferably be the size intended for publication. Tables and Figures should be carefully marked. Legends should be typed single-spaced separately from the figures. Photographs must be originals of high quality. Photocopies are not acceptable. Those wishing to submit color photographs should contact the Editor regarding charges.

JCMR Open Access Policy: Journal of Cell and Molecular Research follows the terms outlined by the Creative Common's Attribution-Only license (CC-BY) to be the standard terms for Open Access. Creative Commons License.

Note: All manuscripts submitted to JCMR are tracked by using "iThenticate" and "Plagiarism Tracker X" for possible plagiarism before acceptance.

Table of Contents

Expressed Cellobiohydrolase Enzyme of Thermobifidia fusca in Pichia pastoris as Host Can Act on Cotton Substrate 1

Karim Imangholiloo; Nasrin Moshtaghi; Seyed Hasan Marashi; Abdolreza Bagheri; Ahmad Sharifi

Phytochemical Analysis of Volatile and Non-volatile Fractions, Antioxidant, and Anti-Cancer Activities of Dracocephalum polychaetum and Dracocephalum kotschyi 11

Marzieh Taghizadeh; Sara Soltanian; Nahid Nasibi

Effect of Intramuscular and Intraperitoneal Injections of conjugated MSTN-siRNA-cholesterol on Inhibition of Myostatin Gene expression 20

Mitra Riasi; Sina Mozaffari Jovin; Ali Javadmanesh

Conversion of Membrane Lipids to Jasmonates as a Key Pathway to Develop Somatic Embryos in Arabidopsis thaliana 28

Azadeh Khadem; Nasrin Moshtaghi; Abdolreza Bagheri

Evaluation of CD86 rs17281995Gene Polymorphism in Gastric and Intestinal Cancer Subjects in Tehran and Khorramabad Cities 37

Masoumeh Aalipour; Asghar Aalipour; Mohammad Mousaei Ghasroldasht

Comparative Transcriptome Analyses of a Transgenic Sugar Beet Resistant to Beet Necrotic Yellow Vein Virus 44

Mahdieh Yousefiara; Mohammad Ali Malboobi; Abdolreza Bagheri; Nasrin Moshtaghi

Investigating the Effect of Stable Glutamine on the Neuronal Differentiation of PC-12 Cells in 2D- and 3D-Culture Media 54

Seyed Majid Jalalian Hosseini; Javad Baharara; Shahrbanoo Oryan; Mohammad Amin Kerachian

Study of lncRNA NEAT1 Gene Expression in Ovarian Cancer 63

Amin Moqadami; Mohammad Khalaj-Kondori

Journal of Cell and Molecular Research

Volume 14, Number 1, Summer, 2022